Finite Element Modelling and Response Spectrum Analysis of Rubble-Stone Masonry Buildings

by

QAZI SULAIMAN NAEEM

A Dissertation
Submitted to the Department Civil, Chemical,
Environmental and Material Engineering (DICAM)
University of Bologna

In Partial Fulfilment of the Requirement
for the Degree of Master of Science
July 2021

Supervised by Prof. Stefano Silvestri

ABSTRACT

Finite element modelling is an efficient tool for performance assessment of masonry structures. In particular, it facilitates the accurate prediction of seismic response of a structure to earthquakes using dynamic analysis procedures. Numerical models using response spectrum analysis based on modal analysis allow to predict realistic failure modes observed after preceding seismic events with reasonable computational effort, a characteristic which is suitable for engineering practice. This thesis deals with modelling as a finite element model and analyse using response spectrum analysis of masonry buildings and the subsequent discussion of the obtained results. SAP2000 software is used for developing the numerical models, which are then analysed on the basis of design acceleration response spectra obtained according to the different building codes for different regions. Different structural demands under static and dynamic loading are obtained from the models and compared with theoretical results made with various mathematical models.

Keywords: Finite element modelling, Response spectrum analysis, Masonry structures, Base Shear

TABLE OF CONTENTS

LIST OF TABLES

LIST OF FIGURES

1. Introduction

Stone masonry is a traditional form of construction that has been exercised for centuries in regions where stone is locally available. Stone masonry has been used for the construction of some of the most important monuments and structures around the world. Buildings of this type range from cultural and historical landmarks, often built by highly skilled stonemasons, to ordinary dwellings built by their owners or local laborers in developing countries where stone is an affordable and cost-effective building material for housing construction. Stone has long served as the choice material of construction for these structures and its relevancy is evident when their vast distribution and ease of access, Stone masonry buildings can be found in many earthquake-prone regions and countries.

Masonry offers a varying multitude of salient features which must be taken into consideration when opting for it as a material for construction. It can be strong, durable and weather resistant. While on the other hand its thick and heavy and reduces the floor space. Masonry possesses an inherent weakness against tensile and shear stresses, aspects which must be compensated for when considering its usage. In areas where non-engineered construction is predominant, vulnerability further increases due to inconsistent and poor quality of materials and workmanship.

This paper is a case study of such masonry structures in which modern analysis tools for seismic assessment and design is carried out. The focus will be on the reaction of these models to different response spectrums using finite element modelling software. The case study comprises two buildings with a layout typical for Himalayan region, which is known for its high seismic activity as well as great number on non-engineering constructions made of rubble stone.

2. Vernacular construction techniques in developing countries

Himalayan regions present a significant seismic activity. Many examples can be found of load-bearing masonry with mortar and reinforced concrete beltings or with horizontal wood lacing and also with covering of steel wire meshes.

Stone masonry can essentially be divided into two major categories: Rubble stone and Ashlar. When rocks are cut into rectangular units with straight adjoining sides it is called Ashlar, also known as cut, squared or dressed stone. To cut such neat units by hand involves lots of intensive labour, which is highly dependent on the hardness of the stone and the required level of shaping and finishing. This makes Ashlar much more expensive than rubble stone and it is therefore less often used in the rural areas. The shape of the stone is important for the structural stability of the wall. Generally said, the rounder the boulder, or the more irregular the shape of the rock, the more difficult it is to build a consistent and stable wall. Of equal importance is the type of masonry mortar that is used. Mud is the main choice in the rural and remote areas in most developing countries, followed by cement mortar if the people can afford it, or lime-sand mortar if lime is available, although this is not very common in the Himalayan regions. (Schildkamp & Araki, 2019)

Another type of construction technique is known as "Bhatar," in which the buildings predominantly consist of dry-stacked stone walls. the Pashto word "Bhatar" specifically indicates beams with a cross section of 3″–4″, which are then combined into continuous wooden ladders with cross pieces, used to reinforce the walls. In some cases, a weak mud or lime mortar is used, which may result in lower quality of masonry, as the masons take less care in proper placement of the stones. This vernacular architecture is still practiced in the Himalayan regions of developing countries, such as India and Pakistan, due to its advantages from both economical and constructive point of view with respect to the conventional construction techniques. On the other hand, Himalayan regions present a significant seismic activity and the "weight issues" concerning Bhatar are not negligible due to the significant mass of walls and roof. Nonetheless, Bhatar buildings are known to have a strong resistance to seismic forces. (Carabbio, Pieraccini, Silvestri, & Schildkamp, 2018)

A gabion-box is a rectangular cage made with steel wire mesh and filled with stones. A gabion-box wall is built-up by stacking vertically each single gabion-box and then joining them with steel wires in order to provide some tensile strength to the entire wall, until the specified height of the wall is reached. In placing the gabion-boxes the vertical joints must be alternated. A gabion-box walls building is a structure composed of adequately interconnected gabion-box walls. Gabion-boxes, made with steel wire mesh and filled with stones of appropriated size, are normally stacked up one into another to form a retaining wall. Given their reduced costs and the easy availability of their constituting materials, gabion-box walls have been extensively used in developing countries (such as Nepal) also to realize simple one-storey residential buildings. In the recent years, gabion structures have been increasingly used in the engineering field. This interest is due to the fact that gabions are environmental friendly and they present several other advantages: versatility, durability, flexibility, permeability, noise proofing, and limited costs. On the other hand, from a seismic point of view, there are "weight issues" given that the gabions are characterized by significant mass due to the rock filling (it is well known that the seismic forces acting on the structure are proportional to the weight). (Samayoa, Baraccani, Pieraccini, & Silvestri, 2018)

Recent research by Smart Shelter Foundation questions the current state-of-the-art methods and knowledge levels referencing to the seismic behaviour of so-called "non-engineered construction techniques" in general, and rubble-stone masonry in particular. In-depth literature reviews (Schildkamp & Araki, 2019) show that the available information in the national codes, technical regulations, and practical manuals are largely outdated, filled with contradictory dead-ends, and often tend towards ambiguity.

Thus, the recommendations and solutions to the aforementioned shortcomings are proposed under the project name SMARTnet, an acronym for "Seismic Methodologies for Applied Research and Testing of non-engineered techniques". It is a world-wide initiative whose strategy is to ensure an international collaboration of experts and scientists. The ultimate goal of the project is to reduce casualties and alleviate financial loss as a result of damage to property and belongings by reducing risk of damage and collapse of indigenous, traditional non-engineered buildings and improving their overall structural response to seismic events in areas particularly prone to earthquakes.

To achieve a balance between accurately predicting and significantly enhancing the seismic performance of such structures and keeping them affordable and accessible with basic engineering principles, a thorough, systematic and scientifically based long-term approach must be adopted. Ideally, the approach should be borne out of an amalgamation of comprehensive material study, laboratory experiments, and computer modelling, which significantly improves upon the standard of proficiency and expertise, leading to the development of new, structured methodology of executing non-engineered construction.

3. Case study

A simple typical layout of two buildings for mountainous regions were taken in which one is a school structure and another one serves as a residential structure (house) representing the type of buildings that were constructed by Smart Shelter Foundation between 2007 and 2012. A detailed description of the buildings structural arrangement and construction materials is given in Section 3.1.

Descriptive information on the models is given in Section 4.

3.1 Description of case study buildings

The buildings used for the case study were inspired by the constructions executed in Nepal by Smart Shelter Foundation and designed by architect Martijn Schildkamp. The materials used in the construction are common for rural areas and easily available sandstone and cement mortar.

The layout of both buildings is simple, regular in plan and elevation, to minimize the unfavourable torsional effects during the seismic events. The structures have reinforcing concrete beams encircling masonry walls. Special attention was paid to lessening of the seismic weight, therefore, both buildings have light-weight roofs and floors, thus making the walls to be the main contribution to the total structural mass.

3.1.1 School building

The school building layout and elevations are demonstrated in Figure 1 - 4. It is a one-storey structure that consists of three classrooms of equal dimensions placed along X axis. The structural layout is regular and symmetric around both axes.

The load-bearing masonry walls comprise a plinth which is a part of the foundation above ground level. The first-storey floor consists of a bed of mountain stones and earth with a layer of compacted soil covered with concrete slab. It reaches the top of the plinth level and is not connected to the walls, therefore having no impact on the mass and rigidity of the structure.

The structure is enhanced by reinforced concrete beams of variable height placed on several levels: on top of the plinth, at the bottom and top level of doors and windows, on the top of the building, with discontinuous RC bands at the mid-window level.

All openings are positioned in the walls along X axis, with only windows on one side and doors and windows on the other. Doors and windows frames are made of wood.

The roof is a light-weight wooden truss structure covered with tin sheets. It is important to note that roof does not affect in a significant way the overall weight and stiffness of the building. The building is constructed with irregular shaped sandstone masonry with cement mortar joints. All walls have the same thickness of 35 cm and total height of 3.4 m. Interior walls are finished with sand-cement plaster.

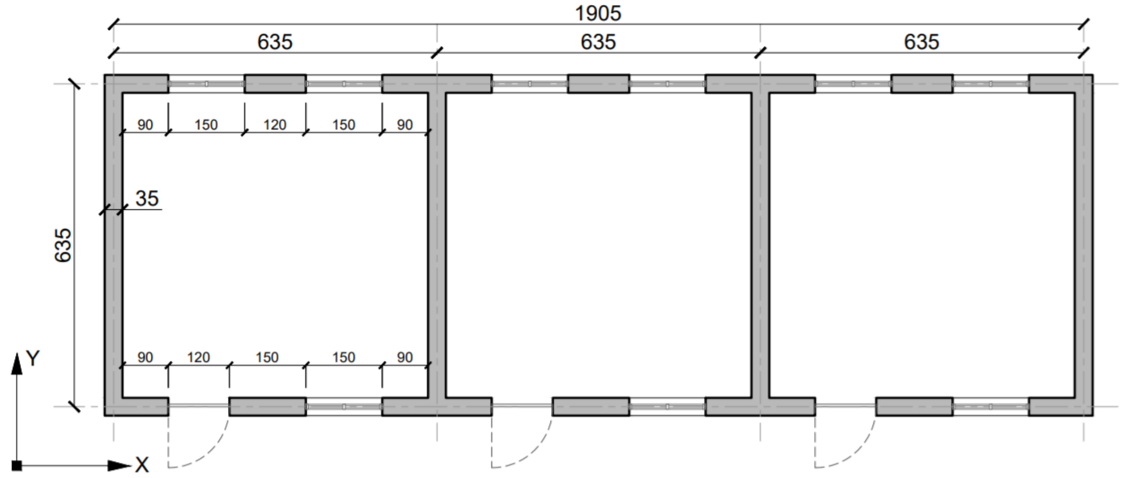

Figure 1 School layout

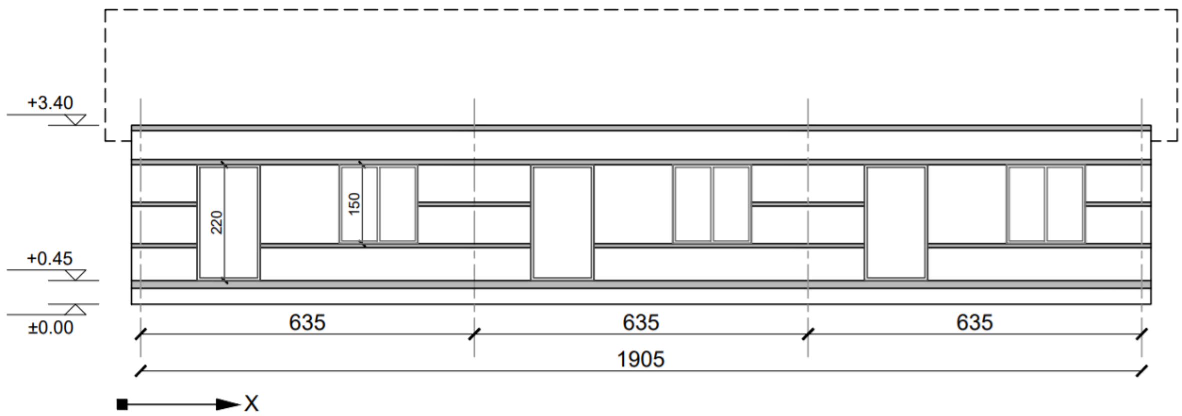

Figure 2 School elevation along X axis, door wall

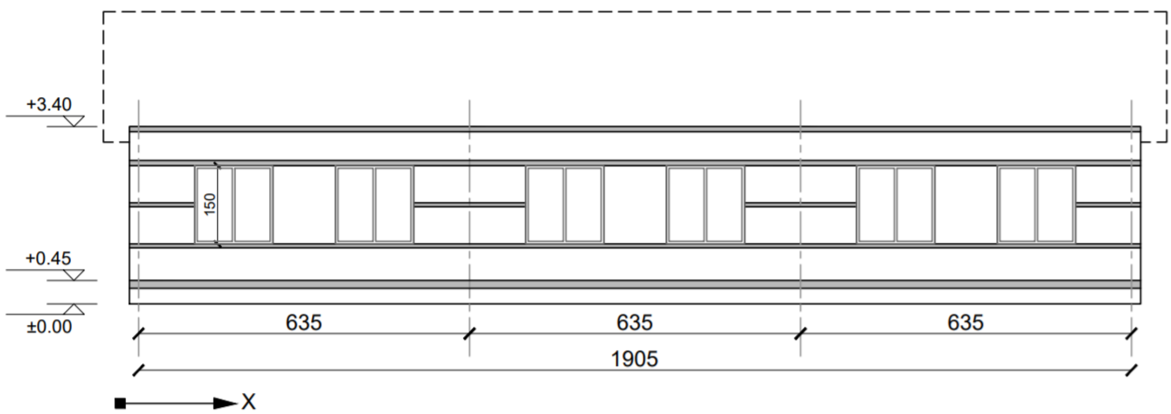

Figure 3 School elevation along X axis, window wall

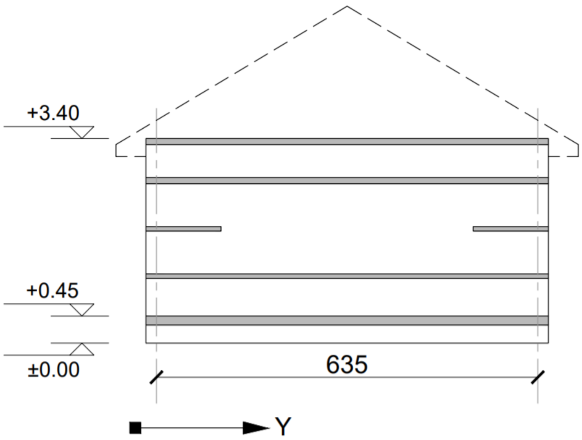

Figure 4 School elevation, wall along Y axis

3.1.2 House building

The house building layout and elevations are demonstrated in Figure 5 - 7. It is a two-storey structure that consists of two rooms of equal dimensions and a terrace on each floor. The rooms are placed along X axis. The structural layout is regular and symmetric around Y axis.

Similar to the school building, the load-bearing masonry walls comprise a plinth which is a part of the foundation above ground level. The first-storey floor consists of a bed of mountain stones and earth with a layer of compacted soil covered with concrete slab. It reaches the top of the plinth level and is not connected to the walls. The second-storey floor is made of wooden beams covered with wooden planks. Neither the first nor the second floor has significant impact on the structural rigidity.

Two floors are connected by an exterior light-weight wooden staircase located on the terrace.

The structure is enhanced by reinforced concrete beams of variable height placed on several levels: on top of the plinth, at the bottom and top level of doors and windows of each storey, on the top of the building, with discontinuous RC bands at the mid-window level.

Most openings are positioned along X axis, with only windows on one side and doors and windows on the other. One door opening is placed on the inner wall along Y axis. Doors and windows frames are made of wood.

The roof is a light-weight wooden truss structure covered with tin sheets. It is important to note that, similarly to the school building, roof, as well as the second story floor, does not affect in a significant way the overall weight and stiffness of the building.

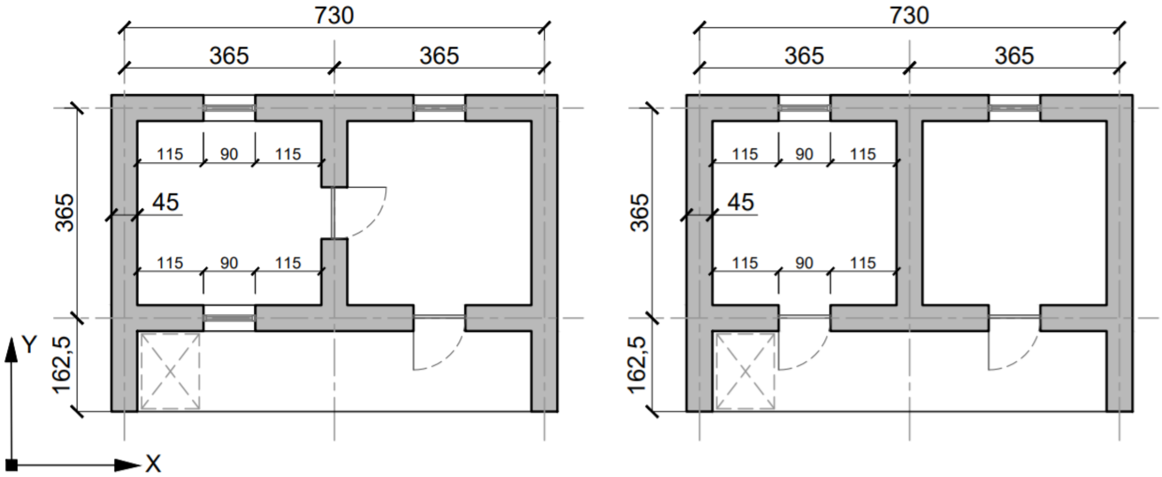

Figure 5 House layout: First floor (left); Second floor (right)

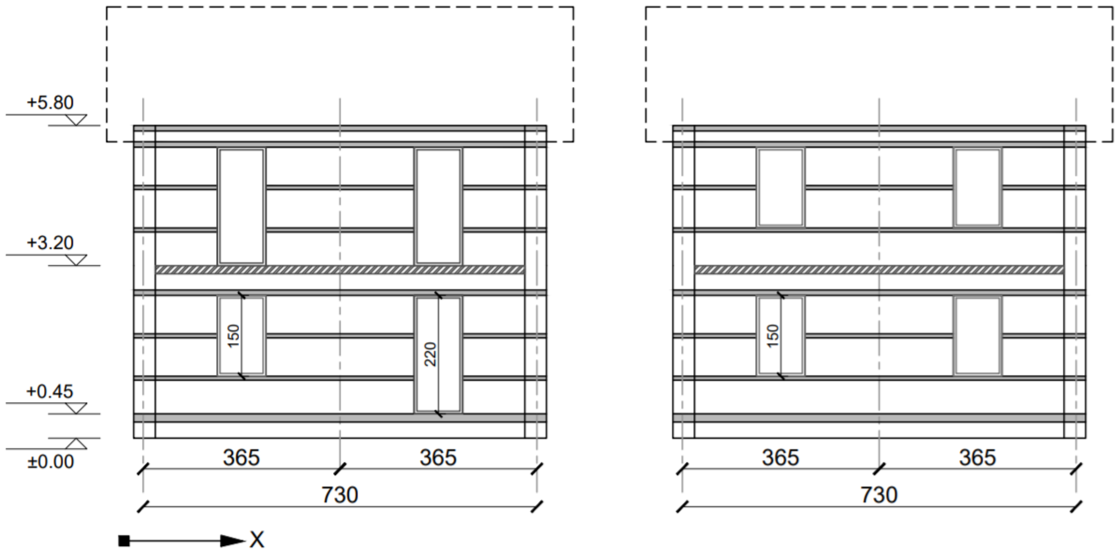

Figure 6 House elevations along X axis: Door wall (left); Window wall (right)

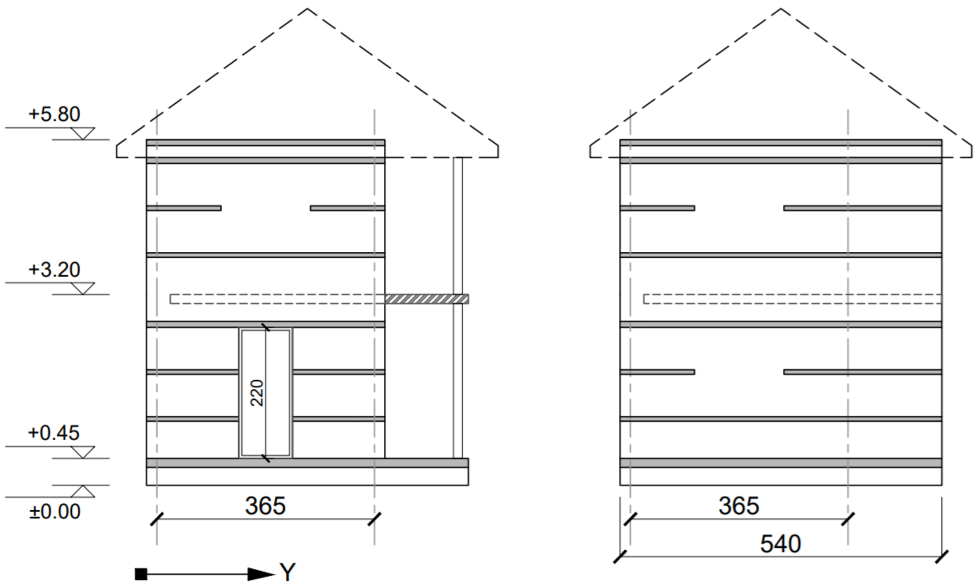

Figure 7 House elevations along Y axis: Interior wall (left); Exterior wall (right)

The building is constructed with irregular shaped sandstone masonry with cement mortar joints. All walls have the same thickness of 45 cm; interior walls are finished with sand-cement plaster. Height of the first storey including the plinth is 3.2 m, second storey – 2.6 m.

4. Description of numerical models

Using SAP2000 software, different model configurations were prepared both for school and house structures changing the material properties as per specific region and code. Using these material properties, two different types of models were then created to analyse the effect of various aspects on structural performance:

- With plinth level (PL)
- Without plinth level (WPL).

Figure 8 shows the difference between two different type of models with an example of school wall along y-axis: With plinth level (PL) and Without plinth level (WPL).

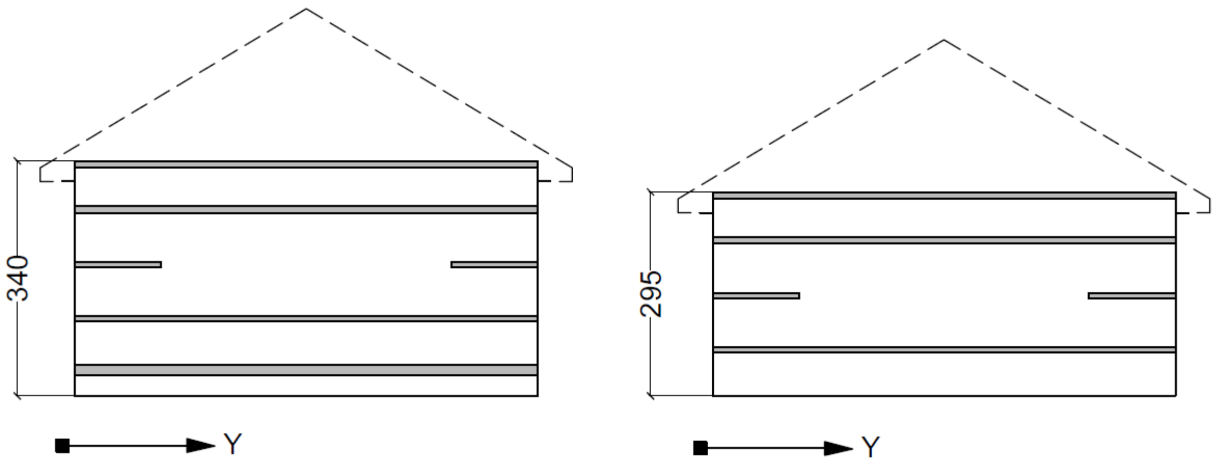

Figure 8 School elevations along Y axis: With plinth level (PL) (left); Without plinth level (WPL) (right)

Few assumptions were taken into consideration while creating these models:

- Manual meshing was done instead of using automatic mesh option of software.
- Hinge support was provided to every node at base level.
- Reinforced concrete beams were placed at specified levels as per building drawings. Width of the beam is always the same as the width of the wall and the thickness of the beams varies along the height. Figure 9-Figure 10 shows the different thicknesses of these beams at different levels for school PL building.

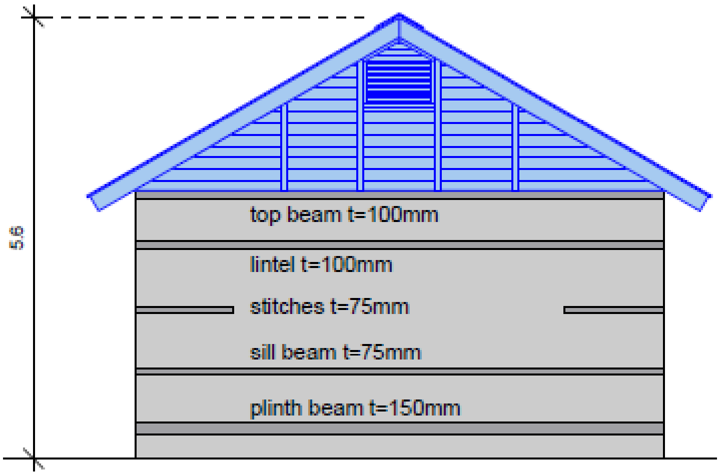

Figure 9 Thicknesses of beams

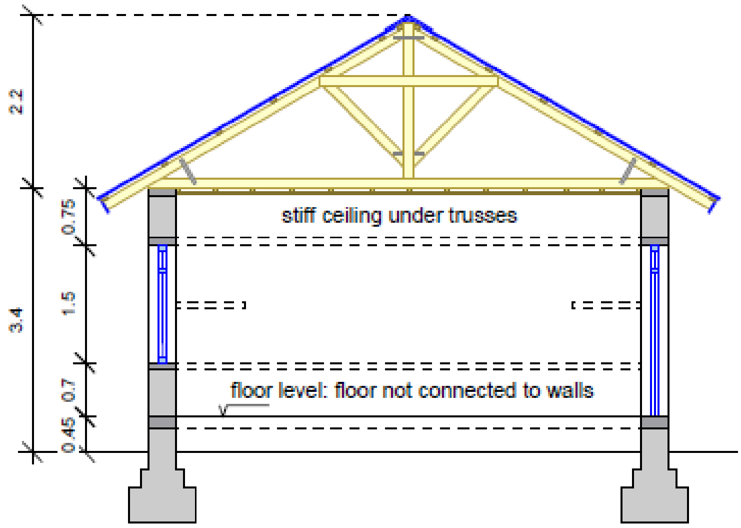

Figure 10 Elevation levels of beams, School PL

4.1 Load analysis

In total 24 different models were prepared with slight input data changed. In which 12 are school models and remaining 12 are house models. These 12 School models were further subdivided into group of 6 as “School PL” models and other 6 as “School WPL” models. The same subdivision was done for 12 house models. Every region’s response spectrum data and material properties values were distinct.

Properties of materials such as sandstone masonry, mortar/plaster, reinforced concrete and wood were taken from the building codes of all the selected regions.

- Nepal: Nepal NBC 102-1994
- India: India IS.875(pt.1)-2007
- Pakistan: Pakistan ASCE-7-1993

- Iran: NBRI-6 (2013)
- China: China GB 50009-2012
- Europe: EN 1991-1-1:2002

Detailed description of the material properties provided by the codes, is given in Table 1.

Unit weights (KN/m^3)				
Region	**Sand stone**	**Plaster**	**Wood**	**Reinforced Concrete**
India & Nepal	22	20.4	5.05	23.48
Pakistan	21.52	20.42	4.41	23.56
Iran	22.6	20.6	4.02	24.5
China	20.8	20	5	24
Europe	22.5	19	4.4	25

Table 1 Unit weights as per different codes

After creating the models, following points were taken into consideration for the application of service dead loads and live loads.

- The ground level floor is not considered in the design of both structure because it is not connected to the walls and therefore has no effect on the structure output. Therefore, no dead loads or live loads were applied to the ground floor.
- While designing the house building, 0.4788 KN/m^2 of dead load and 1.9152 KN/m^2 of live load was applied on the wooden floor at first floor level. The wooden floor has considerably smaller weight and rigidity compared to masonry walls. Therefore, the dead loads (containing the self-weight of the wooden floor) and the live loads acting upon this floor at first floor level i.e. 3.2m height were transferred to dummy beams located at the same height upon the masonry walls. Dummy beams are supposed to transfer the loads directly to the stone masonry walls. Both the dead loads and the live loads were transferred in a percentage of 80% on the x-axis and 20% on the y-axis. Table 2 provides the data of dead and live loads which were transferred from wooden floor to these dummy beams. The properties of dummy beam were taken as follows:
    - X-section: Depth/Thickness = 50mm, Width = 450mm
    - Unit weight, Modulus of Elasticity (E), Poisson ratio (v) and Shear modulus (G) were all defined as 0 value.

Transferring the Floor loads onto the dummy beam								
Region	**Inner House**				**Verandah**			
	Dead load (KN/m)		Live load (KN/m)		Dead load (KN/m)		Live load (KN/m)	
	X-axis (40%)	Y-axis (10%)	X-axis (40%)	Y-axis (10%)	X-axis (40%)	Y-axis (10%)	X-axis (40%)	Y-axis (10%)
India & Nepal	0.936	0.234	2.451	0.613	0.819	0.501	2.145	1.312
Pakistan	0.895	0.224	2.451	0.613	0.783	0.479	2.145	1.312
Iran	0.870	0.218	2.451	0.613	0.761	0.466	2.145	1.312
China	0.933	0.233	2.451	0.613	0.816	0.499	2.145	1.312
Europe	0.894	0.224	2.451	0.613	0.783	0.479	2.145	1.312

Table 2 Dead and live loads transferred from wooden floor to dummy beams, House building

- To compensate the dead load of plaster layer on the inside of the masonry walls, the unit weight of masonry wall was increased accordingly while keeping the width of the wall as 0.35m for school and 0.45m for house building respectively. Also the unit weights of reinforced concrete will be effected by the centre line methodology on which SAP2000 software works. Using centre line method, software can count for the extra self-weight of stone which is integrated with the frame element provided. These updated unit weights were used for modelling the buildings in SAP2000 software. Table 3 provides the data of updated unit weights of sandstone masonry and reinforced concrete.

Fusion of Unit weights of Stone wall and Plaster				
Region	**School**		**House**	
	Stone Masonry (KN/m^3)	Reinforced Concrete (KN/m^3)	Stone Masonry (KN/m^3)	Reinforced Concrete (KN/m^3)
India & Nepal	23.749	0.010	23.360	0.120
Pakistan	23.270	0.290	22.881	0.679
Iran	24.366	0.134	23.973	0.527
China	22.514	1.486	22.133	1.867
Europe	24.129	0.871	23.767	1.233

Table 3 Updated unit weights of stone masonry and reinforced concrete

- Also the roof structures (truss) had considerably smaller weight and rigidity compared to stone walls and were therefore designed separately only to apply the dead load of this truss structures at the connection points on the top of masonry walls as axial forces. This also helped us in eliminating local failure modes in modal analysis.

4.2 Load combinations

The critical load combinations were defined in software for every region and were taken from their respective building codes.

NEP-20 – 1.0D + 0.3L $\pm$ 1.0E

IND-16 – 1.58D $\pm$ 1.5E

PAK-07 – 1.31D + 0.5L $\pm$ 1.1E

IRN-15 – 1.2D + 1.0L $\pm$ 1.0E

EC8 – 1.0D + 0.3L $\pm$ 1.0E

CN-JGJ – 0.95D + 0.475L $\pm$ 1.0E

Where,

D = Dead loads

L = Live loads

E = Earthquake loads

Section 7.2.2 will use these load combinations to compute internal actions at different levels for all buildings and models.

4.3 School model

Taking into consideration all the modelling predispositions described above, total of twelve school models were developed. To clearly differentiate between these models, "*Country name* school PL" will stand for school structure of a specific country with plinth level and on the other hand, "*Country name* school WPL" will stand for a school structure without plinth level. An example of the model name is as follows:

- *Nepal* school PL: masonry structure with plinth level and material properties taken from Nepal building code.
- *Nepal* School WPL: masonry structure without plinth level and material properties taken from Nepal building code.

4.3.1 School PL model

School PL model layout and elevation views are demonstrated in Figure 11-Figure 16.

The layout is identical to the actual building; it is symmetrical around both X and Y axes, with three classrooms of equal dimensions located along X axis.

The walls are modelled as masonry panels with thickness of 35 cm and height of 340 cm with reinforced concrete beams placed at specified levels. The beam parameters are as described previously in this chapter.

The roof structure was converted into point loads (axial loads) and applied to the walls at contact points.

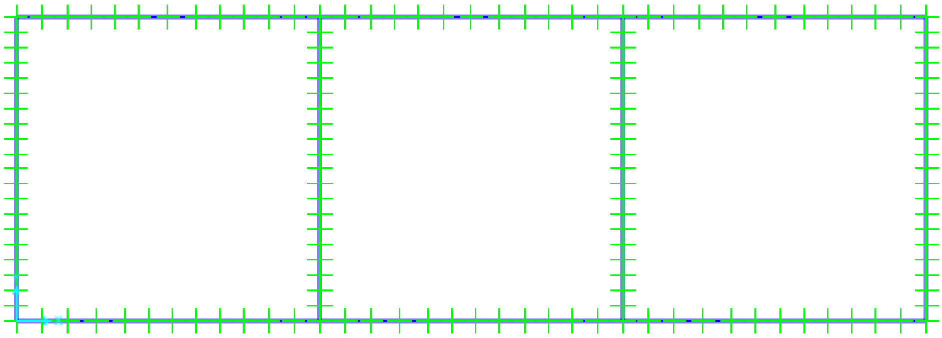

Figure 11 School PL model layout (hinges at every node)

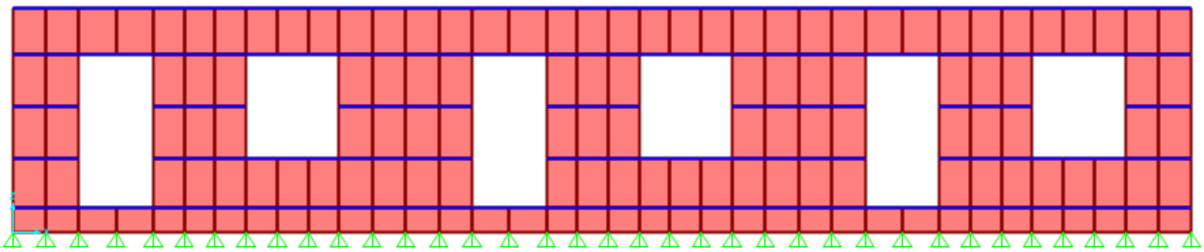

Figure 12 School PL model door wall along X axis

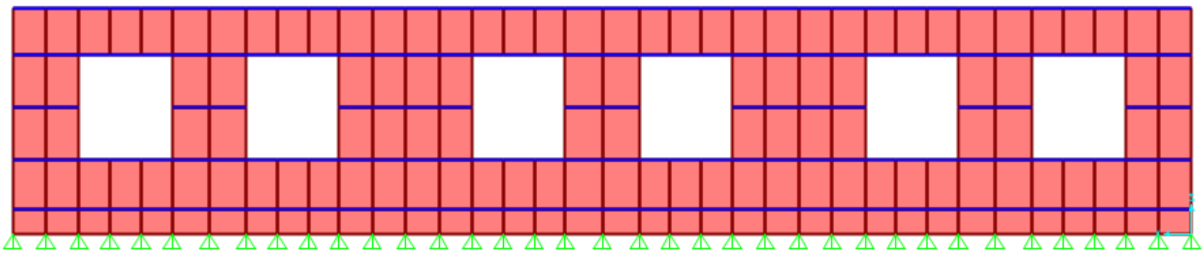

Figure 13 School PL model window wall along X axis

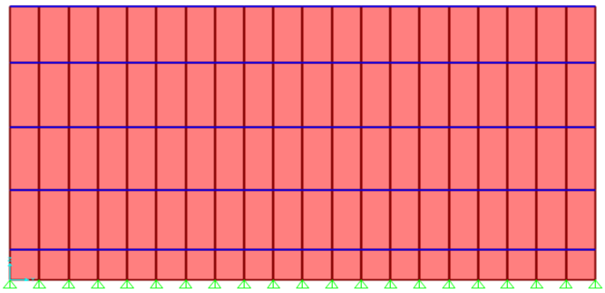

Figure 14 School PL model wall along Y axis

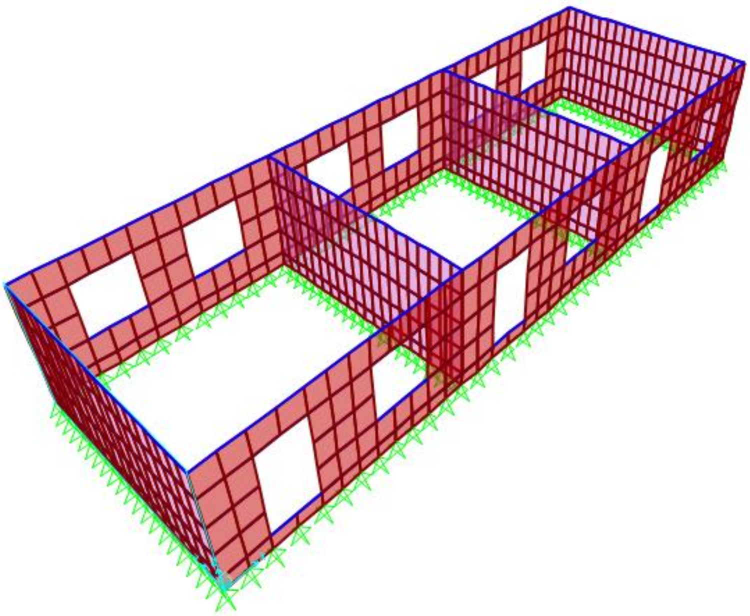

Figure 15 School PL model 3D view: Door wall (front); Window wall (back)

Openings are placed on two walls along X axis, with windows on one side (window wall, WW) and doors and windows on the other (door wall, DW).

Top plan view show the nodes upon which the roof load (converted into point loads) are applied. These point dead loads were same for both school PL and school WPL models. Table 4 shows the values of load (KN) applied upon each node.

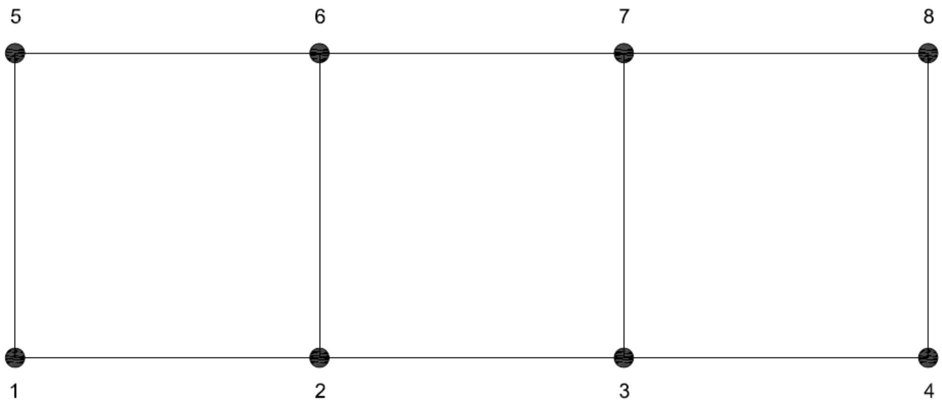

Figure 16 School PL top plan view of nodes

Dead load applied on all nodes (KN)	
Nodes	**School**
1	0.56
2	1.07
3	1.07
4	0.56
5	0.56
6	1.07
7	1.07
8	0.56

Table 4 Dead load for all nodes, School PL and WPL

4.3.2 School WPL model

School WPL model layout is identical to the one of school PL model , and its elevation views is demonstrated in Figure 17-Figure 20.

The walls are modelled as masonry panels with thickness of 35 cm and height of 295 cm with reinforced concrete beams placed at specified levels.

In a similar way to school PL model, openings are placed on two walls along X axis, with windows on one side (window wall, WW) and doors and windows on the other (door wall, DW).

Also the roof structure was converted into point loads (axial loads) and applied to the walls at contact points. The axial load values applied are the same as described in Table 4.

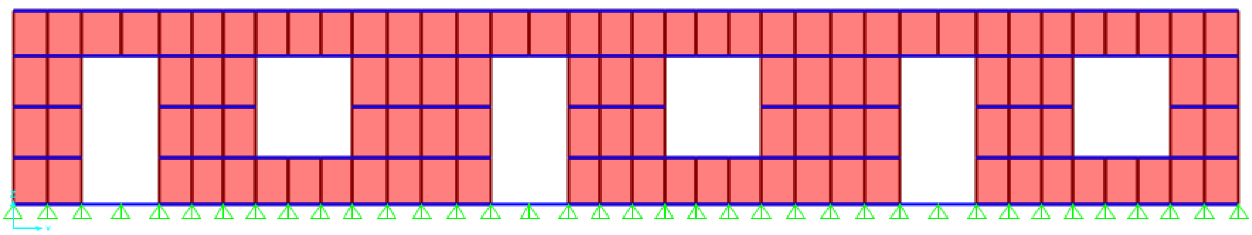

Figure 17 School WPL model door wall along X axis

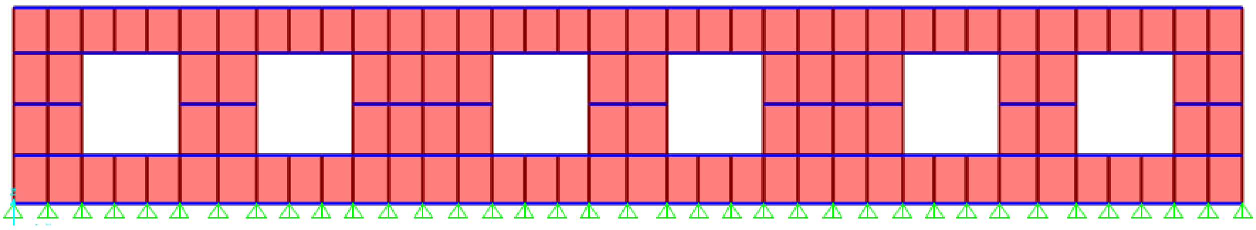

Figure 18 School WPL model window wall along X axis

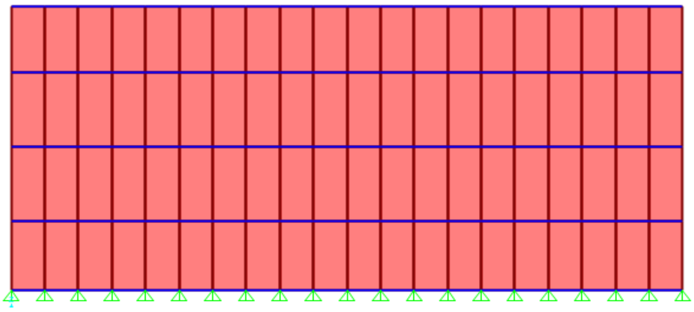

Figure 19 School WPL model wall along Y axis

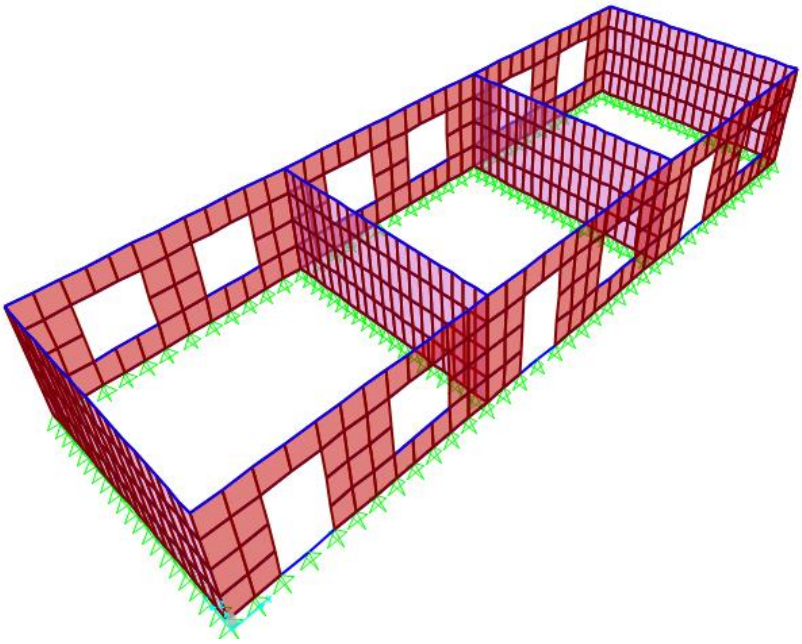

Figure 20 School WPL model 3D view: Door wall (front); Window wall (back)

4.4 House model

Taking into consideration all the modelling predispositions described previously in this chapter, total of twelve house models were developed out of which 6 are “House PL model” and remaining six are labelled as “House WPL model”.

4.4.1 House PL model

The layout and elevation views of house PL model are shown in Figure 21-Figure 25. It is a two-storey structure with two rooms and a terrace on each floor, symmetrical around Y axis.

The walls are modelled as masonry panels with thickness of 45 cm and the height of the first storey is equal to 320 cm with the plinth level, and total height of building is 575 cm with reinforced concrete beams placed at specified levels.

Openings are placed on two walls along X axis, with windows on one side (window wall, WW) and doors and windows on the other (door wall, DW). One door opening is located on the interior wall along Y direction.

As described earlier, the wooden floor has considerably smaller weight and rigidity compared to masonry walls. Therefore, the dead loads (containing the self-weight of the wooden floor) and the live loads acting upon this floor at first floor level were transferred to dummy beams located at the same height upon the masonry walls. Dummy beams are supposed to transfer the loads directly to the stone masonry walls. Both the dead loads and the live loads were transferred in a percentage of 80% on the x-axis and 20% on the y-axis. Table 2 shows the values of load transferred to these walls.

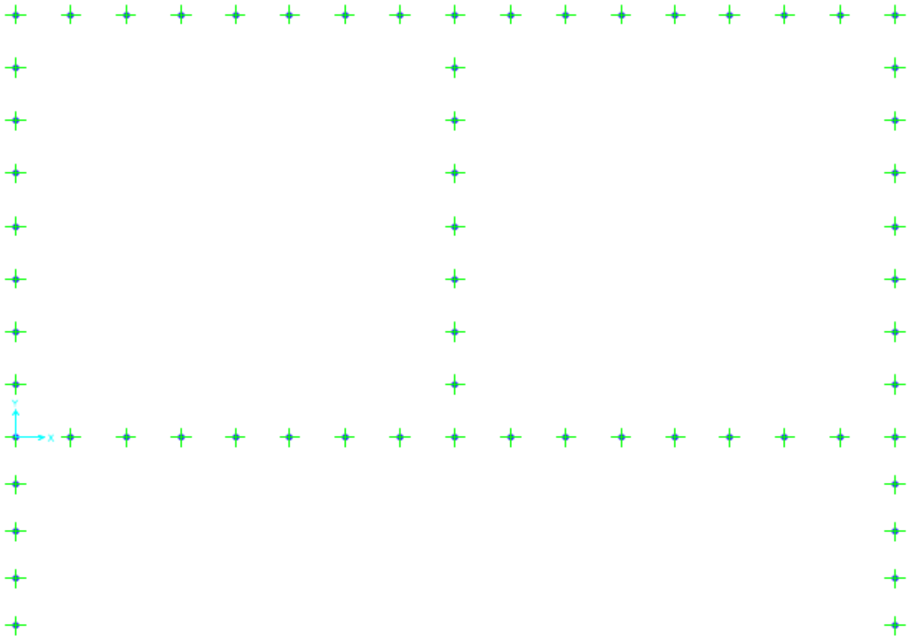

Figure 21 House PL model layout

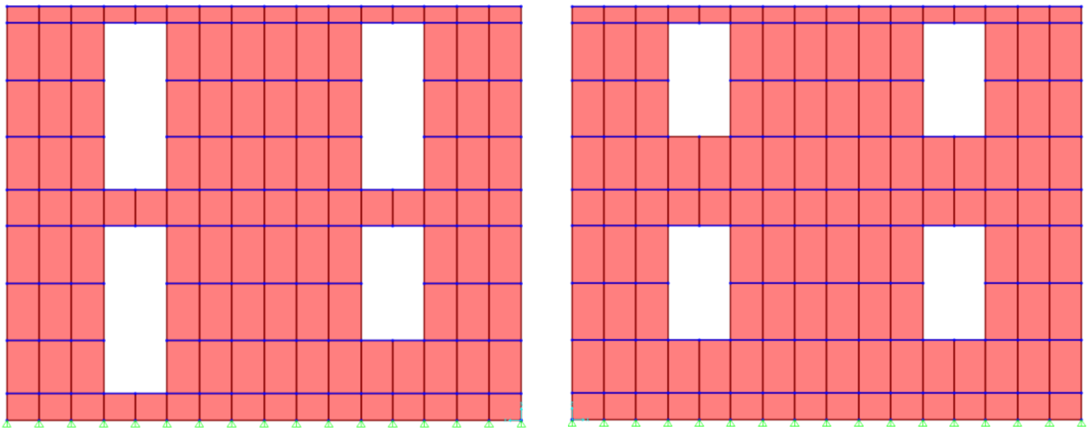

Figure 22 House PL model elevation view, walls along X axis: Door wall (left), Window wall (right)

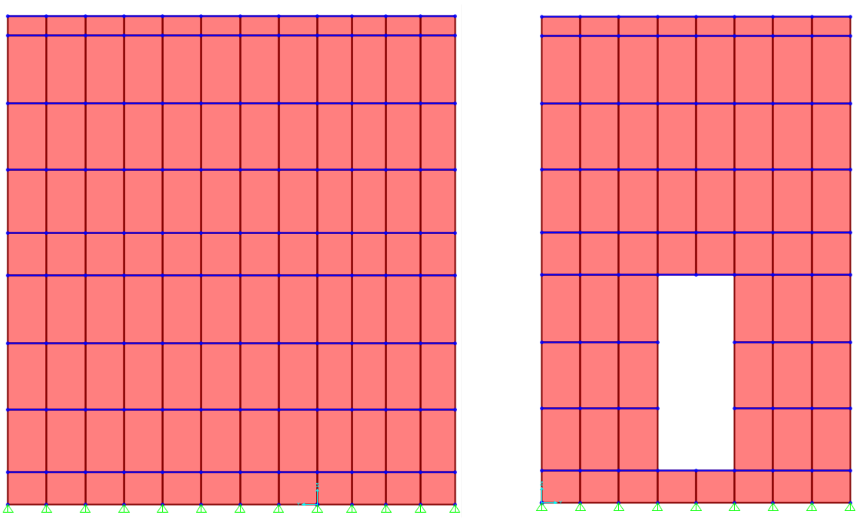

Figure 23 House PL model elevation view, walls along Y axis: Exterior wall (left),Interior wall (right)

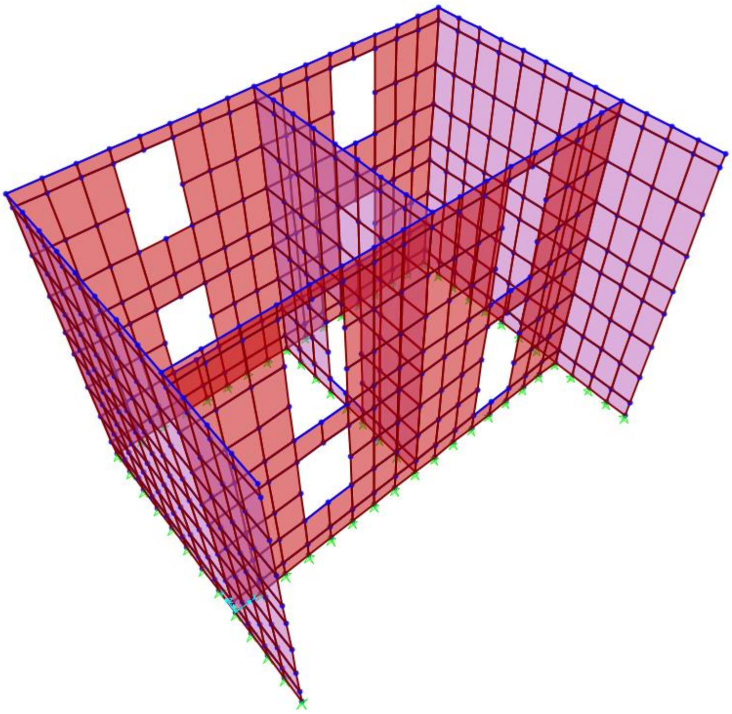

Figure 24 House PL model 3D view

Top plan view show the nodes upon which the roof load (converted into point loads) are applied. This table remains the same for both house PL & WPL same. Table 5 shows the values of load (KN) applied upon each node.

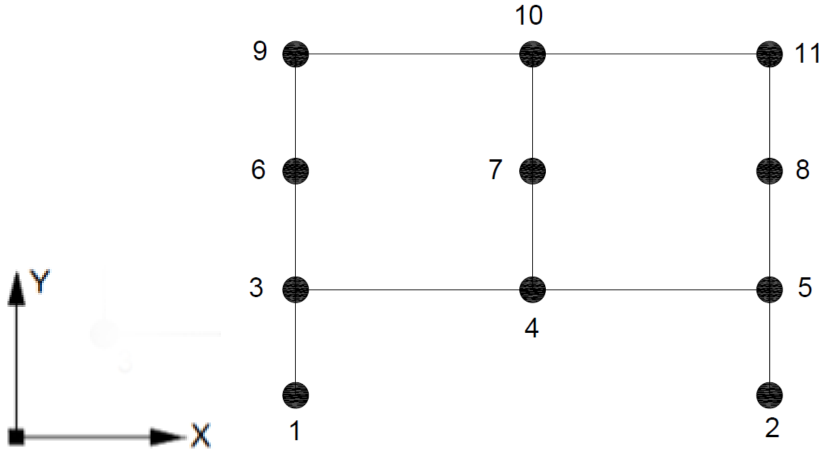

Figure 25 House PL top plan view of nodes

Dead load applied on all nodes (KN)	
Nodes	**House**
1	0.76
2	0.76
3	1.15
4	2.02
5	1.15
6	0.93
7	0.95
8	0.93
9	0.44
10	0.39
11	0.44

Table 5 Dead load for all nodes, House PL and WPL

4.4.2 House WPL model

House WPL model layout is identical to the one of house PL model. The elevation views of house WPL model are shown in Figure 26-Figure 28. The thickness of walls is 45 cm; the plinth level is omitted thus the height of the first storey is equal to 282.5 cm, and total height of building is 537.5 cm with reinforced concrete beams placed at specified levels.
Openings are placed on two walls along X axis, with windows on one side (window wall, WW) and doors and windows on the other (door wall, DW). One door opening is located on the interior wall along Y direction.

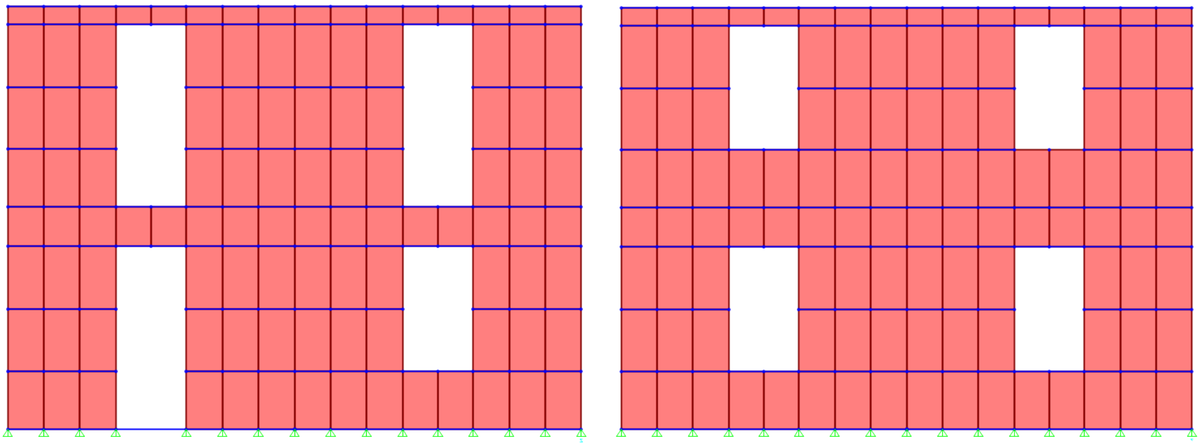

Figure 26 House WPL model elevation view, along X axis: Door wall (left), Window wall (right)

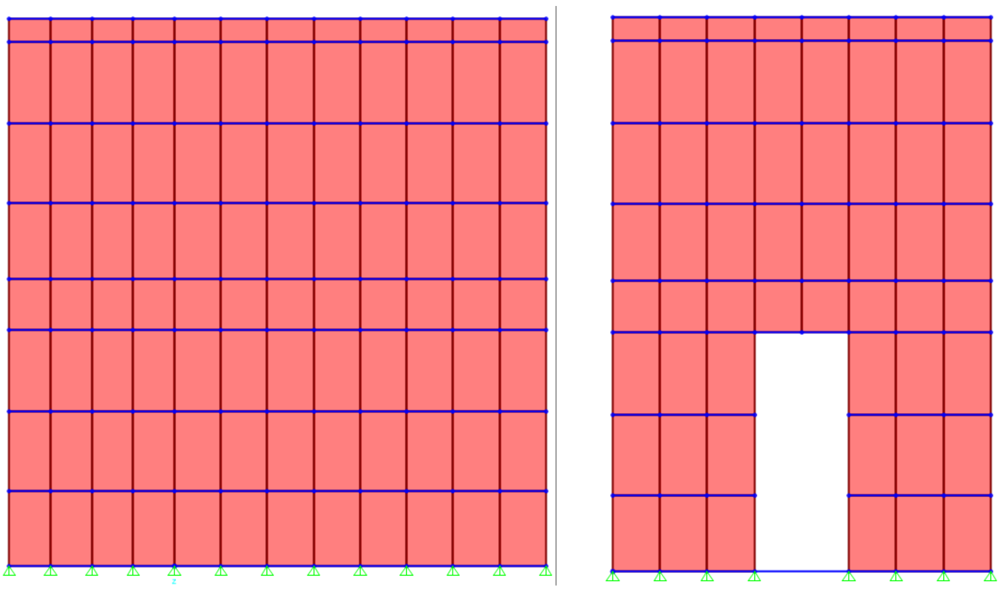

Figure 27 House WPL model elevation view, along Y axis: Exterior wall (left), Interior wall (right)

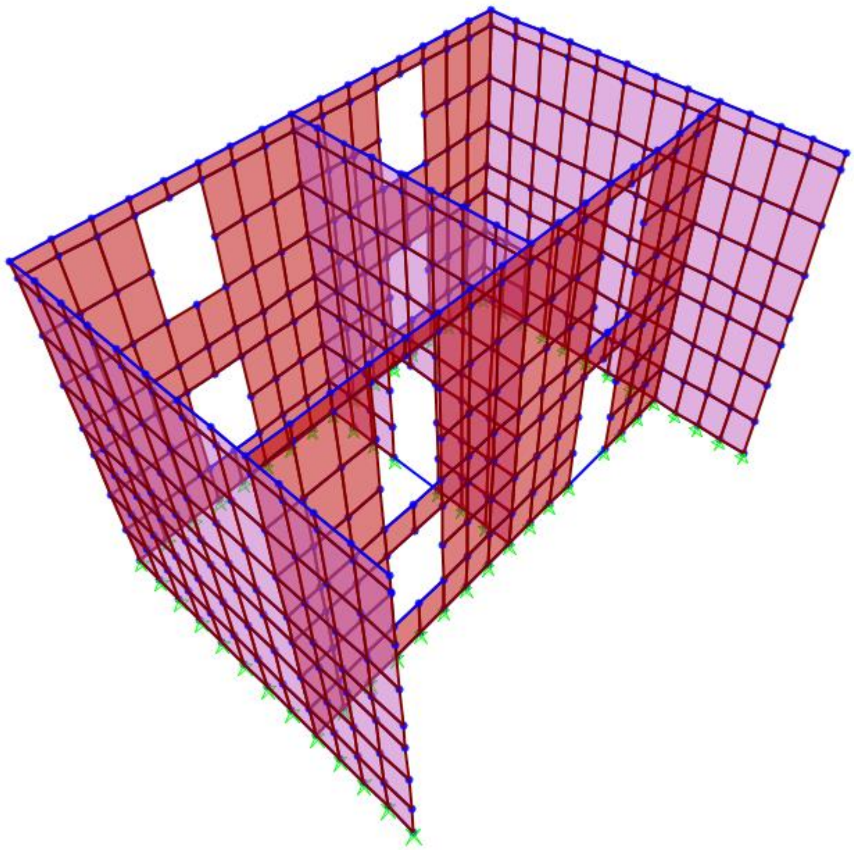

Figure 28 House WPL model 3D view

5. Static analysis

Unreinforced masonry buildings bear a specific sensitivity towards seismic events. Due to this potentially high vulnerability it is necessary to inquire about their structural response and behaviour in the face of such events and the subsequent analytical and numerical modelling for their structural assessment. Therefore, the reliability of these models is certainly important, serving as the primary aspect around which the assessment and viability of existing structures and the design requirements of new ones are conceived.

5.1 Dead load results

In rural and mountain areas the construction materials are generally heavy, such as bricks, stones and earth. An important factor that determines earthquake inertia forces in a building is its mass. For both buildings the self-weight, or total Dead Load (DL) of structural is determined according to the national codes for “Design Loads,” which mention characteristic densities of materials. The total dead loads obtained in these sections are used later for base shear calculation.

SAP2000 software was used in the case study presented in this paper for the discussion of the results in terms of dead load of the school models and house models in Section 5.1.1 and Section 5.1.2 respectively.

5.1.1 School models

The total Dead Load (DL) which include self-weight and the dead loads applied on the model, is determined according to the national codes for "Design Loads," which mention characteristic densities of materials. The densities for stone masonry, concretes, plaster and woods are expressed in KN/m^3 in Table 1. Table 10 at the end of report shows the data of dead loads for all region of school Pl and WPL models.

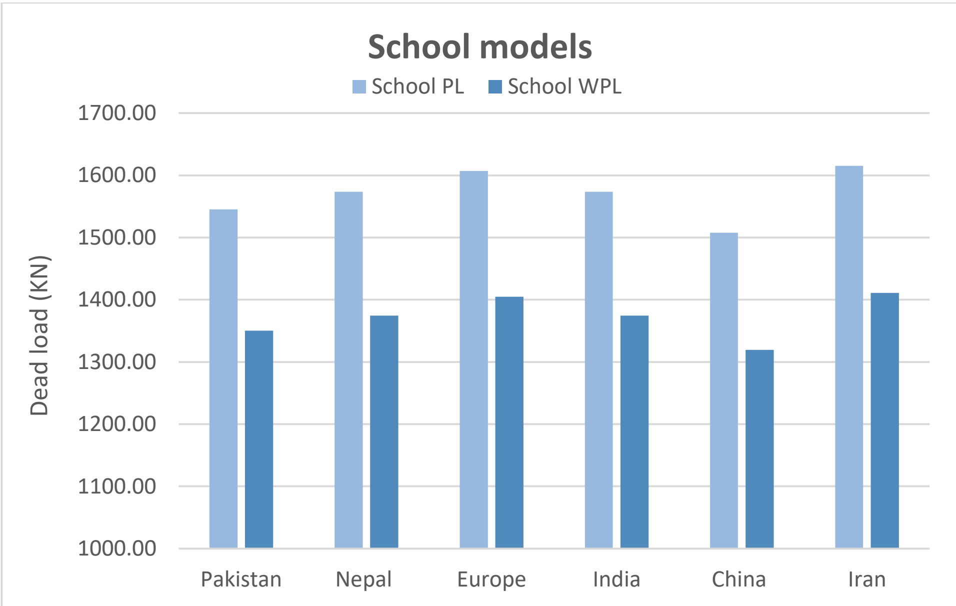

Figure 29 Dead loads for all regions, School PL and School WPL

5.1.2 House models

The total Dead Load (DL) which include self-weight and dead loads applied on the model, is determined according to the national codes for "Design Loads," which mention characteristic densities of materials. The densities for stone masonry, concretes, plaster and woods are expressed in KN/m^3 in Table 1. Table 11 at the end of report shows the data of dead loads for all region of house Pl and WPL models.

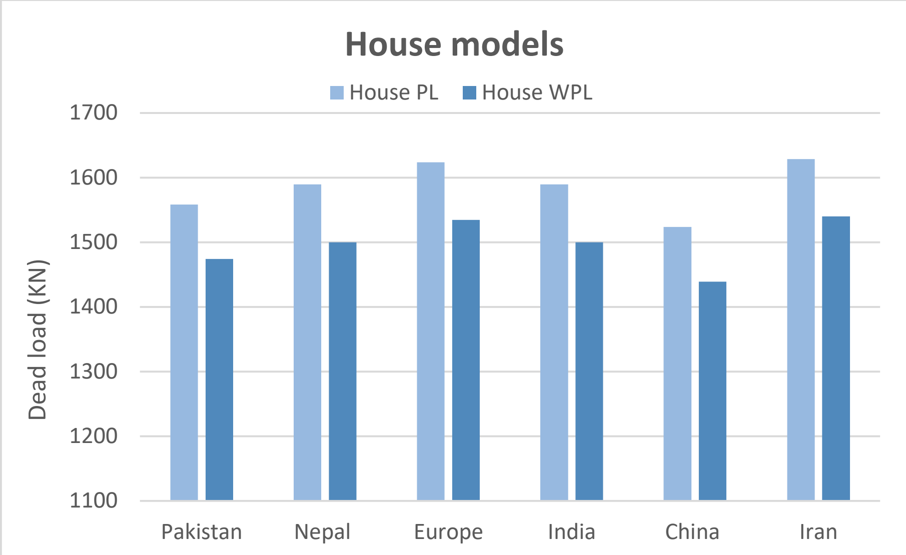

Figure 30 Dead loads for all regions, House PL and House WPL

5.1 Live load results

Live load of 1.9152 KN/m^2 was applied on wooden floor at first floor level in house models for all regions. No live load was applied on any school model.

5.1.1 House models

Due to the reason that a constant value for live load was selected to be applied on all models for all regions, all the live loads results for all models were similar. Table 12 at the end of report shows the data of live loads for all region of house Pl and WPL models.

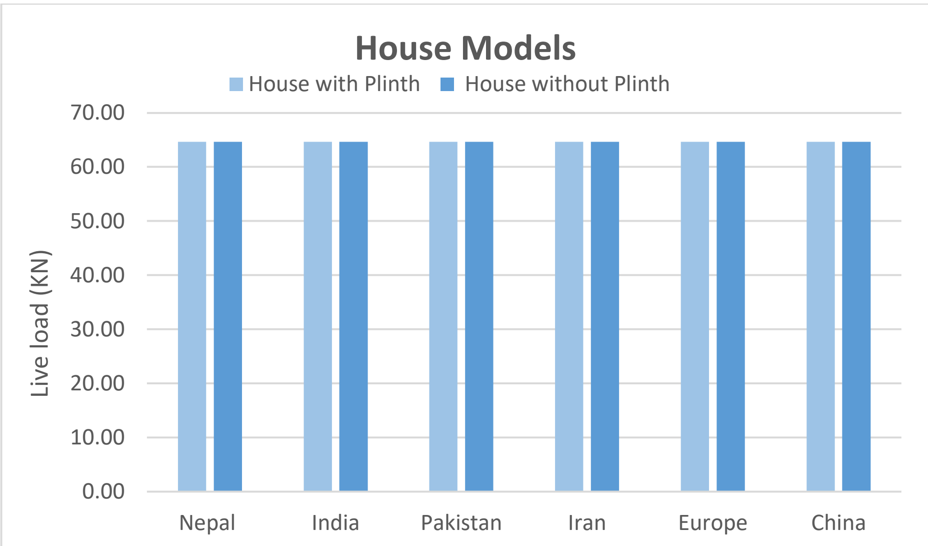

Figure 31 Live loads for all regions, House PL and House WPL

5.2 Static results for seismic load combination

The picture of the building right before the earthquake load hits it or the static weight of the building when it is subjected to earthquake will be the load combination which includes the dead and live load with their respective coefficients according to different building codes as per Section 4.2. The earthquake loads will be excluded from these load combinations and a constant value of 1.9152 KN/m^2 was considered for all models. Following load combinations were considered to get static results for seismic load combination:

NEP-20 – 1.0D + 0.3L

IND-16 – 1.58D

PAK-07 – 1.31D + 0.5L

IRN-15 – 1.2D + 1.0L

EC8 – 1.0D + 0.3L

CN-JGJ – 0.95D + 0.475L

Where,

D = Dead loads

L = Live loads

5.2.1 School models

Both school Pl and school WPL models for all regions were analysed on the basis of the load combinations described in Section 5.2. As there is only the ground floor level in school buildings, the factor of live load will not be effective because of the fact that there is no live load applied on school buildings. The results for both buildings in terms of load in z direction were taken and put together in Figure 32. Table 13 shows the data of static results for seismic load combinations in KN.

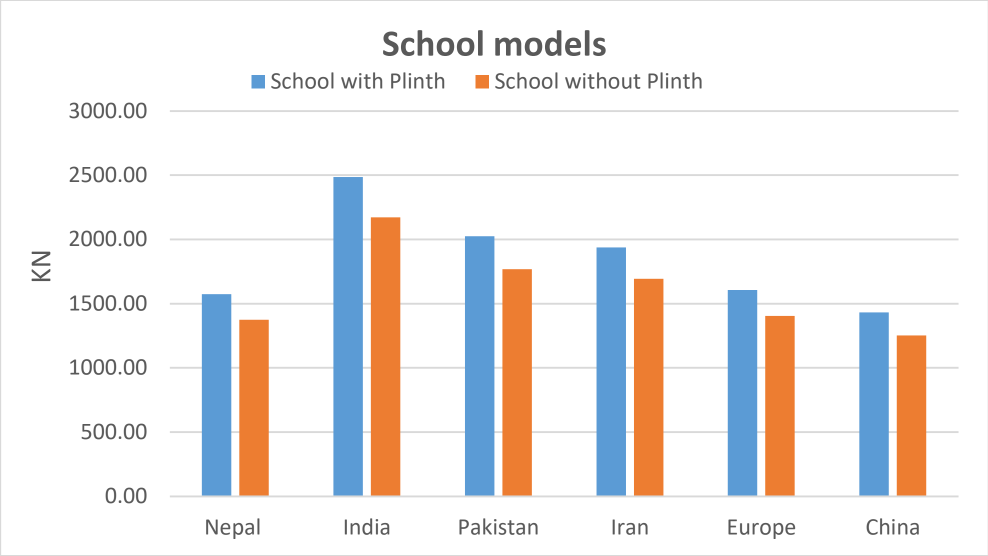

Figure 32 Static load combination results for all regions, School PL & School WPL

Static load combination for India gives us the maximum static load in KN because of its huge multiplier of 1.58 with the dead load. On the other hand, Nepal, Europe and China had the lowest static load results due to the dead load multiplier of around 1.

5.2.2 House models

Both house Pl and house WPL models for all regions were analysed on the basis of the load combinations described in Section 5.2. The results for both buildings in terms of load in z direction were taken and put together in Figure 33. Table 14 shows the data of static results for seismic load combinations in KN.

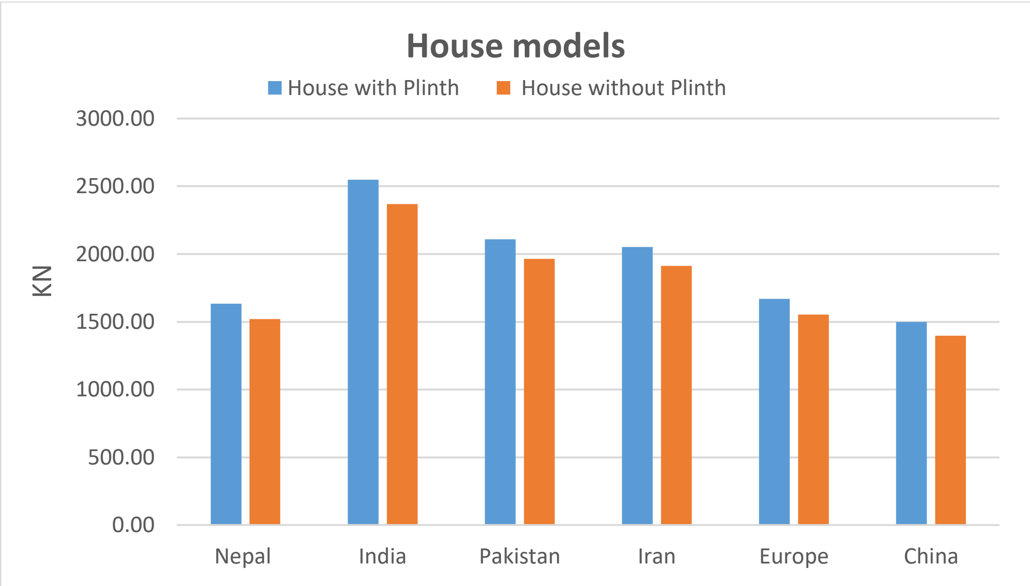

Figure 33 Static load combination results for all regions, House PL & House WPL

Static load combination for India gives us the maximum static load in KN because of its huge multiplier of 1.58 with the dead load. On the other hand, Nepal, Europe and China had the lowest static load results due to the dead load multiplier of around 1. Effect of live load is almost negligible on static load results because of the fact that live load is pretty small as compared to dead load and also because of small coefficient values of live loads in load combinations.

6. Modal analysis

Modal analysis is the study of the dynamic properties of systems in the frequency domain. It helps to determine the vibration characteristics (natural frequencies and mode shapes) of a mechanical structure or component, showing the movement of different parts of the structure under dynamic loading condition. The natural frequencies and mode shapes are important parameters in the design of a structure for dynamic loading conditions. The model assumes the number of degrees of freedom of the structure. It converts the vibration signals of excitation and responses measured on a complex structure that is difficult to perceive, into a set of modal parameters which can be straightforward to foresee. (Uttamchandani, 2006)

6.1 Modal shape and period of vibration

In structural engineering, modal analysis uses the overall mass and stiffness of a structure to find the various periods at which it will naturally resonate. In any kind of structural simulation, a modal analysis will help the engineer to understand the global behavior of the system. By performing a modal analysis first, it is possible to identify the natural frequencies, periods of vibration and modal shapes of the system. It helps to predict the dynamic responses that this system will have.

The spectral acceleration on a structure mainly depends on its fundamental (or natural) period of vibration T (in seconds). Main parameters affecting T are the weight and height of the building, as well as the stiffness of the lateral-resisting elements in relation to their distribution in plan and elevation within the structure.

The first fundamental periods of vibration which corresponds to different percentages of mass ratio activated in school and house structure were taken from the modal analysis of all models and the shapes of those fundamental modes in both axes are described in subsequent chapters.

6.1.1 School PL

To achieve at least 90 percent of mass ratio activated of the model, 100 number of modes were defined in modal analysis of load case data. Table 6 shows the data of fundamental periods along with the percentage of mass ratio activate by that particular mode. Figure 34 shows the first fundamental period of vibration of the first mode corresponding to substantial percentage of mass ratio activated in both x and y axis. Figure 35 shows the modal shapes of mode number 5 for x-axis and mode number 7 considering y axis direction.

School with Plinth				
Region	**First Fundamental period**		**% of mass ratio activated**	
	X-axis (s)	Y-axis (s)	X-axis (%)	Y-axis (%)
Pakistan	0.0707	0.0593	30.29	28.56
Nepal	0.0713	0.0599	30.30	28.56
Europe	0.0721	0.0606	30.26	28.57
India	0.0713	0.0599	30.30	28.56
China	0.0698	0.0587	30.23	28.58
Iran	0.0723	0.0607	30.29	28.56

Table 6 Period of vibrations, % of mass ratio activated for all regions, x and y axis, school PL

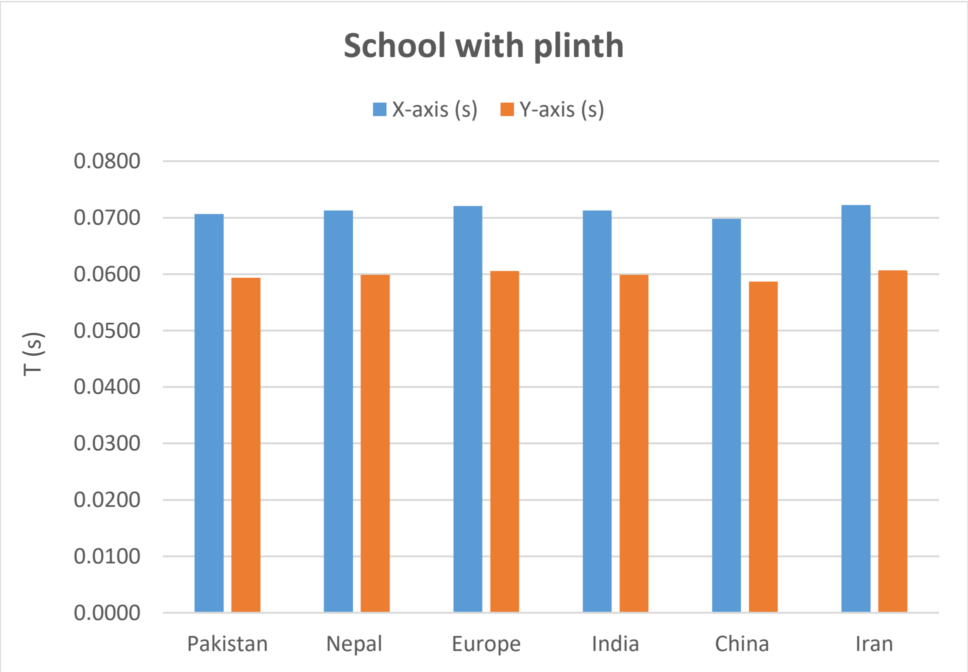

Figure 34 Period of vibration for all regions, x and y axis school PL

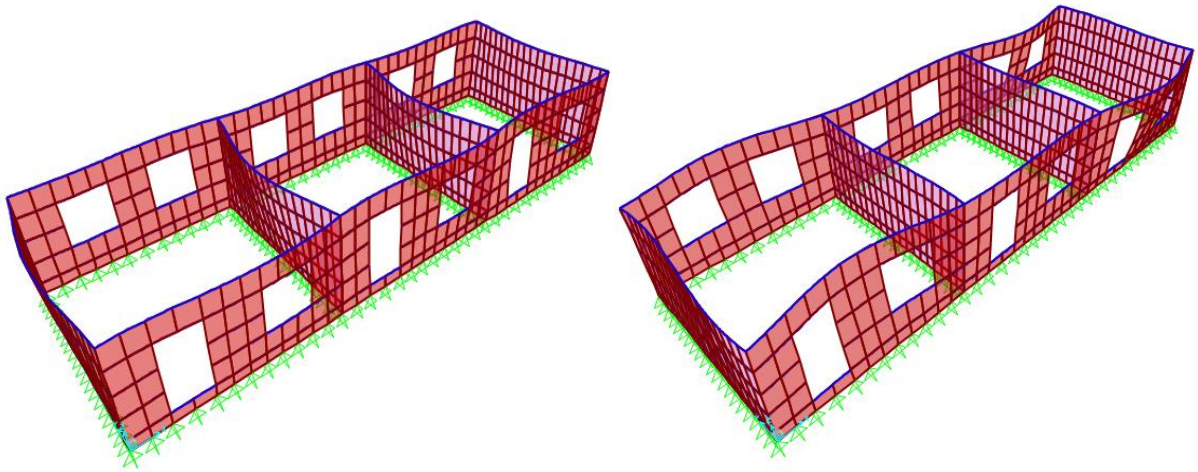

Figure 35 Shape of mode 5, x axis (left), shape of mode 7, y axis (right), school PL

6.1.2 School WPL

To achieve at least 90 percent of mass ratio activated of the model, 100 number of modes were defined in modal analysis of load case data. Table 7 shows the data of fundamental periods along with the percentage of mass ratio activate by that particular mode. Figure 36 shows the first fundamental period of vibration of the first mode corresponding to substantial percentage of mass ratio activated in both x and y axis. Figure 37 shows the modal shapes of mode number 5 for x-axis and mode number 7 considering y axis direction.

School without Plinth				
Region	First Fundamental period		% of mass ratio activated	
	X-axis (s)	Y-axis (s)	X-axis (%)	Y-axis (%)
Pakistan	0.0673	0.0578	32.81	29.36
Nepal	0.0679	0.0583	32.81	29.34
Europe	0.0687	0.0590	32.79	29.38
India	0.0679	0.0583	32.81	29.34
China	0.0688	0.0591	32.81	29.35
Iran	0.0688	0.0591	32.81	29.35

Table 7 Period of vibrations, % of mass ratio activated for all regions, x and y axis, school WPL

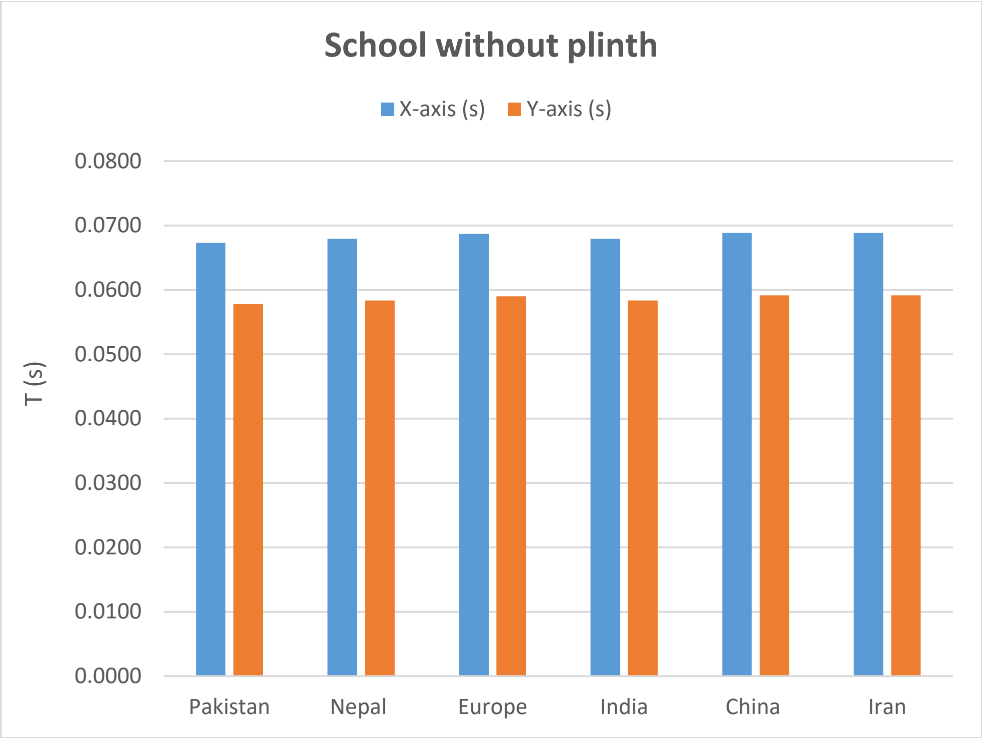

Figure 36 Period of vibration for all regions, x and y axis, school WPL

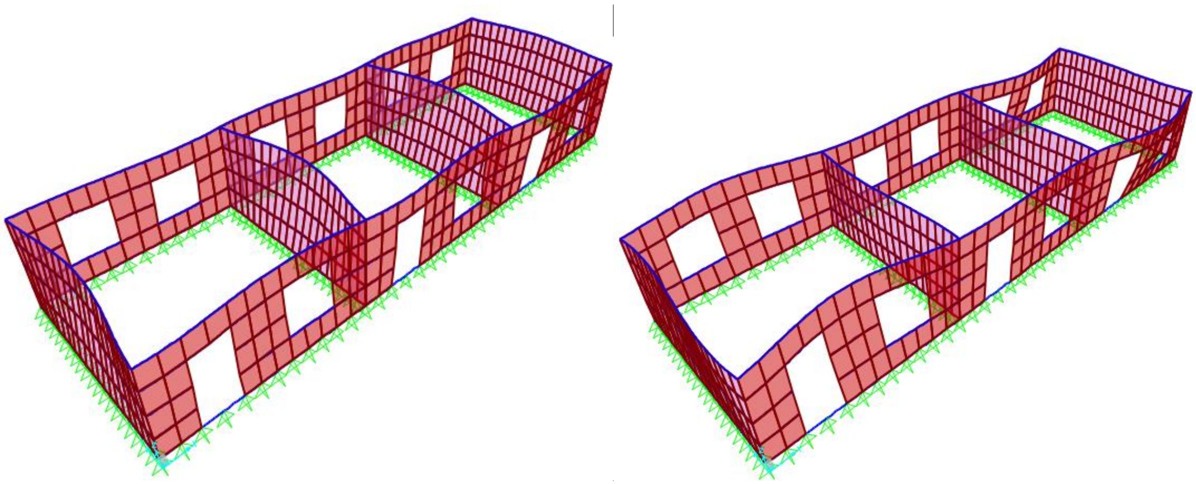

Figure 37 Shape of mode 5, x axis (left), shape of mode 7, y axis (right), school WPL

6.1.3 House PL

To achieve at least 90 percent of mass ratio activated of the model, 75 number of modes were defined in modal analysis of load case data. Table 8 shows the data of fundamental periods along with the percentage of mass ratio activate by that particular mode. Figure 38 shows the first fundamental period of vibration of the first mode corresponding to substantial percentage of mass ratio activated in both x and y axis. Figure 39 shows the modal shapes of mode number 1 for x-axis and mode number 2 considering y axis direction.

House with Plinth				
Region	**First Fundamental period**		**% of mass ratio activated**	
	X-axis (s)	Y-axis (s)	X-axis (%)	Y-axis (%)
Pakistan	0.0559	0.0545	58.20	56.95
Nepal	0.0563	0.0550	58.20	56.94
Europe	0.0570	0.0557	58.20	56.96
India	0.0563	0.0550	58.20	56.94
China	0.0552	0.0538	58.19	56.97
Iran	0.0571	0.0558	58.20	56.94

Table 8 Period of vibrations, % of mass ratio activated for all regions, x and y axis, house PL

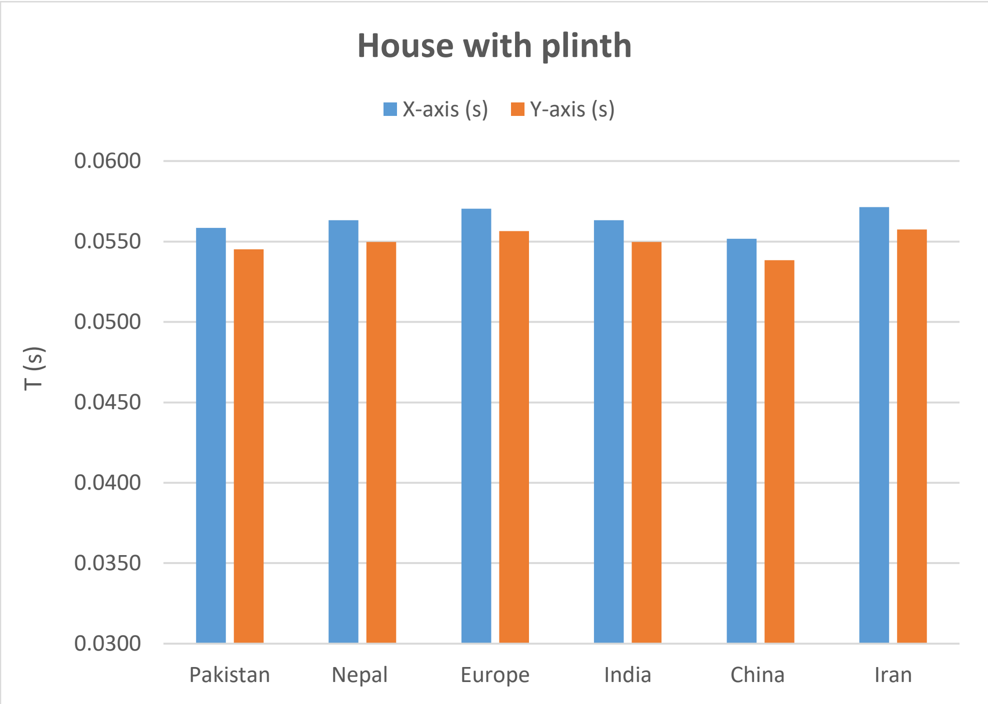

Figure 38 Period of vibration for all regions, x and y axis, house PL

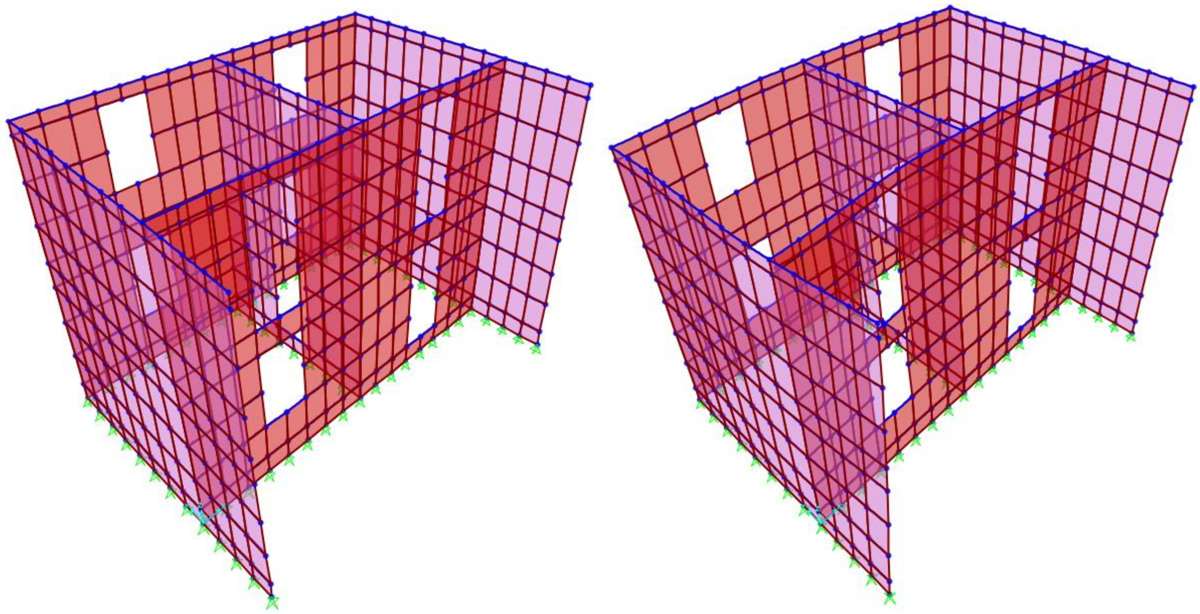

Figure 39 Shape of mode 1, x axis (left), shape of mode 2, y axis (right), house PL

6.1.4 House WPL

To achieve at least 90 percent of mass ratio activated of the model, 75 number of modes were defined in modal analysis of load case data. Table 9 shows the data of fundamental periods along with the percentage of mass ratio activate by that particular mode. Figure 40 shows the first fundamental period of vibration of the first mode corresponding to substantial percentage of mass ratio activated in both x and y axis. Figure 41 shows the modal shapes of mode number 1 for x-axis and mode number 2 considering y axis direction.

House without Plinth				
Region	**First Fundamental period**		**% of mass ratio activated**	
	X-axis (s)	Y-axis (s)	X-axis (%)	Y-axis (%)
Pakistan	0.0532	0.0507	61.95	59.88
Nepal	0.0536	0.0512	61.96	59.86
Europe	0.0543	0.0518	61.95	59.89
India	0.0536	0.0512	61.96	59.86
China	0.0526	0.0501	61.95	59.91
Iran	0.0544	0.0519	61.95	59.87

Table 9 Period of vibrations, % of mass ratio activated for all regions, x and y axis, house WPL

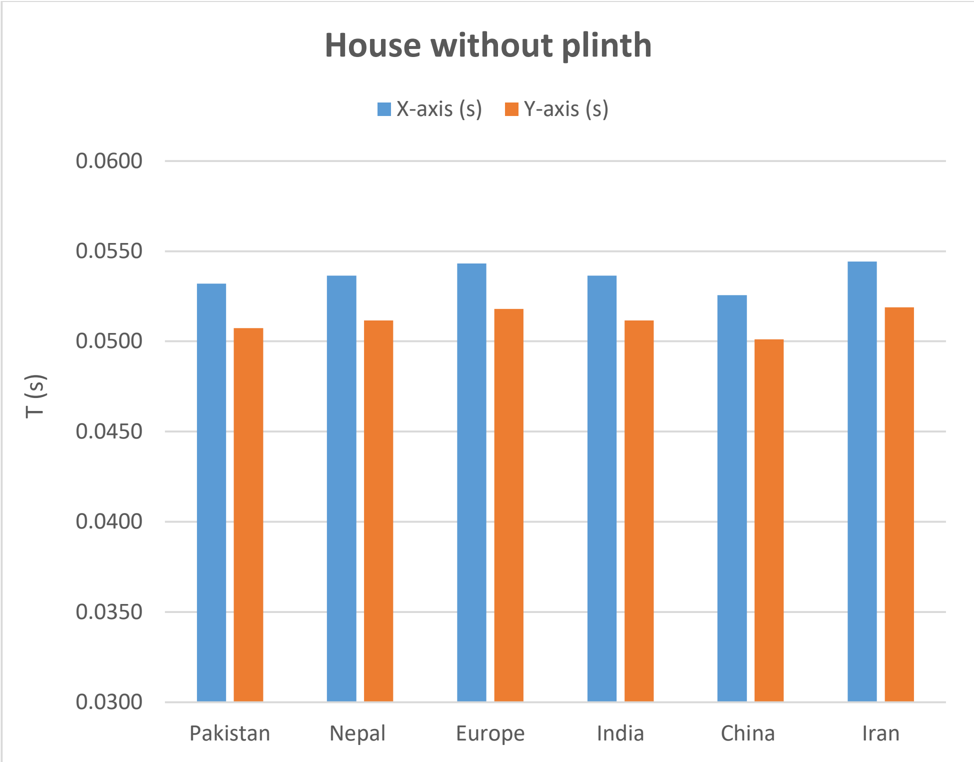

Figure 40 Period of vibration for all regions, x and y axis, house WPL

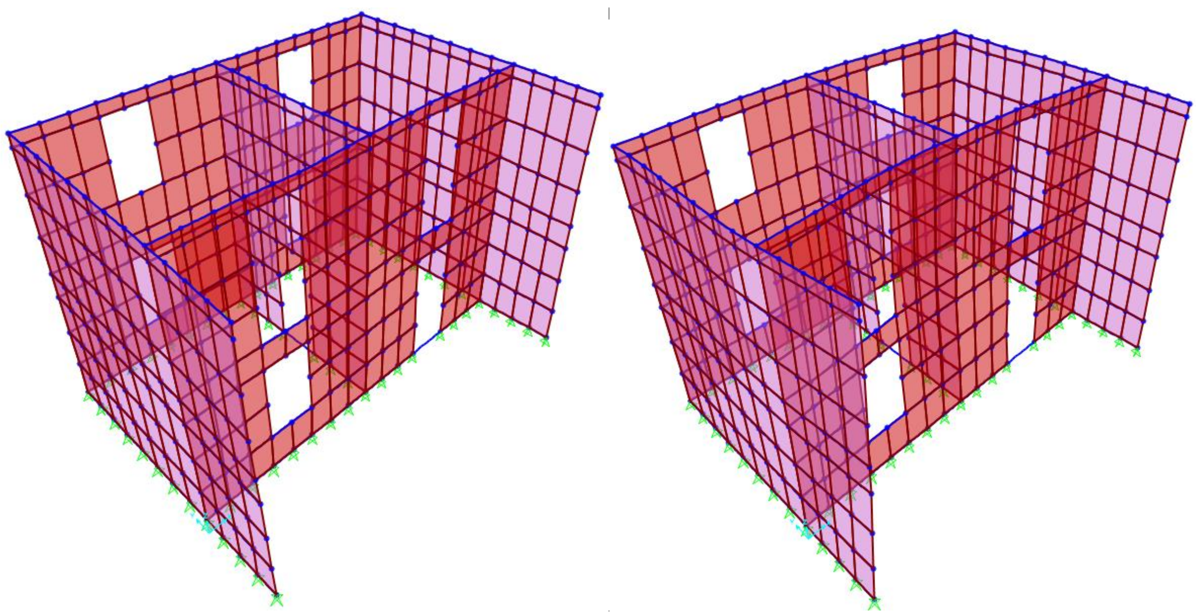

Figure 41 Shape of mode 1, x axis (left), shape of mode 2, y axis (right), house WPL

7. Response spectrum analysis

Response-spectrum analysis (RSA) is a linear-dynamic statistical analysis method which measures the contribution from each natural mode of vibration to indicate the likely maximum seismic response of an essentially elastic structure. Response-spectrum analysis provides insight into dynamic behaviour by measuring pseudo-spectral acceleration, velocity, or displacement as a function of structural period for a given time history and level of damping. It is practical to envelope response spectra such that a smooth curve represents the peak response for each realization of structural period. (Ondrej & Napier, 2014)

Response spectrum analysis (RSA) is a method widely used for the design of buildings. Conceptually the method is a simplification of modal analysis, i.e., response history (or time history) analysis (RHA) using modal decomposition, that benefits from the properties of the response spectrum concept. The purpose of the method is to provide quick estimates of the peak response without the need to carry out response history analysis. This is very important because response spectrum analysis (RSA) is based on a series of quick and simple calculations, while time history analysis requires the solution of the differential equation of motion over time. Despite its approximate nature, the method is very useful since it allows the use of response spectrum, a very convenient way to describe seismic hazard. (Fragiadakis, 2013)

The Finite Element Method (FEM) is a numerical technique to find approximate solutions of partial differential equations. Finite element analysis (FEA) is a computerized method for predicting how a product reacts to real-world forces, vibration, heat, fluid flow, and other physical effects. Finite element analysis shows whether a product will break, wear out, or work the way it was designed. It is called analysis, but in the product development process, it is used to predict what is going to happen when the product is used.

FEA works by breaking down a real object into a large number (thousands to hundreds of thousands) of finite elements, such as little cubes. Mathematical equations help predict the behavior of each element. A computer then adds up all the individual behaviors to predict the behavior of the actual object.

In a structural simulation, FEM helps in producing stiffness and strength visualizations. It also helps to minimize material weight and its cost of the structures. FEM allows for detailed visualization and indicates the distribution of stresses and strains inside the body of a structure. FEM allows for easier modelling of complex geometrical and irregular shapes. Because the designer is able to model both the interior and exterior, he or she can determine how critical factors might affect the entire structure and why failures might occur. While modelling a complex physical deformity by hand can be impractical, a computer using FEM can solve the problem with a high degree of accuracy. FEM is highly useful for certain time-dependent simulations, such as impact of earthquake on structures, in which deformations in one area depend on deformation in another area.

One of the modern tools available in structural analysis field is SAP2000 software, a program that implements Response spectrum analysis based on Finite element method. The software was used in the case study presented in this paper with further discussion of the obtained results.

7.1 Response spectrums for different regions

As described earlier both structures were evaluated for seismic safety according to six different response spectrums for six different regions as a part of case study.

7.1.1 Nepal response spectra according to NBC 150: 2020

According to Nepal National Building Code (NBC 150: 2020), the elastic site spectra for horizontal loading are given as,

$$C(T) = C_h(T) \cdot Z \cdot I$$

Where,

$C_h(T)$ – Spectral shape factor

Z – Seismic zoning factor

I – Importance factor

The spectral shape factor $C_h(T)$ is a parameter calculated on the existing soil type which is calculated as,

$$C_h(T) \begin{cases} 1 + (\alpha - 1)\dfrac{T}{T_a}; if\ T < T_a \\ \alpha; if\ T_a < T < T_C \\ \alpha\left[K + (1-K)\left(\dfrac{T_C}{T}\right)^2\right]\left(\dfrac{T_C}{T}\right)^2; if\ T_C < T < 6 \end{cases}$$

Where,

α – Peak spectral acceleration normalized by PGA

T_a and T_C – Lower and upper bounds of the flat part of the spectrum

K – Coefficient affecting the descent of the spectrum

Parameters required for calculating spectral shape factor can be found in table ---.

Soil type considered in the case study is of type A – stiff or hard soil.

With respect to the local seismic hazard, Nepal is divided into a number of different seismic zones, based on the assumption that the seismic hazard within each zone remains constant. The seismic zoning factor (Z) represents the peak ground acceleration (PGA) for a 475-year return period. For the case study,

$$Z = PGA = 0.2g$$

Design response spectra was applied eventually upon the structures. To get design response spectra, ductility factor (Rμ) and over strength factor (Ωμ) were used. Table 15 shows the values of these parameters. Having defined the required parameters, eventual elastic response spectra were calculated for school and house buildings and are demonstrated in Figure 42.

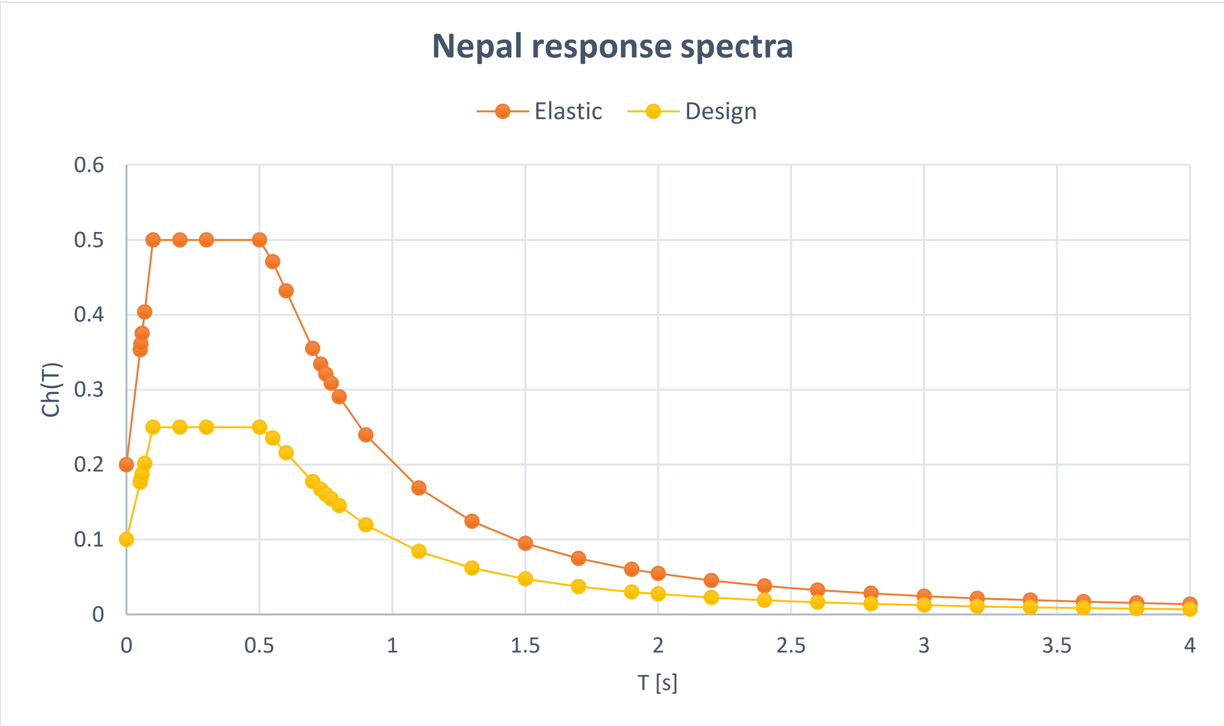

Figure 42 Acceleration response spectra for Nepal

7.1.2 India response spectra according to IS1893 (part 1): 2016

The design horizontal seismic coefficient A_h for a structure should be determined by:

$$A_h = \frac{\left(\frac{Z}{2}\right)\times\left(\frac{Sa}{g}\right)}{\left(\frac{R}{I}\right)}$$

Where,

Z – Seismic zone factor

I – Importance factor

R – Response reduction factor

$\frac{Sa}{g}$ – Design acceleration coefficient for different soil types, normalized with peak ground acceleration, corresponding to natural period of structure T.

$$\frac{Sa}{g} \text{ (for Rocky or hard soil sites) } \begin{cases} 1 + 15T \,; T < 0.10s \\ 2.5 \,; 0.10s < T < 0.40s \\ \frac{1}{T} \,; 0.40s < T < 4s \\ 0.25 \,; T > 4s \end{cases}$$

Soil type was selected as type I as rocky or hard soil sites.

The region of India is divided in four seismic zone. Zone IV was the part of our case study. Table 16 shows the value of seismic zone factor that should be taken considering zone IV, but considering the fact that while calculating design horizontal coefficient, $\left(\frac{Z}{2}\right)$ factor converts elastic horizontal coefficient to design horizontal coefficient. Therefore, seismic zone factor was taken as Z=0.4.

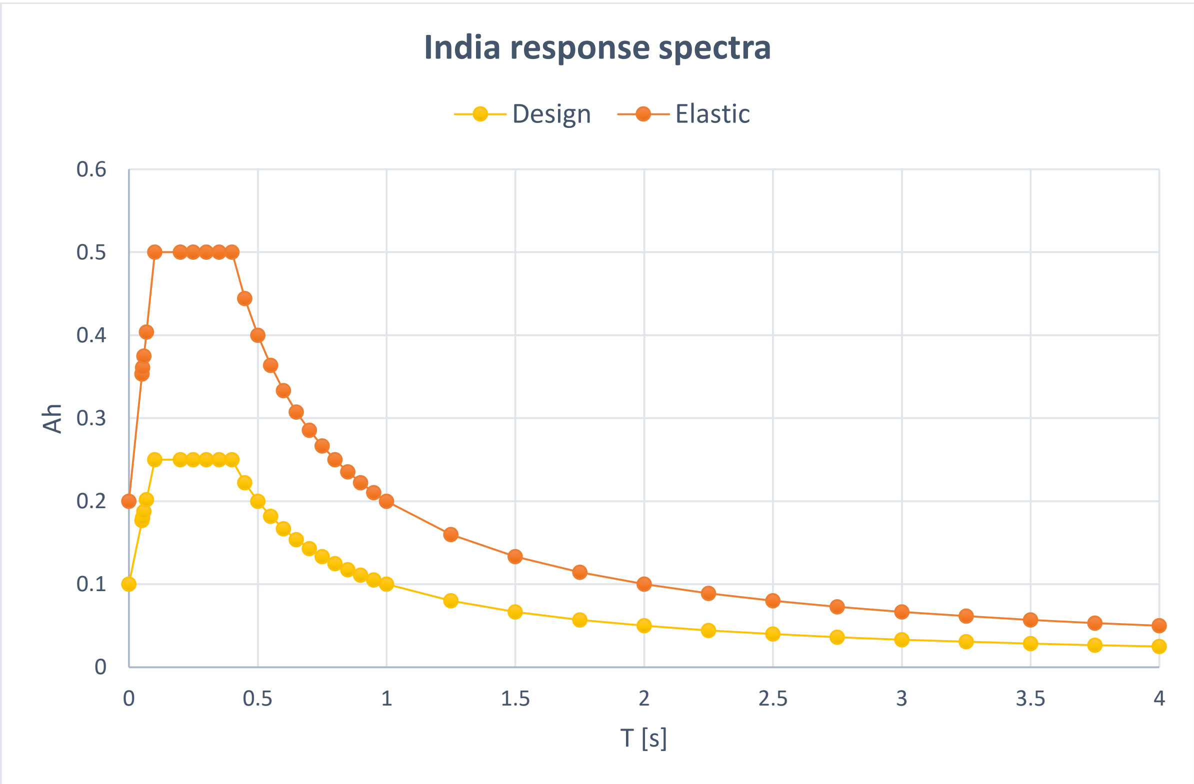

Figure 43 Acceleration response spectra as per IS1893

7.1.3 Pakistan response spectra according to SP-07

Keeping the ground acceleration Z = 0.2g (zone 2B) value constant while detailing all these response spectrums for different regions; An elastic design response spectrum constructed according to Figure 44, using the values of Ca and Cv consistent with the specific site. Rock type of soil categorized as S_B as was selected. The values of Ca = 0.2 and Cv = 0.2 shows in Table 17.

$$Spectral\ accelaration \begin{cases} Ca\,; T = 0 \\ 2.5Ca\,; To < T < Ts \\ \dfrac{Cv}{T}\,; T > Ts \end{cases}$$

While, $T_S = \dfrac{Cv}{2.5Ca}$; $T_O = 0.2Ts$

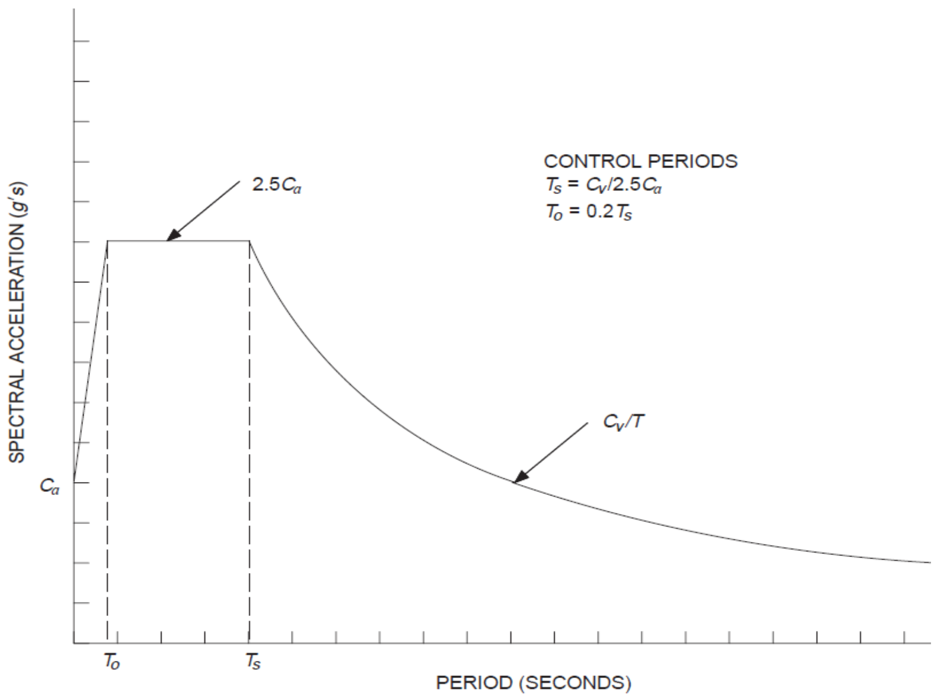

Figure 44 Response spectra

Over strength factor R was taken as 4.5 for bearing masonry wall system.

Design response spectrum was achieved by reducing the elastic response spectrum by the factor of R.

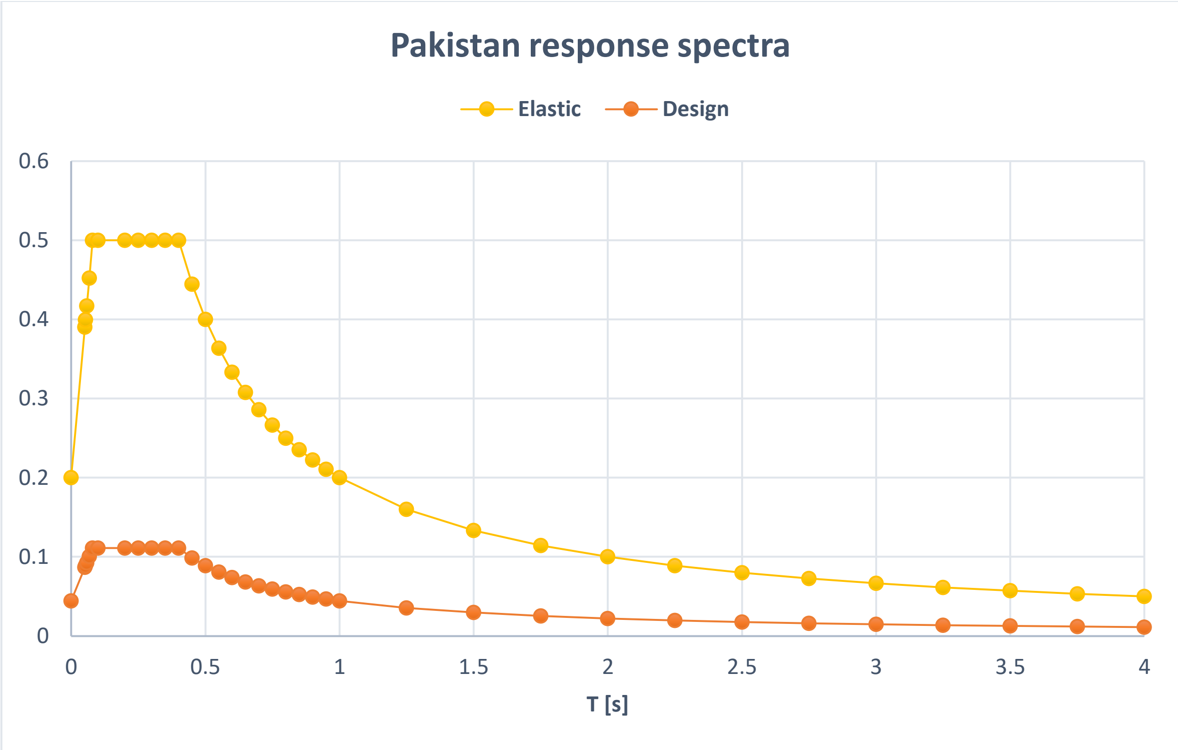

Figure 45 Acceleration response spectra as per SP-07

7.1.4 Iran response spectra according to Standard 2800 (2015)

Iran is divided into four different seismic zones according to their level of seismicity. Design base acceleration was selected as A = 0.2g shown in Table 18. The building response factor B represents the building response to the ground motion. This factor shall be determined from the following formulae

$$B \begin{cases} 1 + S\left(\dfrac{T}{T_0}\right); 0 \leq T \leq T_0 \\ S + 1\,; T_0 \leq T \leq T_s \\ (S+1)\left(\dfrac{T_s}{T}\right)^{\frac{2}{3}}\,; T > T_s \end{cases}$$

While,

T = Fundamental period of vibration of the structure

T_O, T_S and S are parameters determined from the soil profile type and level of seismicity. Selecting soil profile type I classified as stiff soils or igneous rocks type, Table 18 shows the input values selected for T_O, T_S and S parameters.

To achieve the design response spectra, building behavior factor R was selected to be 2 for bearing masonry wall system.

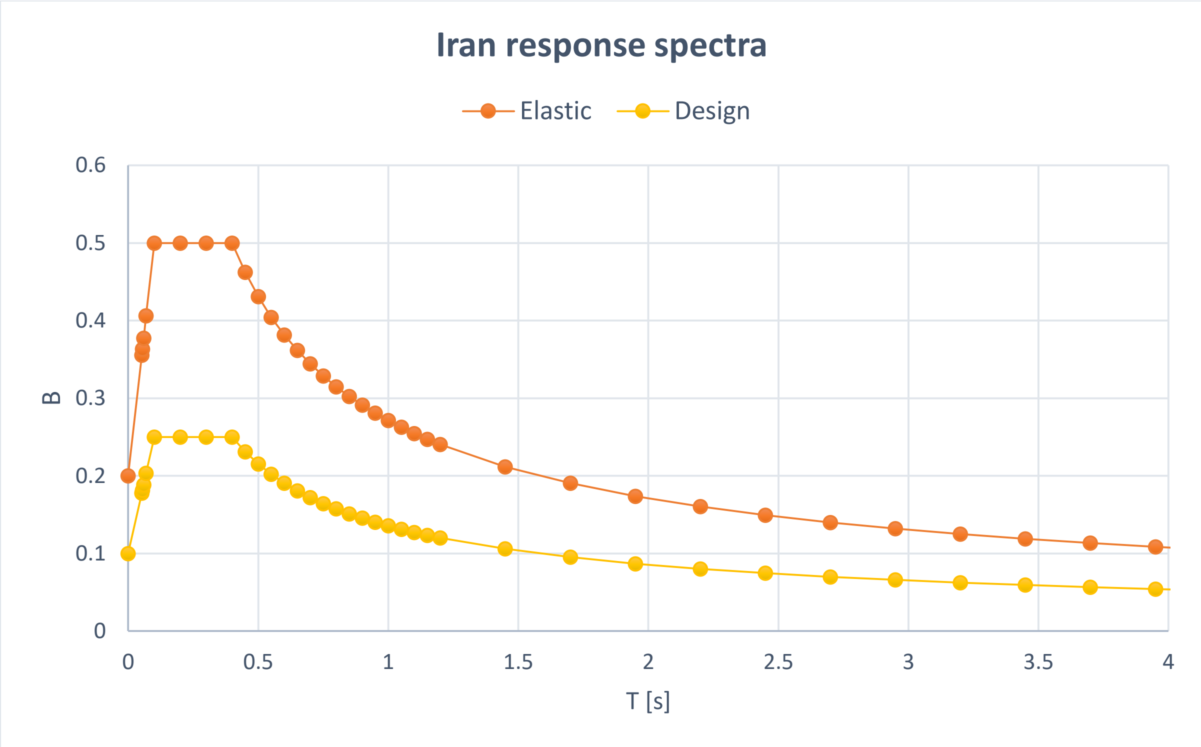

Figure 46 Acceleration response spectra as per standard 2800 (2015)

7.1.5 China response spectra according to GB0011-2010

Seismic intensity of 8 was selected which corresponds to 0.2g of design basic acceleration of ground motion.

Selected soil category of I_o corresponds to stiff hard and complete rocks.

The characteristic period value T_g is taken from Table 19 as 0.3s.

Seismic influence coefficient of a building structure shall be determined according to Intensity, site-category, natural period and damping ratio of the structure. The maximum seismic influence coefficient α_{max} of the precautionary earthquake for the seismic intensity of 8 (0.2g) was defined as 0.45 as per the code.

The seismic influence coefficient was defined by following formulas/diagram:

$$\alpha \begin{cases} 0.45\alpha_{max}\,;\ T = 0 \\ \eta_2\alpha_{max}\,;\ 0.1 \le T \le T_g \\ (\frac{Tg}{T})^{\gamma}\ \eta_2\alpha_{max}\,; T\ g \le T \le 5T_g \\ \left[\eta_2 0.2^{\gamma} - \eta(\mathrm{T} - 5T_g)\right]\alpha_{max}\,;\ T \ge 5T_g \end{cases}$$

Where,

α = Seismic influence coefficient

α_{max} = The maximum value of seismic influence coefficient = 0.45

η_1 = Adjusting coefficient of declined slope at straight-line declining section;

$\eta 1 = 0.02+\frac{0.05-\xi}{4+32\xi}$

η_2 = Damping adjusting coefficient; $\eta 2 = 1+\frac{0.05-\xi}{0.06+1.6\xi}$

γ = Attenuation index number; $\gamma = 0.9+ \frac{0.05-\xi}{0.5+\xi}$

ξ = Damping ratio = 5%

T_g = Characteristic period = 0.3s

T = Natural period of vibration for structure

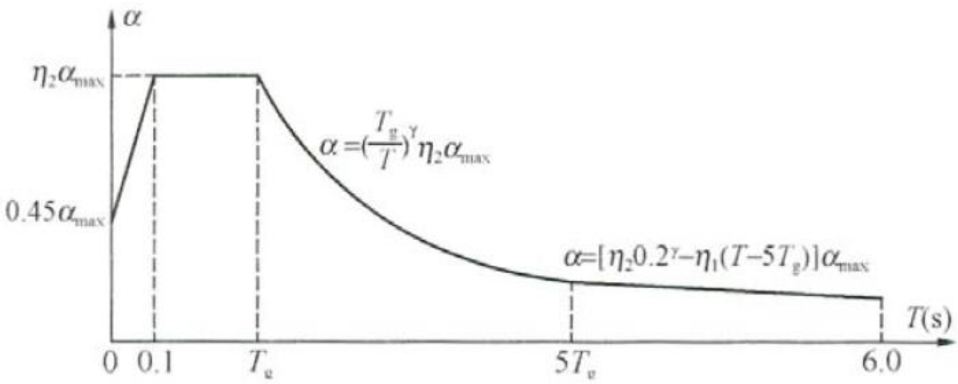

Figure 47 Seismic Influence Coefficient Curve

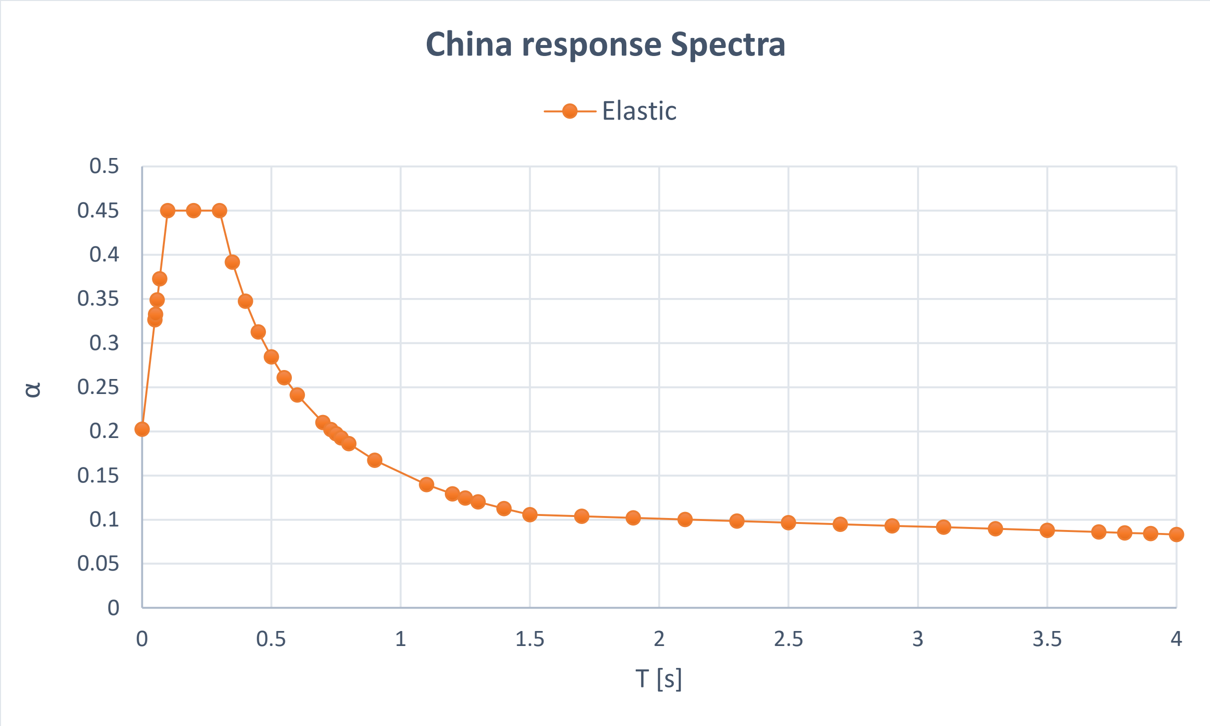

Figure 48 Acceleration response spectra as per GB0011-2010

7.1.6 Europe response spectra according to EC8

If the earthquakes that contribute most to the seismic hazard defined for the site for the purpose of probabilistic hazard assessment have a surface-wave magnitude, M_s, greater than 5.5, it is recommended that the Type 1 spectrum is adopted. For the horizontal components of the seismic action, the Type 1 elastic response spectrum Se(T) is defined by the following expressions:

$$Se(T)\begin{cases} a_g \times S \times \left[1 + \dfrac{T}{T_b} \times (\eta \times 2.5 - 1)\right]; 0 \leq T \leq T_b \\ a_g \times S \times \eta \times 2.5\,; T_b \leq T \leq T_c \\ a_g \times S \times \eta \times 2.5 \left(\dfrac{T_c}{T}\right); T_c \leq T \leq T_d \\ a_g \times S \times \eta \times 2.5 \left(\dfrac{T_c \times T_d}{T^2}\right)\,; T_d \leq T \leq 4s \end{cases}$$

Where,

Se(T) = elastic response spectrum;

T = vibration period of system;

a_g = design ground acceleration

T_b = lower limit of the period of the constant spectral acceleration branch;

T_c = upper limit of the period of the constant spectral acceleration branch;

T_d = value defining the beginning of the constant displacement response range of the spectrum;

S = soil factor;

η = damping correction factor with a reference value of η = 1 for 5% viscous damping

For ground acceleration a_g = 0.2 and soil type selected as A, the values of T_b, T_c, T_d and S are taken from Table 20.

To avoid explicit inelastic structural analysis in design, the capacity of the structure to dissipate energy, through mainly ductile behaviour of its elements and/or other mechanisms, is taken into account by performing an elastic analysis based on a response spectrum reduced with respect to the elastic one, henceforth called a "design spectrum". This reduction is accomplished by introducing the behaviour factor q. To achieve the design response spectra, behaviour factor q is taken as 2 and following expressions will be used to define it

$$Sd(T)\begin{cases} a_g \times S \times \left[\frac{2}{3} + \frac{T}{T_b} \times \left(\frac{2.5}{q} - \frac{2}{3}\right)\right]; 0 \leq T \leq T_b \\ a_g \times S \times \frac{2.5}{q} \; ; T_b \leq T \leq T_c \\ a_g \times S \times \frac{2.5}{q}\left(\frac{T_c}{T}\right); T_c \leq T \leq T_d \\ a_g \times S \times \frac{2.5}{q}\left(\frac{T_c \times T_d}{T^2}\right) \; ; T_d \leq T \end{cases}$$

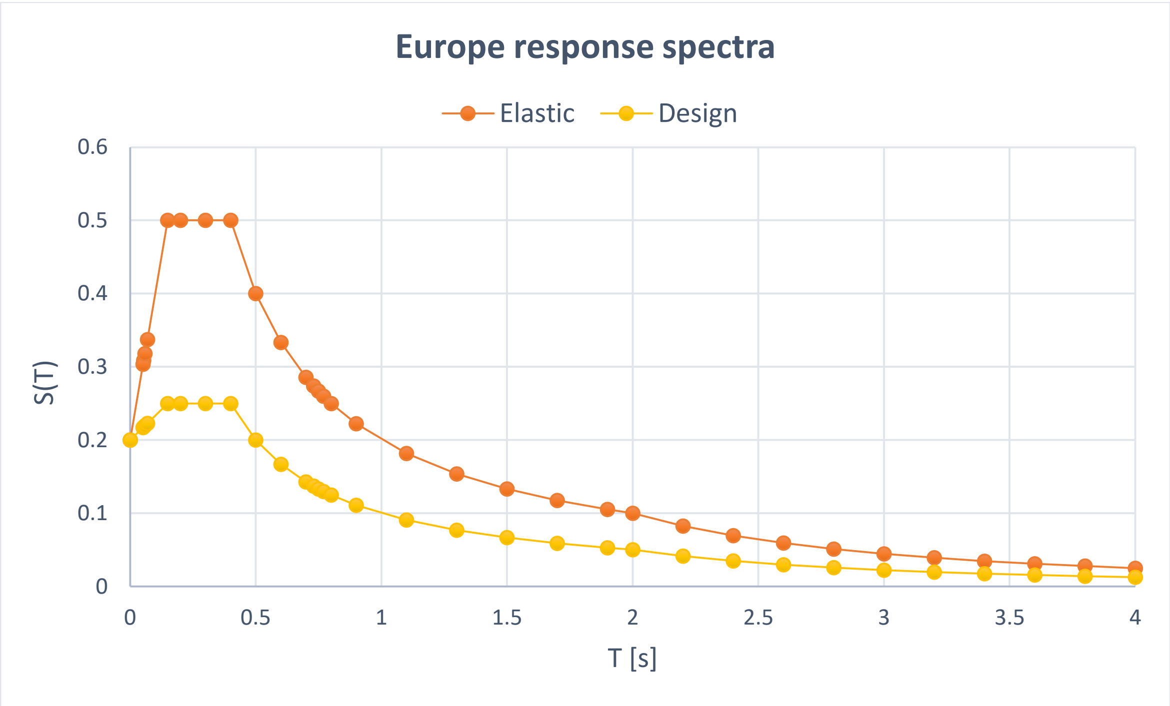

Figure 49 Acceleration response spectra as per EC8

The comparison of elastic response spectra and design response spectra of all regions is shown by Figure 50 and Figure 51 respectively. Keeping in mind that the design spectra were used as input response spectra in SAP2000 software for analysis purposes. The first two segments are of interest for the case study building. The short period response starting from peak ground acceleration point which was kept constant as $a_{g} = 0.2$ and the linearly increasing spectral acceleration, is followed by the constant spectral acceleration plateau. 5% of viscous damping was selected for all regions.

The corner points of plateau are usually fixed and are given by the codes. The starting point of plateau ranges between 0.08s (SP-07) and 0.15s (EC8) whereas the second control point ranges between 0.2s (CN-GB) and 0.5 (NEP-20). This low value for China results in a response spectrum with a very short plateau.

Spectral amplification being the ratio between the spectral acceleration at plateau and the spectral acceleration at starting point (PGA) is 2.5 for all regions except China which stands at 2.22.

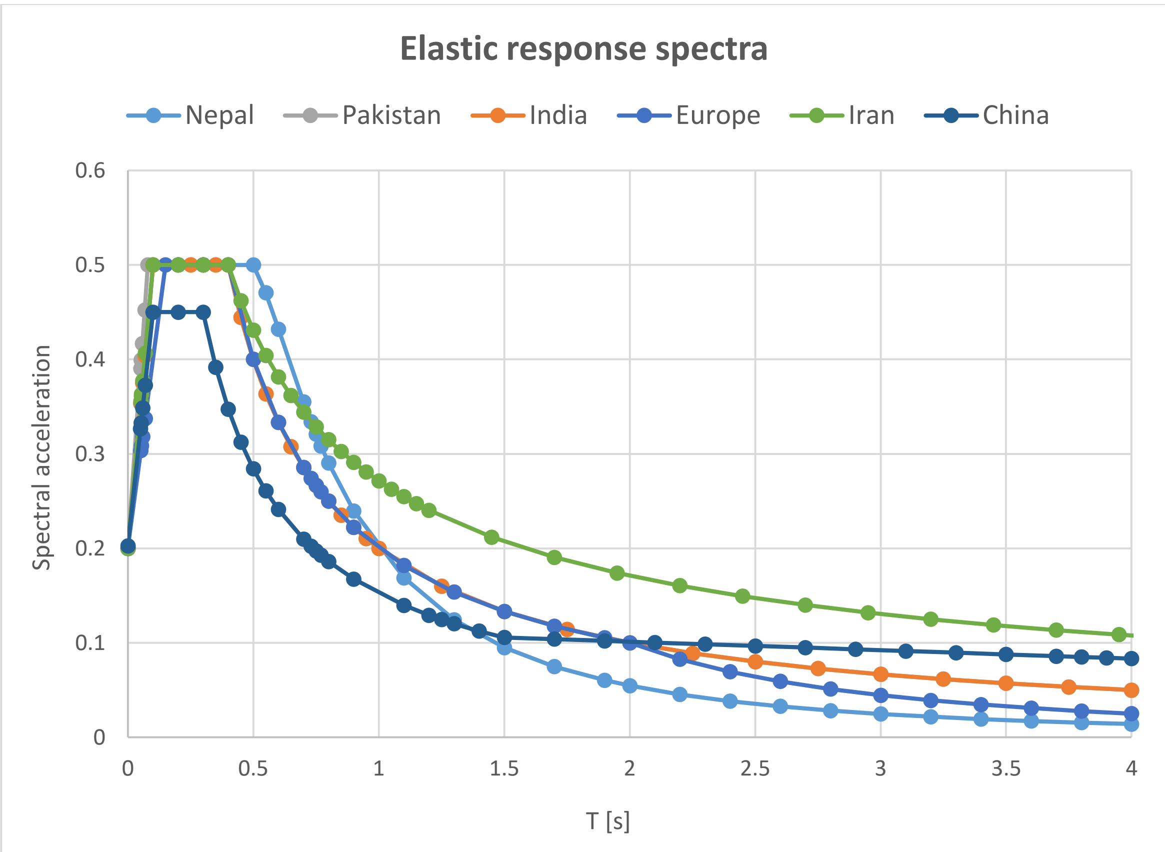

Figure 50 Comparison of elastic response spectra

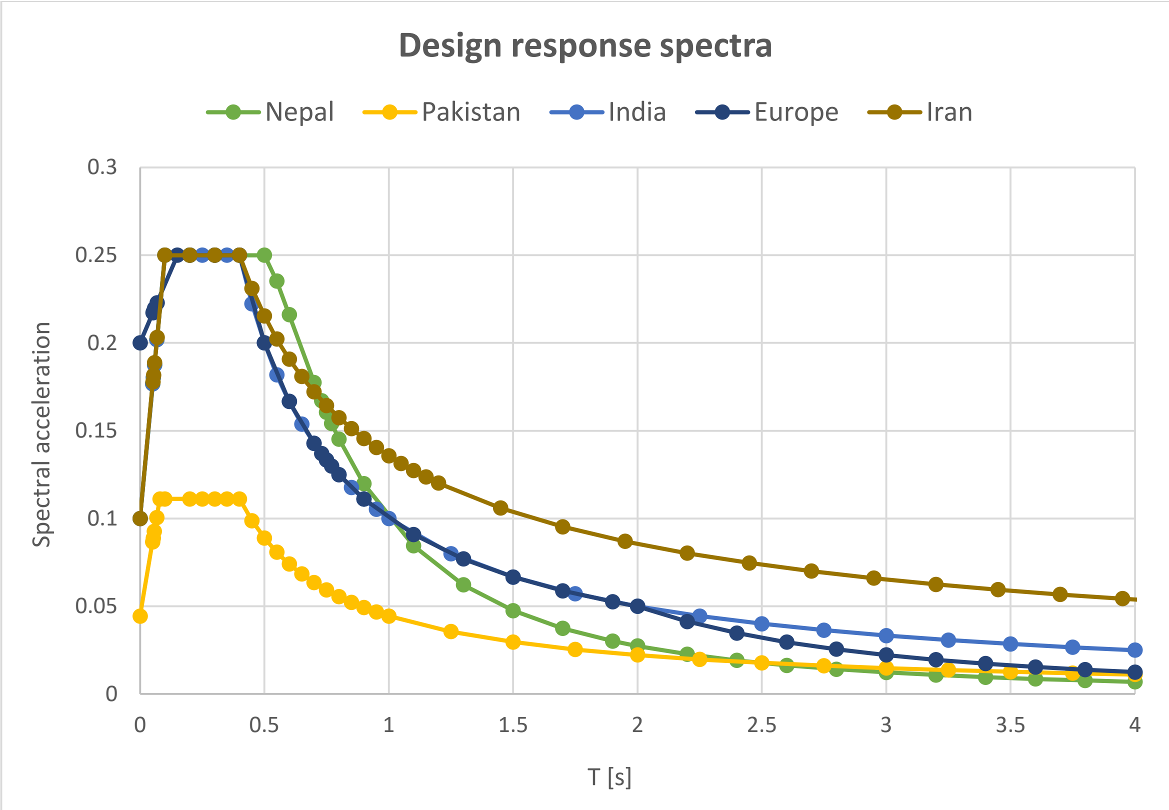

Figure 51 Comparison of design response spectra

7.2 Analysis and results

With the required response spectrum curve inserted in SAP2000, corresponding results in terms of base shear and internal forces at specific cross section are evaluated. It must be mentioned that for both buildings, different material properties and different spectrums were applied according to specified regions. The obtained results provide an important observation on the effect of the design seismic action on the structures, which is further compared to the results achieved by Smart Shelter Foundation during theoretical computations of base shear in later sections.

7.2.1 Base shear

An estimate of the maximum expected lateral force that will occur due to seismic ground motion at the base of a structure is termed as base shear. The results of the executed analyses are represented by graphs for both types of buildings in both X and Y axis direction. These buildings are then subdivided into building with plinth level (PL) and building without plinth level (WPL). By extracting the design PGA and assuming that the seismic weight is constant, the implications for the base shear according to each national code can be easily compared for any given seismic hazard.

7.2.1.1 School PL

School PL building have undergone the six different design seismic action according to each national code to make six various configurations, and their response in terms of base shear force both in X and Y axis direction are demonstrated in Figure 52 and the values are reported in Table 21.

It can be observed that the base shear of Iran (IRN-15), India (IND-16) and Nepal (NEP-20) are almost the same due to the similar short period response segment of their design response spectrums. However, Pakistan is two times more tolerant compared to its neighboring countries, mainly caused by the high value of the behavior factor R = 4.5. China, on the other hand is nearly two times more conservative due to the fact that elastic response spectra was used to compute its base shear.

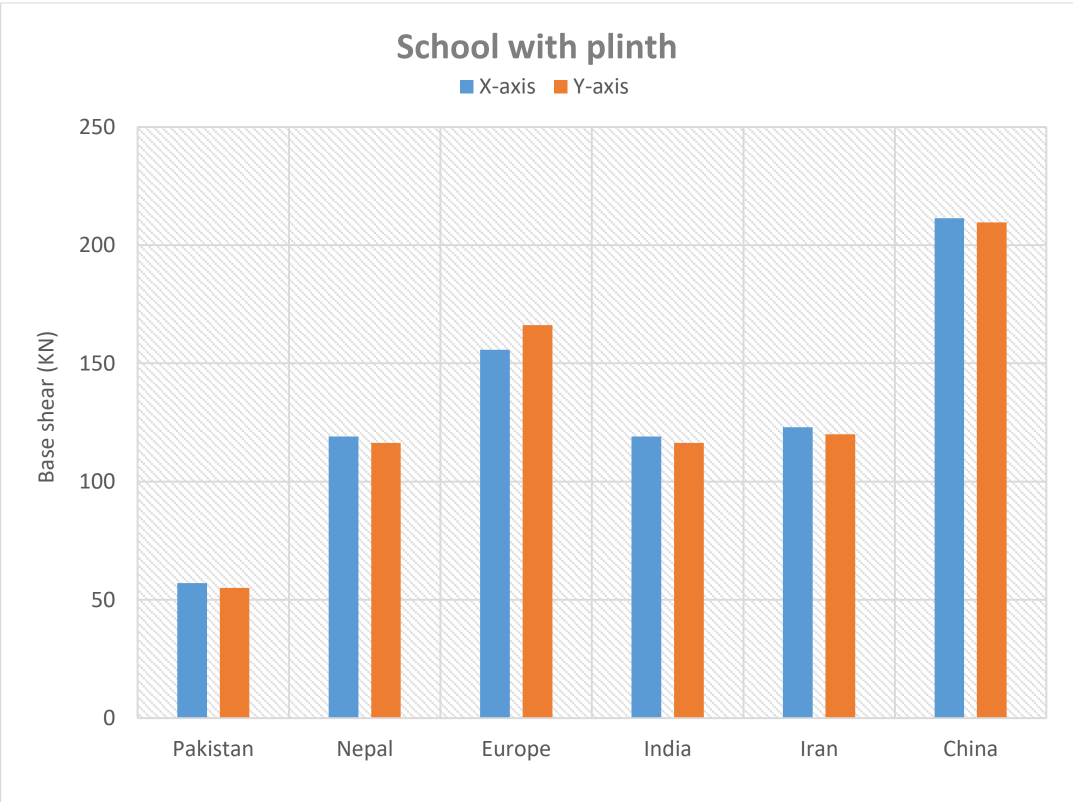

Figure 52 Seismic demand for school PL

7.2.1.2 School WPL

Similarly, school WPL building have also undergone the six different design seismic action according to each national code to make six various configurations, and their response in terms of base shear force both in X and Y axis direction are demonstrated in Figure 53 and the values are reported in Table 22.

With the exclusion of the plinth level from the model, the base shear values, both in X and Y direction have declined a bit.

It can be observed that the response in terms of base shear is approximately the same for all six regions response spectrums as compared to chart of school PL mode.

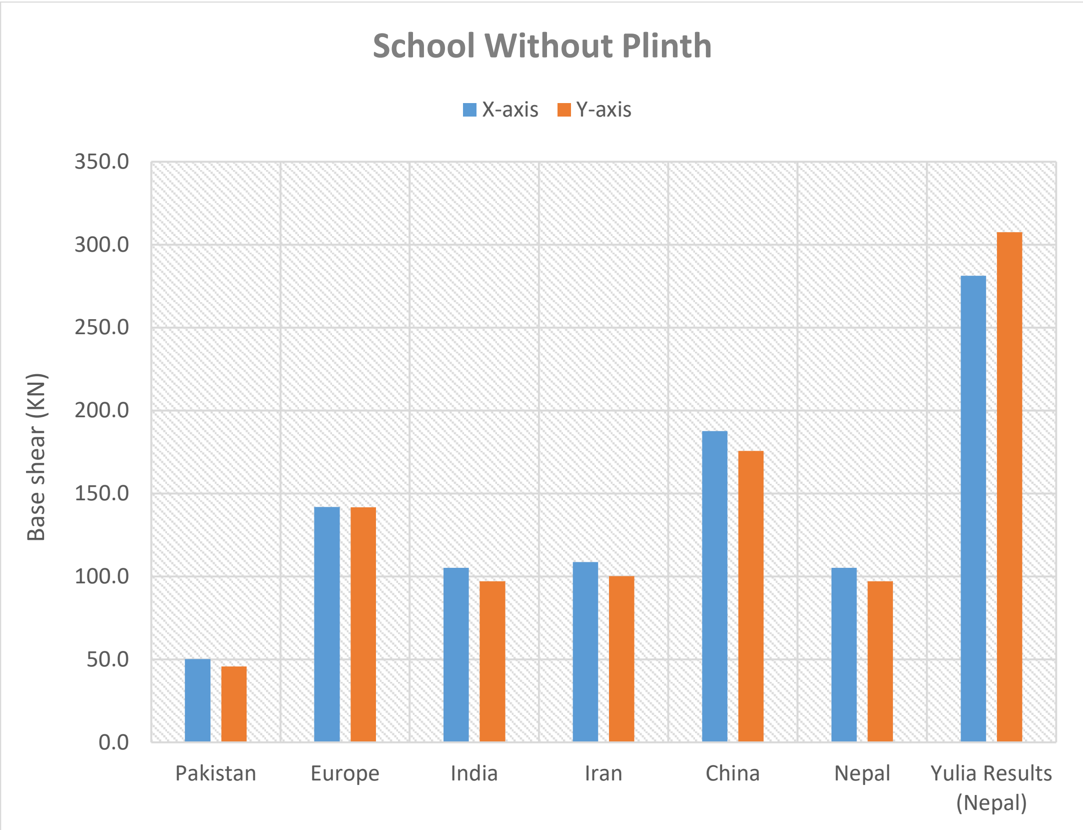

Figure 53 Seismic demand for school WPL

7.2.1.1 House PL

House PL building have undergone the six different design seismic action according to each national code to make six various configurations, and their response in terms of base shear force both in X and Y axis direction are demonstrated in Figure 54 and the values are reported in Table 23.

It can be observed that the base shear of Iran (IRN-15), India (IND-16) and Nepal (NEP-20) are almost the same due to the similar short period response segment of their design response spectrums. However, Pakistan is two times more tolerant compared to its neighboring countries, mainly caused by the high value of the behavior factor R = 4.5. China, on the other hand is nearly two times more conservative due to the fact that elastic response spectra was used to compute its base shear.

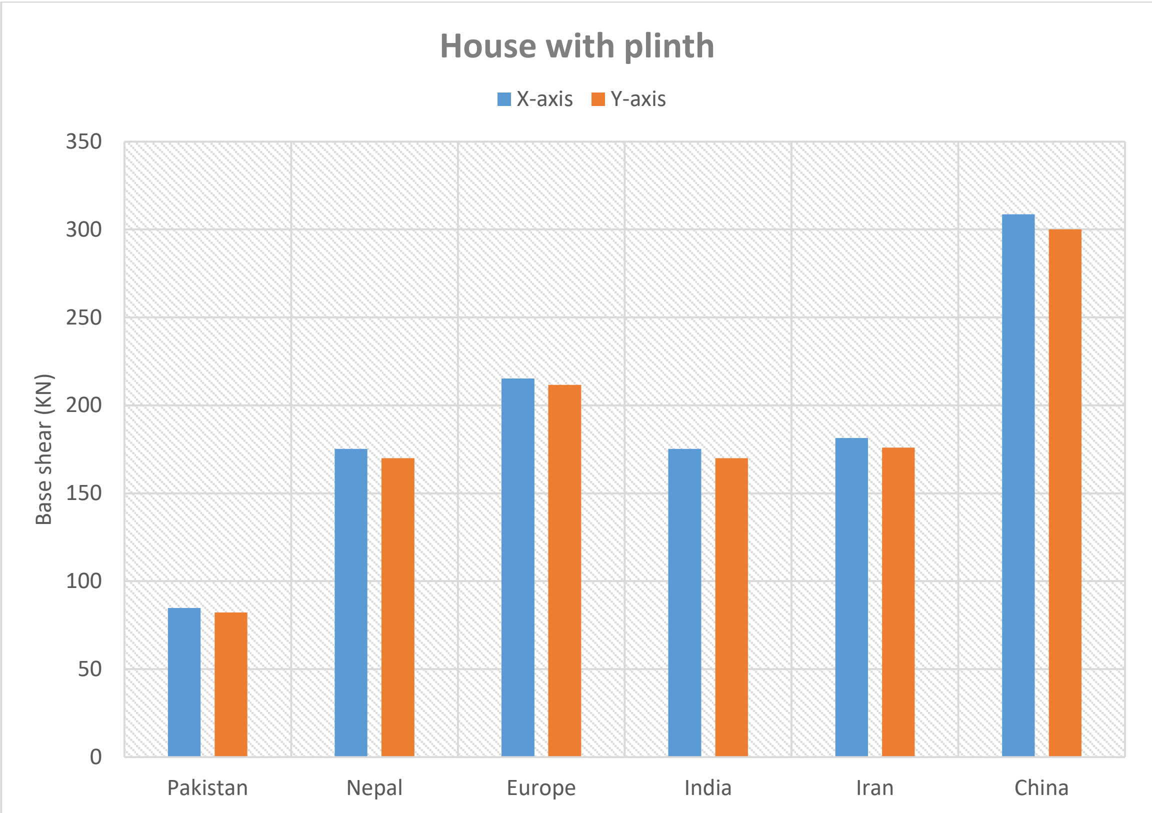

Figure 54 Seismic demand for house PL

7.2.1.2 House WPL

Similarly, house WPL building have also undergone the six different design seismic action according to each national code to make six various configurations, and their response in terms of base shear force both in X and Y axis direction are demonstrated in Figure 55 and the values are reported in Table 24.

With the exclusion of the plinth level from the model, the base shear values, both in X and Y direction have declined a bit.

It can be observed that the response in terms of base shear is approximately the same for all six regions response spectrums as compared to chart of house PL mode.

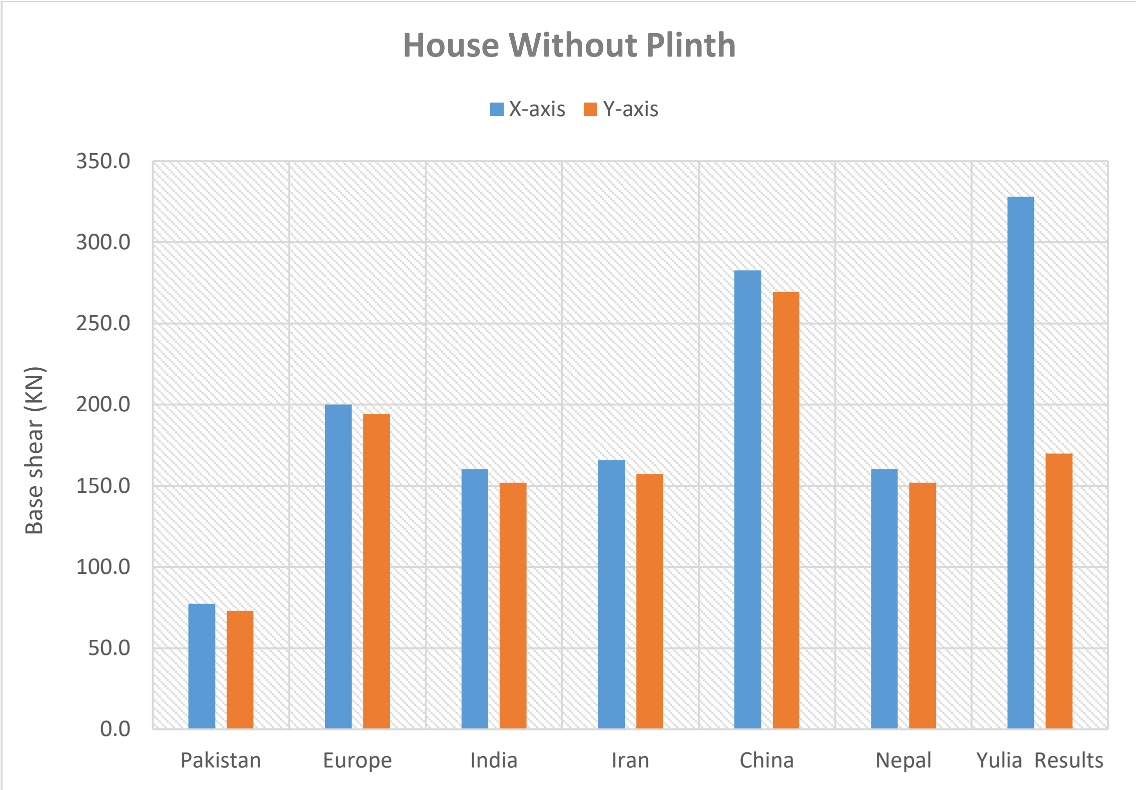

Figure 55 Seismic demand for house WPL

7.2.2 Internal Forces

In order to better understand and interpret the numerical results obtained with SAP2000 software, both school and house structure are represented as combination of cantilevered piers with inherent shear and flexural stiffness to give us insight about the internal forces in terms of axial forces, bending moment and shear forces at cross section located at the bottom end of the structure.

7.2.2.1 Section cut procedure

Section cuts were taken at the base level of all defined piers of the models designed in SAP2000 software to get the idea about internal forces. The efficient procedure to achieve such results is to use the section cut tool of the software. To do so, a group consisting the nodes and the area section lying above this section should be created initially. Figure 56 shows the selection of nodes and area section above cross section level.

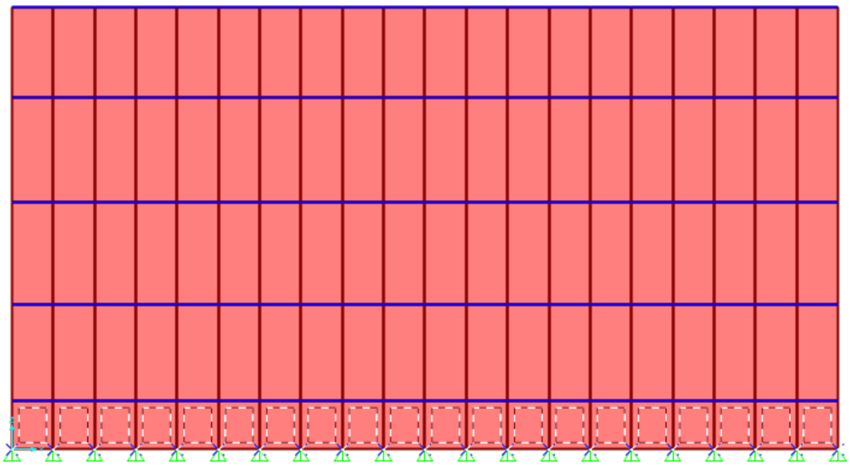

Figure 56 Selection of nodes and area section

After the definition of groups with a unique name, the section cuts are defined which will include a specific group from the list of groups created. Figure 57 shows the dialogue box settings for creating a section cut.

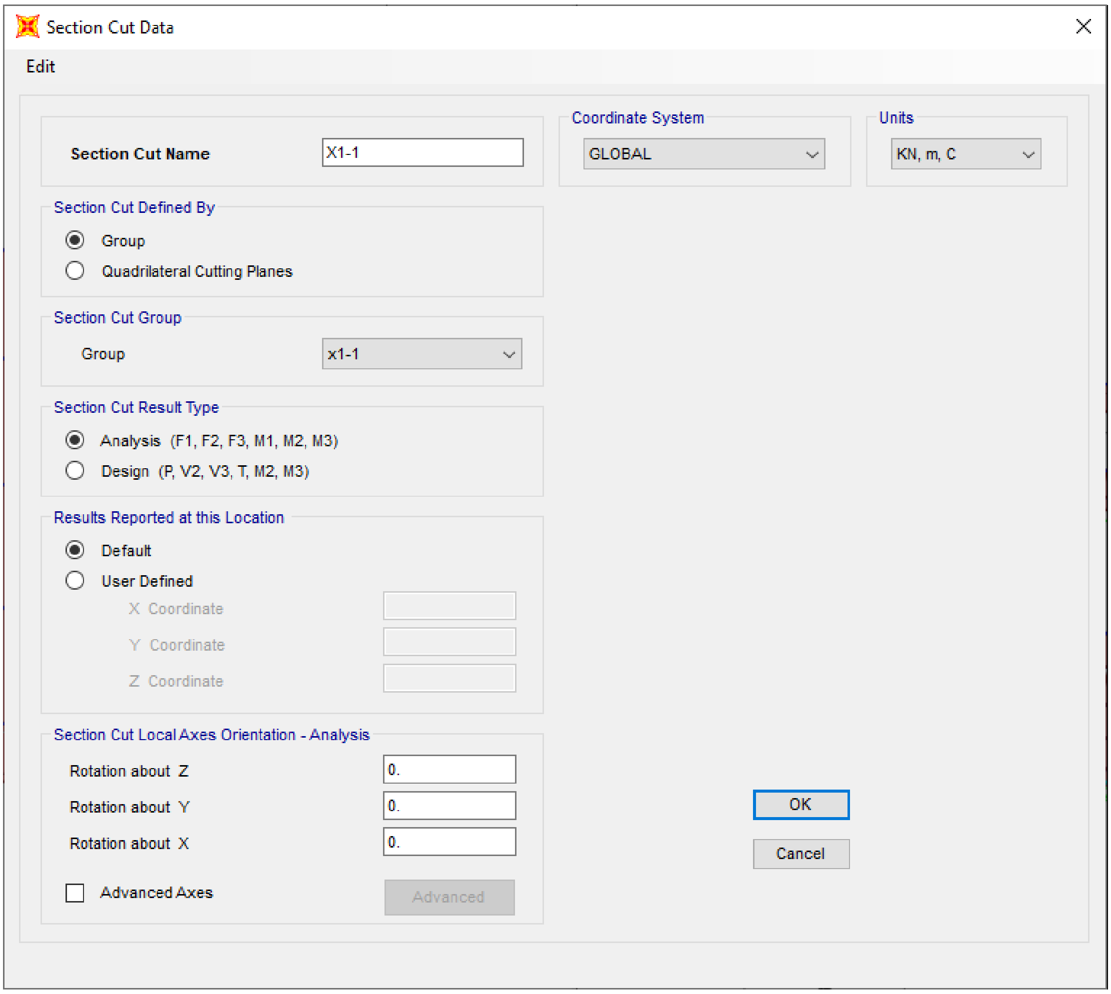

Figure 57 Section cut dialogue box

The critical load combinations were defined in software for every region and were taken from their respective building codes.

NEP-20 – 1.0D + 0.3L $\pm$ 1.0E

IND-16 – 1.58D $\pm$ 1.5E

PAK-07 – 1.31D + 0.5L $\pm$ 1.1E

IRN-15 – 1.2D + 1.0L $\pm$ 1.0E

EC8 – 1.0D + 0.3L $\pm$ 1.0E

CN-JGJ – 0.95D + 0.475L $\pm$ 1.0E

Where,

D = Dead loads

L = Live loads

E = Earthquake loads

7.2.2.2 School PL

For the internal forces estimation of school PL building, the structure is represented as a frame of piers, as is demonstrated in Figure 58. The lower end of each pier is fixed to form a cantilever pier which will represent the worst case scenario. At the plinth or base level there is a vast distribution of forces. To consider the connection of beams with the masonry pier and to be more close to the realistic behaviour of the building, we would also consider cross sections at z levels shown in elevation view in Figure 59 and Figure 60. This schematization will decrease the length of the piers and would also change the restrains of the piers considered.

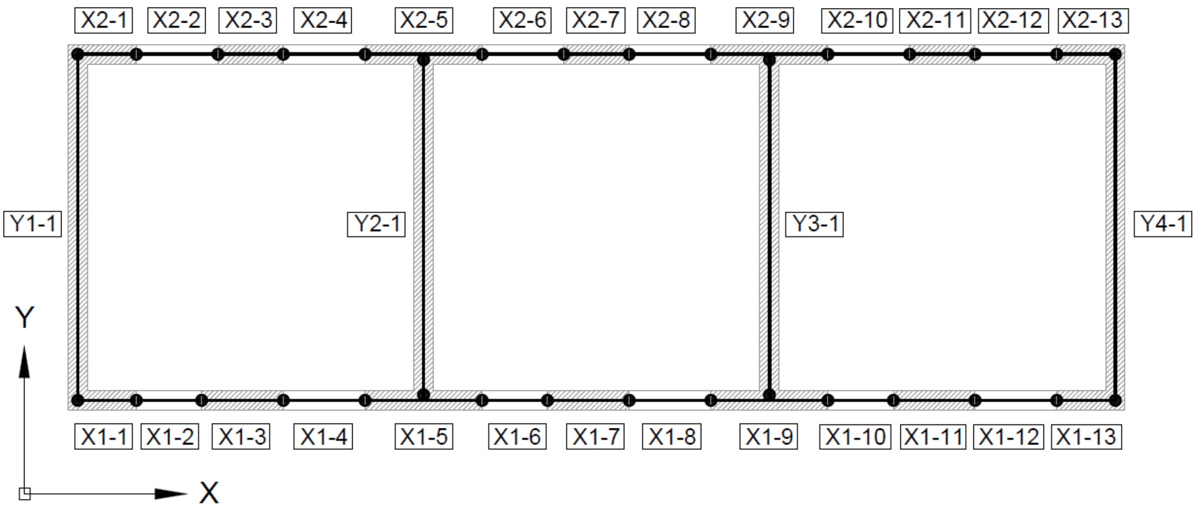

Figure 58 Piers layout for school PL

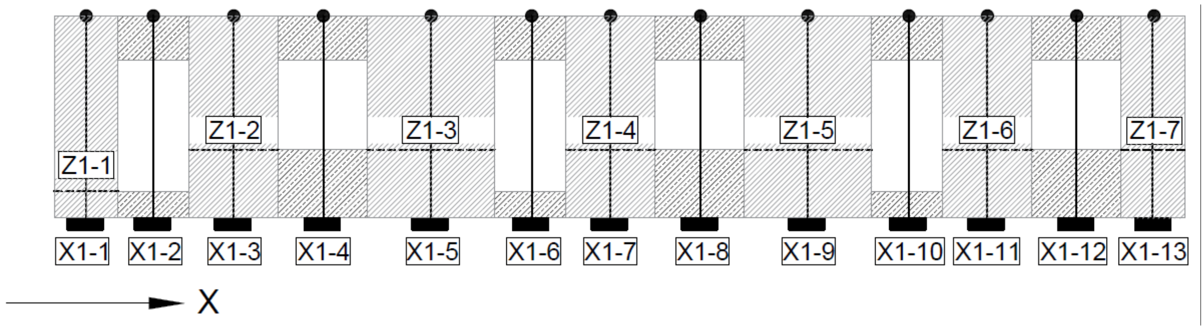

Figure 59 Piers arrangement for school PL along X axis, door wall

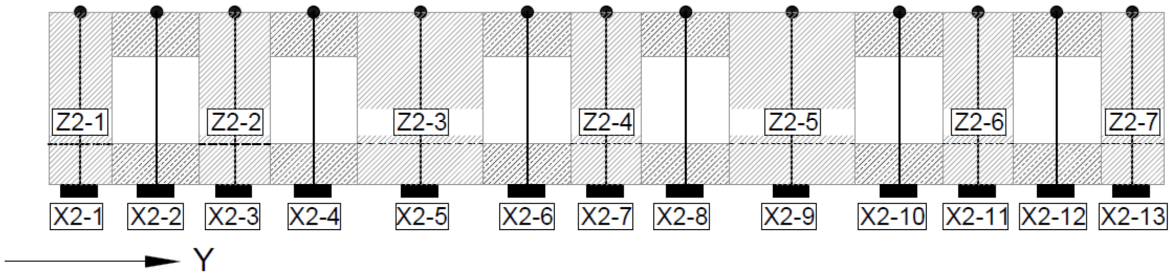

Figure 60 Piers arrangement for school PL along X axis, window wall

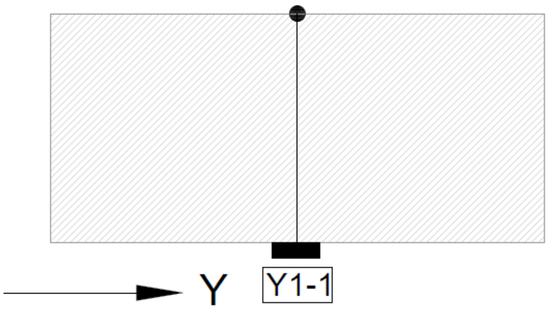

Figure 61 Piers arrangement for all walls of school PL along Y axis

7.2.2.2.1 Axial Force

Using section cut procedure in SAP2000 at base level of building while looking at internal forces in z-direction of local axis, the axial forces at all piers were determined and then plotted in order to compare these results for all regions with different critical load combination. Figure 62 shows the axial forces for door wall along x- axis with piers X1-1, X1-2, X1-3, X1-4, X1-5, X1-6, X1-7, X1-8, X1-9, X1-10, X1-11, X1-12 and X1-13. Figure 63 shows the axial forces for window wall along x-axis with piers X2-1, X2-2, X2-3, X2-4, X2-5, X2-6, X2-7, X2-8, X2-9, X2-10, X2-11, X2-12 and X2-13. Table 25 shows the data for all the piers in door wall along x-axis and Table 26 shows the data for all the piers in window wall along x-axis. Figure

64 shows the axial forces for all the walls along y- axis with piers Y1-1, Y2-1, Y3-1, Y4-1 and Table 27 shows the data for all the piers in all the walls along y-axis. Figure 65 shows the axial forces only for Nepal region for the piers at z section level for both door and window wall: Z1-1, Z1-2, Z1-3, Z1-4, Z1-5, Z1-6 Z1-7, Z2-1, Z2-2, Z2-3, Z2-4, Z2-5, Z2-6 and Z2-7. Table 28 shows the data for all the piers at z level for both door and window wall along x-axis.

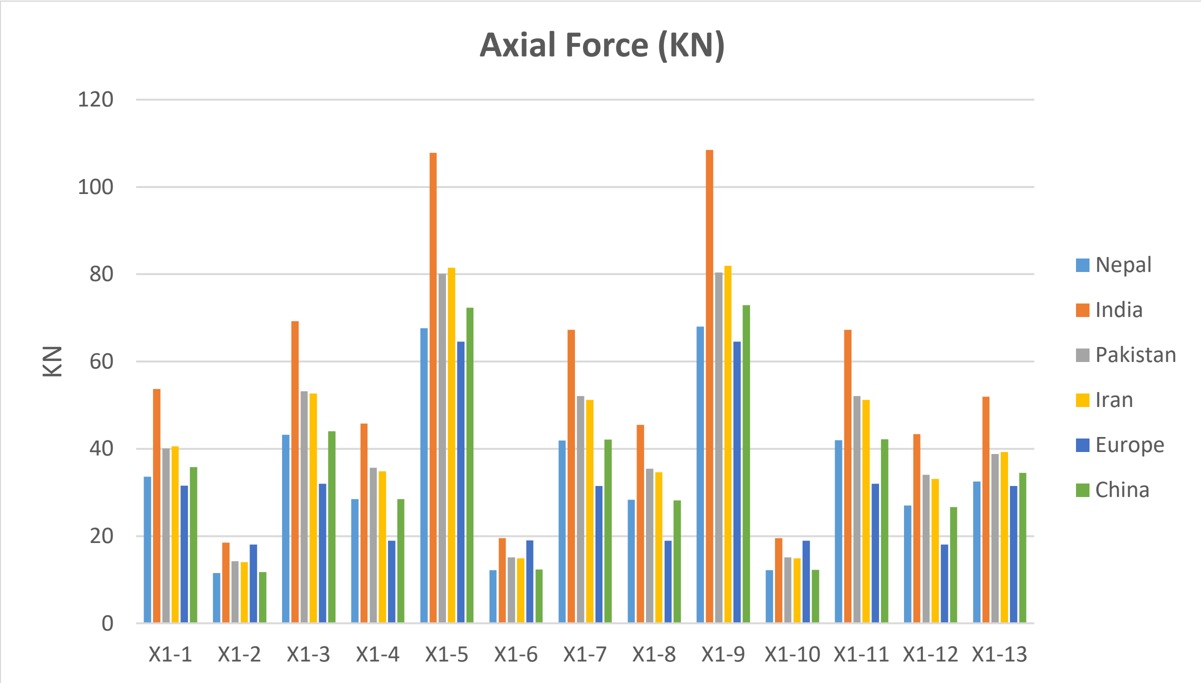

Figure 62 Comparison of axial forces, door wall, school PL

Looking at the elevation view of door wall along x-axis of school PL building, we can generally state that the axial force is lower for the piers having doors or windows portion and is maximum for piers with sizeable width. Results for India were the most conservative among all the countries and the critical load combination of Pakistan and Iran codes were showing almost the same results. Moreover, results of Nepal critical load combination were more similar to the ones of Europe and China.

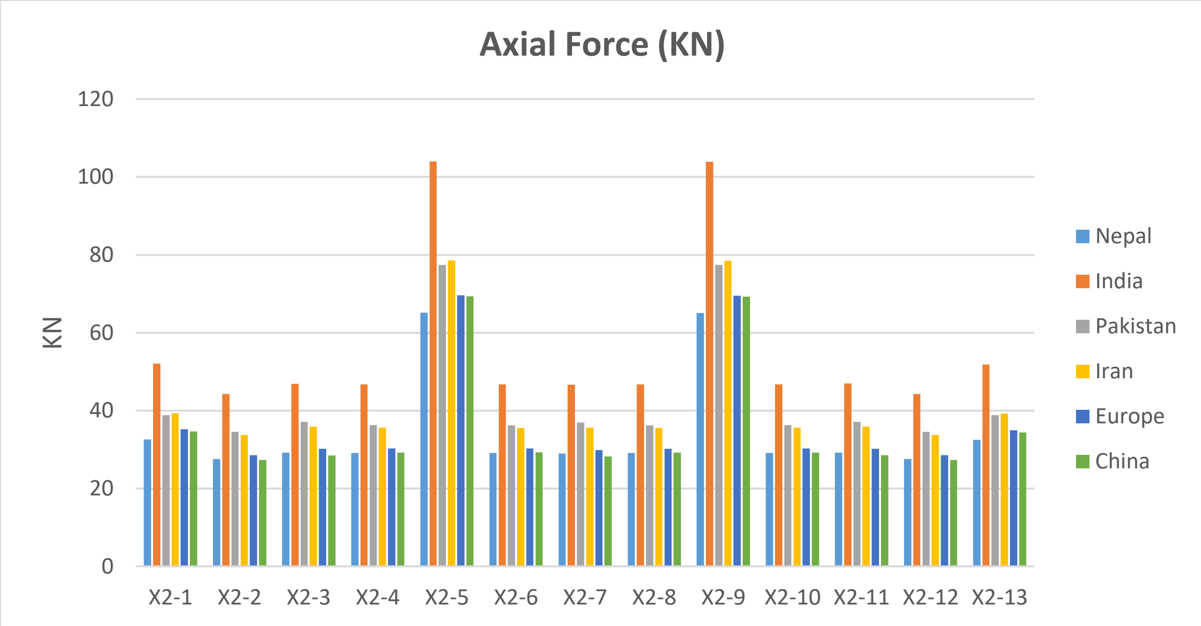

Figure 63 Comparison of axial forces, window wall, school PL

Again looking at the elevation view of window wall along x-axis of school PL building, we can clearly see that the axial forces have large values for the piers with large width and no windows (X2-5, X2-9) while identical distribution can be seen for piers with windows portion and piers with narrow width. Again results for critical load combination of India were the most conservative and critical load combination of Nepal, Europe and China were the most tolerant.

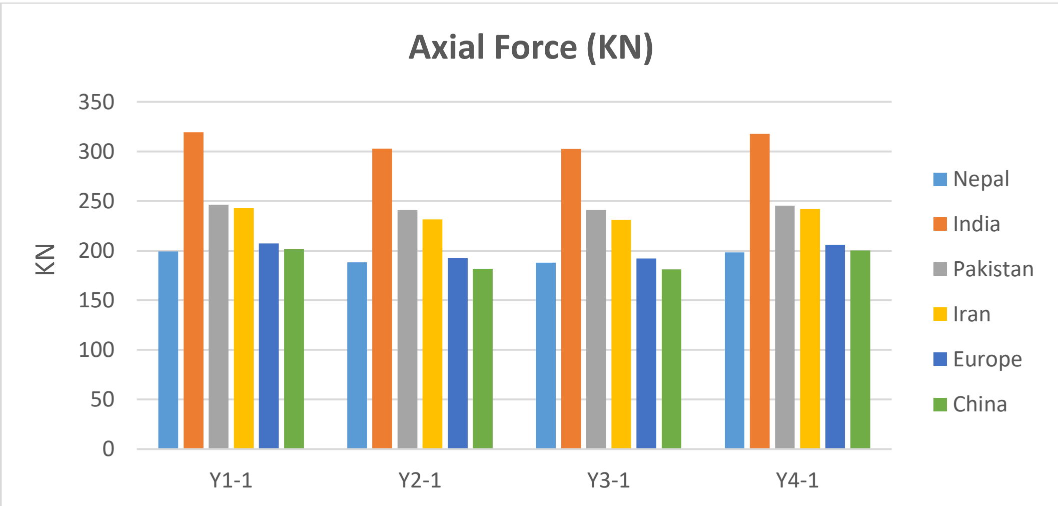

Figure 64 Comparison of axial forces, all walls along y-axis, school PL

Considering the elevation view of walls along y-axis of school PL building, we can notice that due to symmetry of the building, all the walls have approximately same results. Results for critical load combination of India were the most conservative and critical load combination of Nepal, Europe and China were the most tolerant.

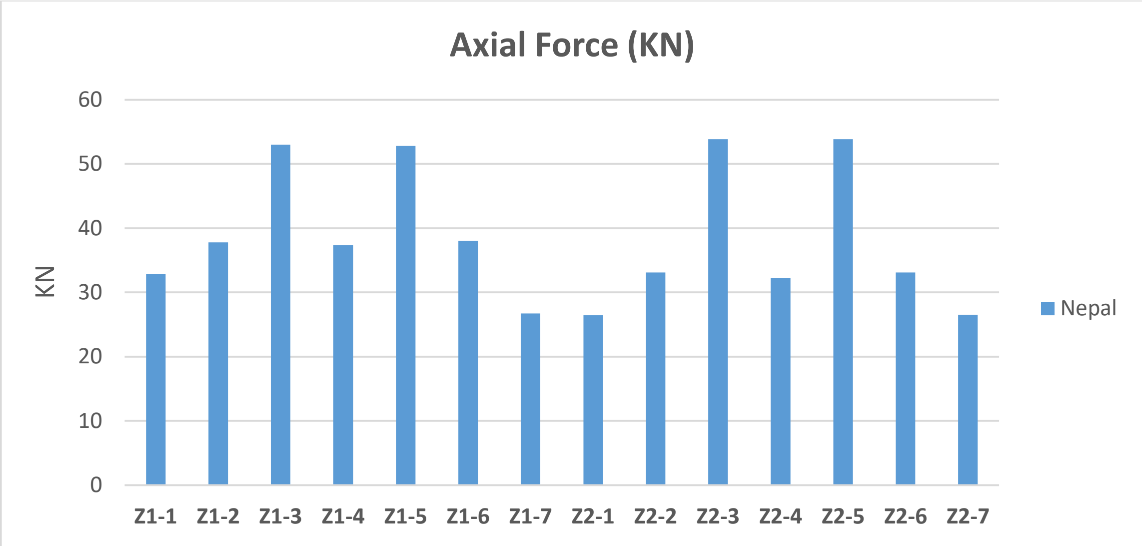

Figure 65 Comparison of axial forces, all walls along x-axis, z level, school PL

Axial forces distribution at z levels shows us that the more is the width of the pier (Z1-3, Z1-5, Z2-3, Z2-5), the higher its axial force level is. Also we can state that the axial forces at z levels are lesser as compared to axial forces at base levels.

7.2.2.2.2 Bending moment

The bending moment at all piers were determined at base cross sections and then plotted in order to compare these results for all regions with different critical load combination. Figure 66 shows the bending moments for door wall along x- axis with piers X1-1, X1-2, X1-3, X1-4, X1-5, X1-6, X1-7, X1-8, X1-9, X1-10, X1-11, X1-12 and X1-13. Figure 67 shows the bending moments for window wall along x-axis with piers X2-1, X2-2, X2-3, X2-4, X2-5, X2-6, X2-7, X2-8, X2-9, X2-10, X2-11, X2-12 and X2-13. Table 29 shows the data for all the piers in door wall along x-axis and Table 30 shows the data for all the piers in window wall along x-axis. Figure 68 shows the bending moments for all the walls along y- axis with piers Y1-1, Y2-1, Y3-1, Y4-1 and Table 31 shows the data for all the piers in all the walls along y-axis. Figure 69 shows the bending moments only for Nepal region for the piers at z section level for both door and window wall: Z1-1, Z1-2, Z1-3, Z1-4, Z1-5, Z1-6 Z1-7, Z2-1, Z2-2, Z2-3, Z2-4, Z2-5, Z2-6 and Z2-7. Table 32 shows the data for all the piers at z level for both door and window wall along x-axis.

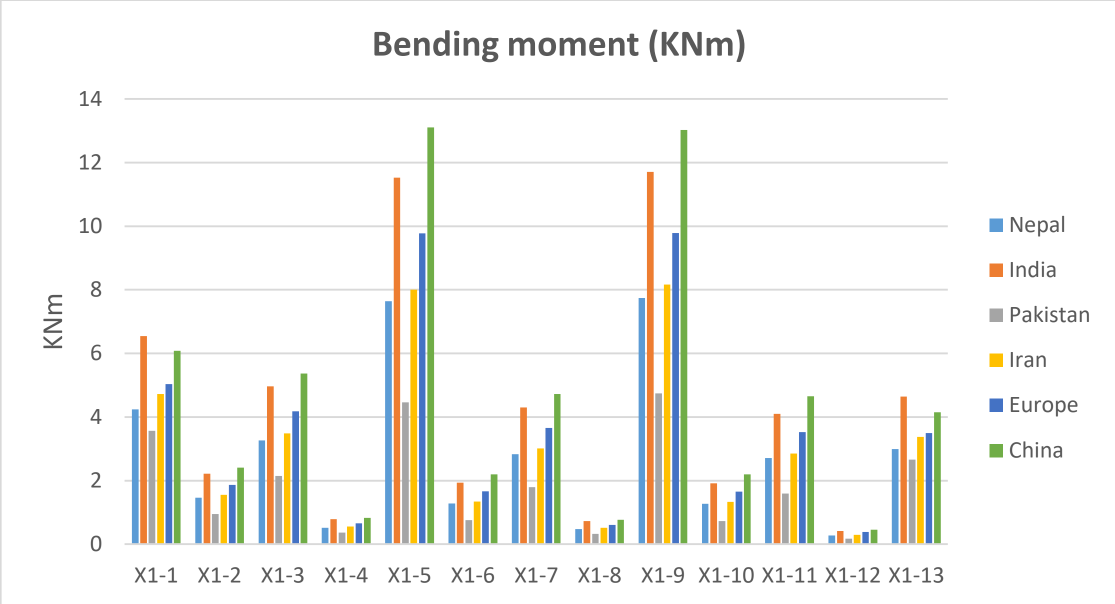

Figure 66 Comparison of bending moments, door wall, school PL

Looking at the elevation view of door wall along x-axis of school PL building, we can generally state that the bending moment is lower for the piers having doors or windows portion and is maximum for piers with sizeable width. Results for China and India were the most conservative among all the countries and the critical load combination of Nepal and Iran codes were showing almost the same results. Moreover, results of Pakistan critical load combination were most tolerant.

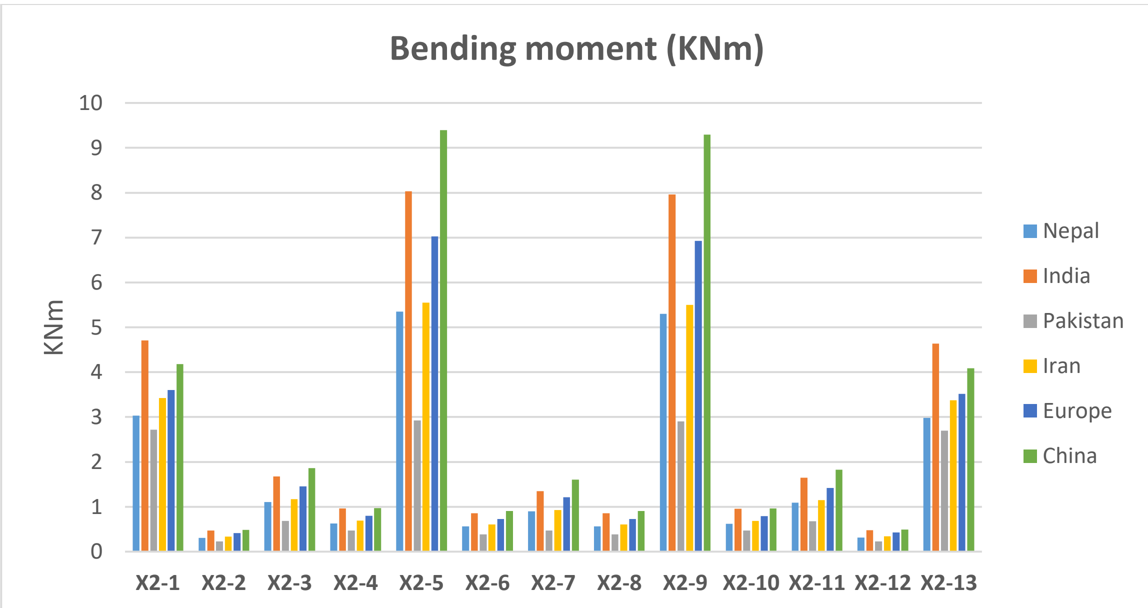

Figure 67 Comparison of bending moments, window wall, school PL

Again looking at the elevation view of window wall along x-axis of school PL building, we can clearly see that the bending moments have large values for the piers with large width and no windows (X2-5, X2-9) while identical distribution can be seen for piers with windows portion (X2-2, X2-4, X2-6, X2-8, X2-10 and X2-12). Piers with narrow width at either ends (X2-1, X2-13) have higher bending moment values. Again results for critical load combination of India and China were the most conservative while Pakistan was most tolerant. Moreover, critical load combination of Nepal and Iran were almost the same.

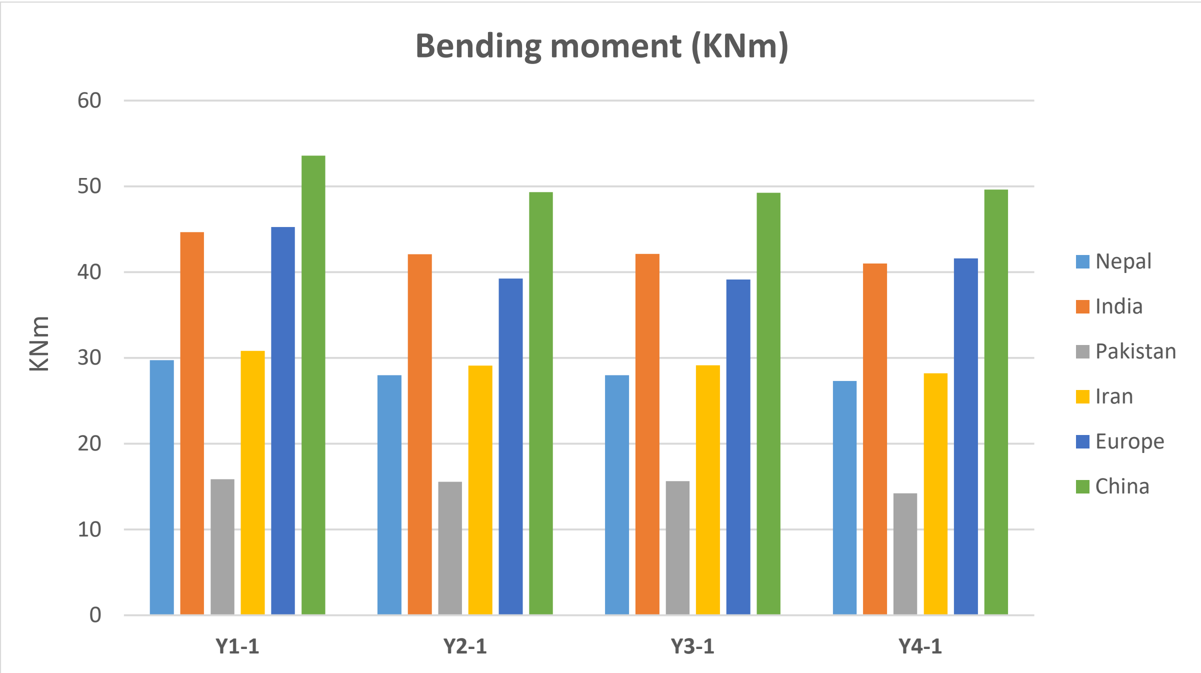

Figure 68 Comparison of bending moments, all walls along y-axis, school PL

Considering the elevation view of walls along y-axis of school PL building, we can notice that due to symmetry of the building, all the walls have approximately same results. Results for critical load combination of China were the most conservative and critical load combination of Pakistan were the most tolerant.

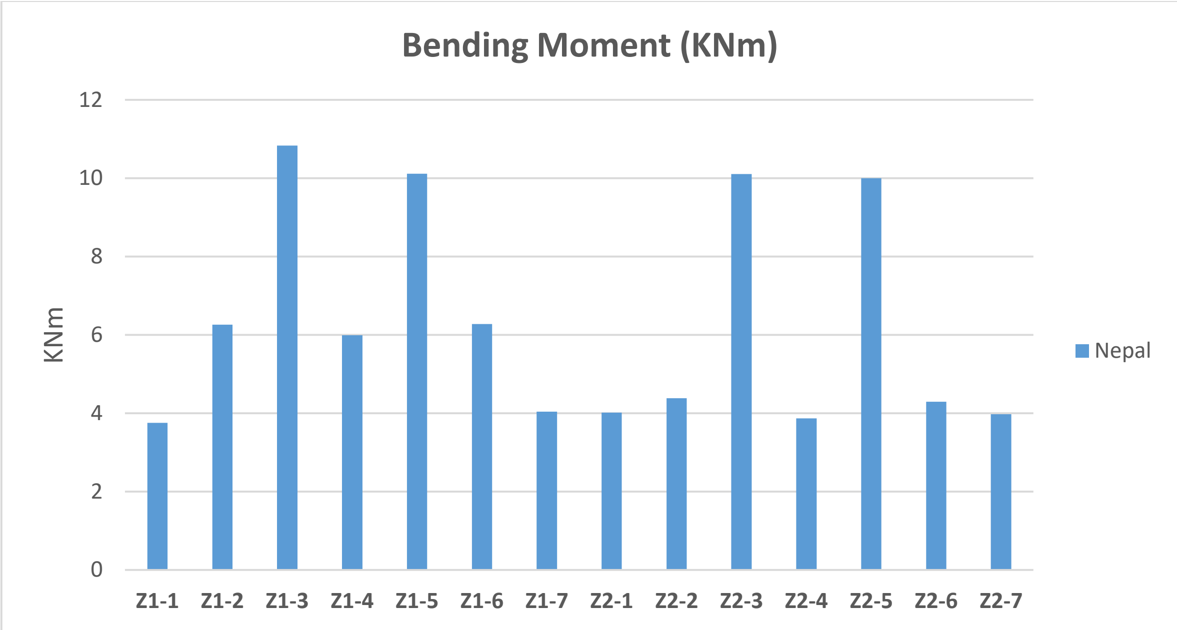

Figure 69 Comparison of bending moments, all walls along x-axis, z level, school PL

Bending moment distribution at z levels shows us that the more is the width of the pier (Z1-3, Z1-5, Z2-3, Z2-5), the higher its bending moment level is.

7.2.2.2.3 Shear force

Shear Forces at all piers were determined at base cross sections and then plotted in order to compare these results for all regions with different critical load combination. Figure 70 shows the shear forces for door wall along x- axis with piers X1-1, X1-2, X1-3, X1-4, X1-5, X1-6, X1-7, X1-8, X1-9, X1-10, X1-11, X1-12 and X1-13. Figure 71 shows the shear forces for window wall along x-axis with piers X2-1, X2-2, X2-3, X2-4, X2-5, X2-6, X2-7, X2-8, X2-9, X2-10, X2-11, X2-12 and X2-13. Table 33 shows the data for all the piers in door wall along x-axis and Table 34 shows the data for all the piers in window wall along x-axis. Figure 72 shows the shear forces for all the walls along y- axis with piers Y1-1, Y2-1, Y3-1, Y4-1 and Table 35 shows the data for all the piers in all the walls along y-axis. Figure 73 shows the shear forces only for Nepal region for the piers at z section level for both door and window wall: Z1-1, Z1-2, Z1-3, Z1-4, Z1-5, Z1-6 Z1-7, Z2-1, Z2-2, Z2-3, Z2-4, Z2-5, Z2-6 and Z2-7. Table 36 shows the data for all the piers at z level for both door and window wall along x-axis.

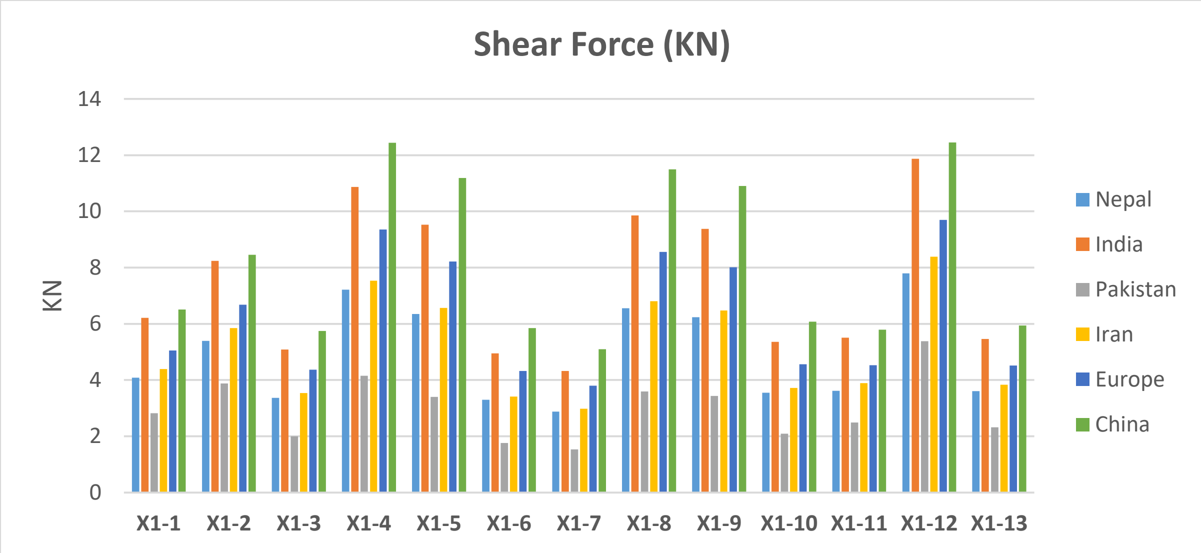

Figure 70 Comparison of shear forces, door wall, school PL

Looking at the elevation view of door wall along x-axis of school PL building, we can state that the shear force is high for the piers having windows portion (X1-4, X1-8, X1-12) and is less for piers with no windows or doors. Results for China and India were the most conservative among all the countries and the critical load combination of Nepal and Iran codes were showing almost the same results. Moreover, results of Pakistan critical load combination were most tolerant.

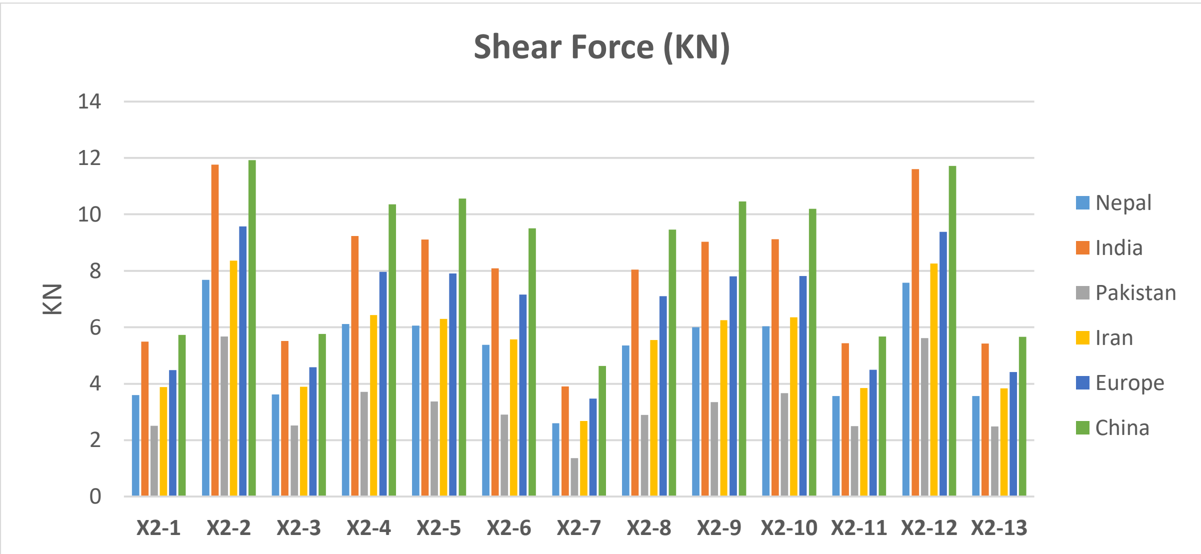

Figure 71 Comparison of shear forces, window wall, school PL

Again looking at the elevation view of window wall along x-axis of school PL building, we can clearly see that the shear force is high for the piers having windows portion (X2-2, X2-4, X2-6, X2-8, X-10 and X2-12) and is less for piers with no windows or doors. Again results for critical load combination of India and China were the most conservative while Pakistan was most tolerant. Moreover, critical load combination of Nepal and Iran were almost the same.

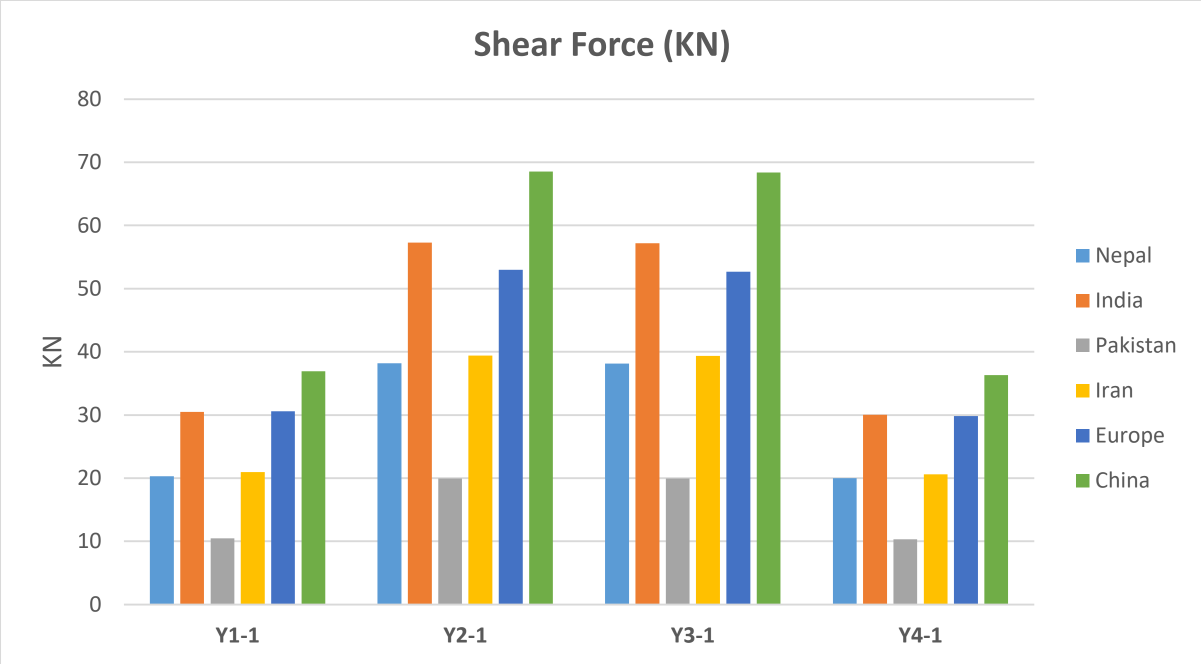

Figure 72 Comparison of shear forces, all walls along y-axis, school PL

Considering the elevation view of walls along y-axis of school PL building, we can notice that due to symmetry of the building, walls on outer side of building have less shear forces and vice versa. Results for critical load combination of China were the most conservative and critical load combination of Pakistan were the most tolerant. Moreover, critical load combination of Nepal and Iran were almost the same.

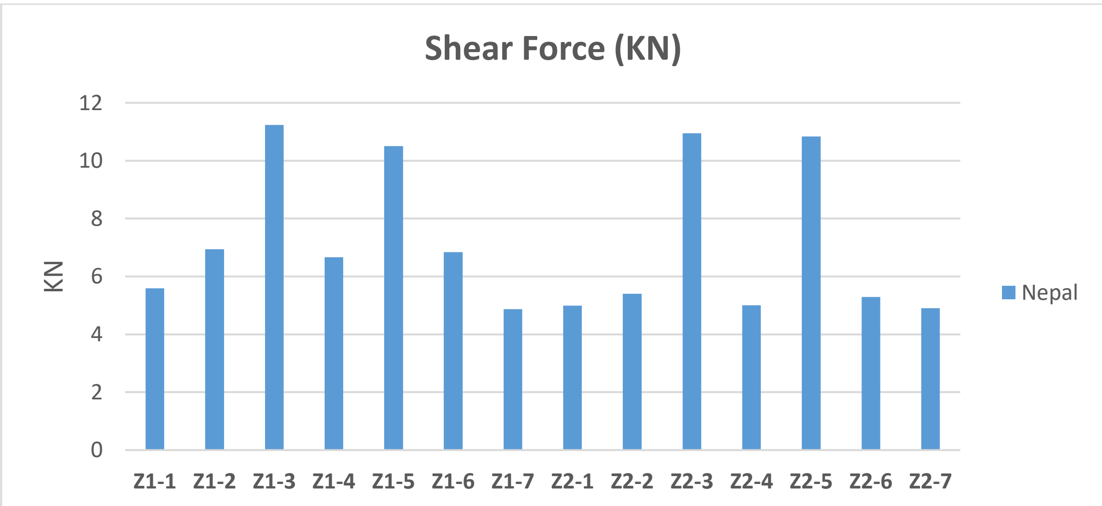

Figure 73 Comparison of shear forces, all walls along x-axis, z level, school PL

Shear force distribution at z levels shows us that the more is the width of the pier (Z1-3, Z1-5, Z2-3, Z2-5), the higher its shear force level is.

7.2.2.3 School WPL

Similar to school PL building, for the internal forces estimation of school WPL building, without the plinth level, the internal actions were reduced in the buildings as compared to school with plinth level. The structure is represented as a frame of piers, as is demonstrated in Figure 74-Figure 77.

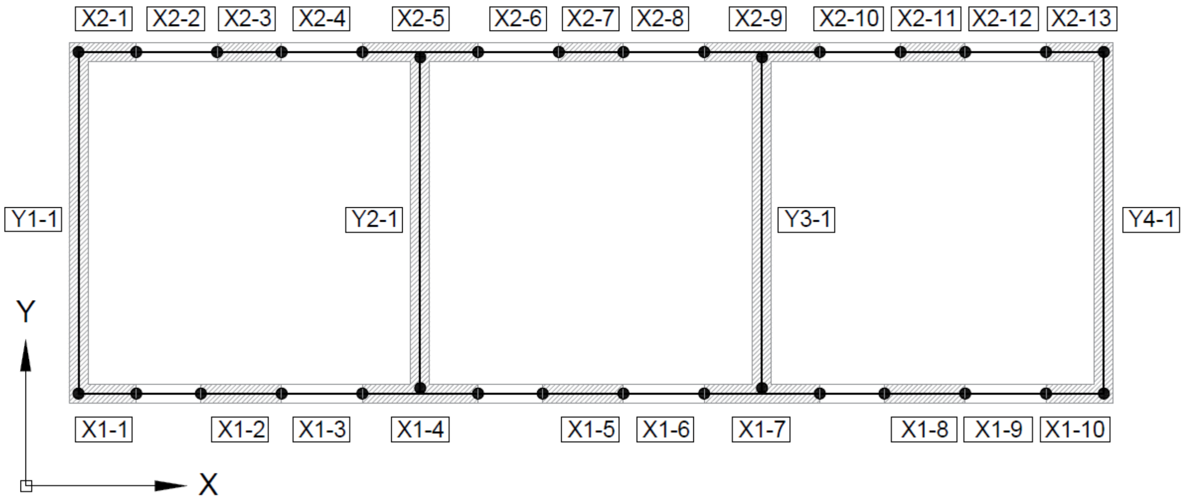

Figure 74 Piers layout for School WPL

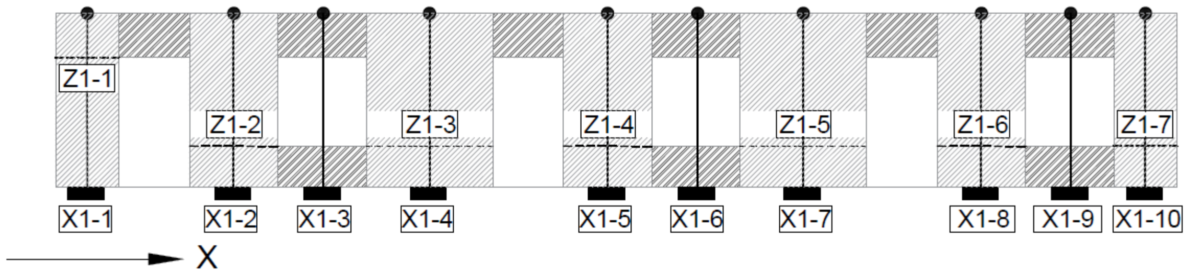

Figure 75 Piers arrangement for school WPL along X axis, door wall

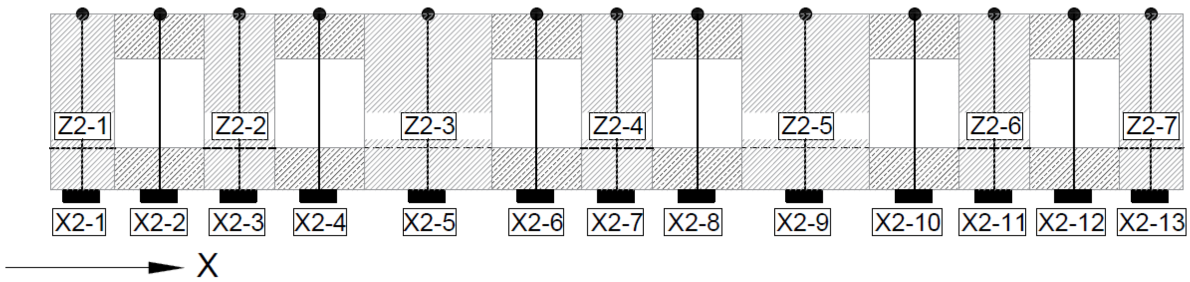

Figure 76 Piers arrangement for school WPL along X axis, window wall

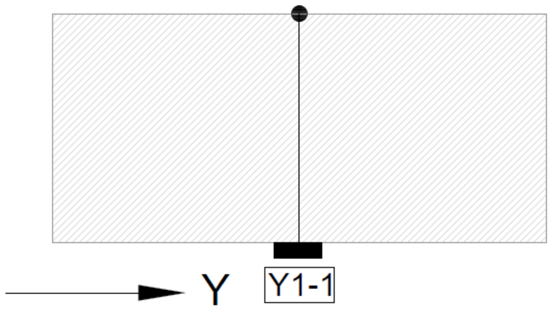

Figure 77 Piers arrangement for all walls of school WPL along Y axis

7.2.2.3.1 Axial Force

Using section cut procedure in SAP2000 at base level of school WPL building while looking at internal forces in z-direction of local axis, the axial forces at all piers were determined and then plotted in order to compare these results for all regions with different critical load combination. Figure 78 shows the axial forces for door wall along x- axis with piers X1-1, X1-2, X1-3, X1-4, X1-5, X1-6, X1-7, X1-8, X1-9 and X1-10. Figure 79 shows the axial forces for window wall along x-axis with piers X2-1, X2-2, X2-3, X2-4, X2-5, X2-6, X2-7, X2-8, X2-9, X2-10, X2-11, X2-12 and X2-13. Table 37 shows the data for all the piers in door wall along x-axis and Table 38 shows the data for all the piers in window wall along x-axis. Figure 80 shows the axial forces for all the walls along y- axis with piers Y1-1, Y2-1, Y3-1, Y4-1 and Table 39 shows the data for all the piers in all the walls along y-axis. Figure 81 shows the axial forces only for Nepal region for the piers at z section level for both door and window wall: Z1-1, Z1-2, Z1-3, Z1-4, Z1-5, Z1-6 Z1-7, Z2-1, Z2-2, Z2-3, Z2-4, Z2-5, Z2-6 and Z2-7. Table 40 shows the data for all the piers at z level for both door and window wall along x-axis.

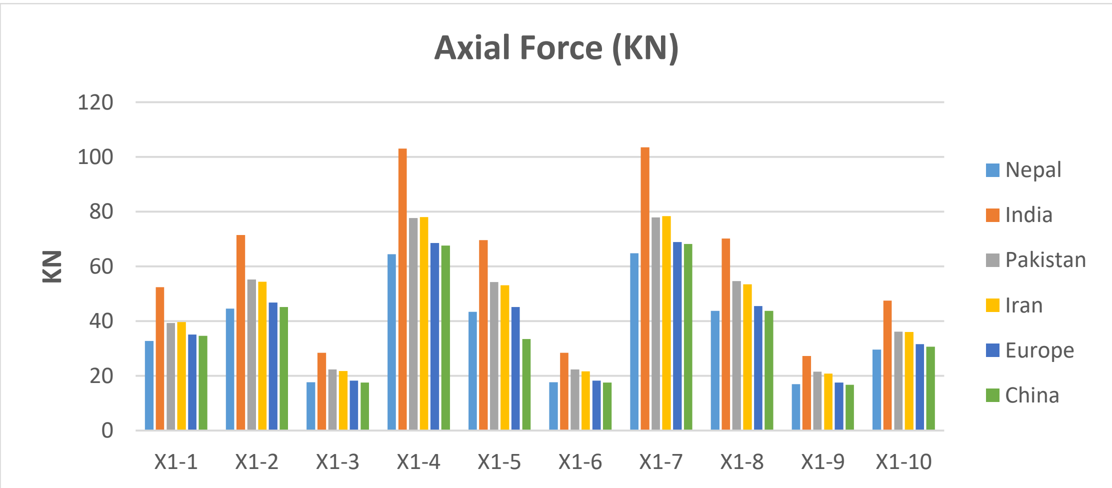

Figure 78 Comparison of axial forces, door wall, school WPL

Looking at the elevation view of door wall along x-axis of school WPL building, we can generally state that the axial force is lower for the piers having windows portion and is maximum for piers with sizeable width. Results for India were the most conservative among all the countries and the critical load combination of Pakistan and Iran codes were showing almost the same results. Moreover, results of Nepal critical load combination were more similar to the ones of Europe and China.

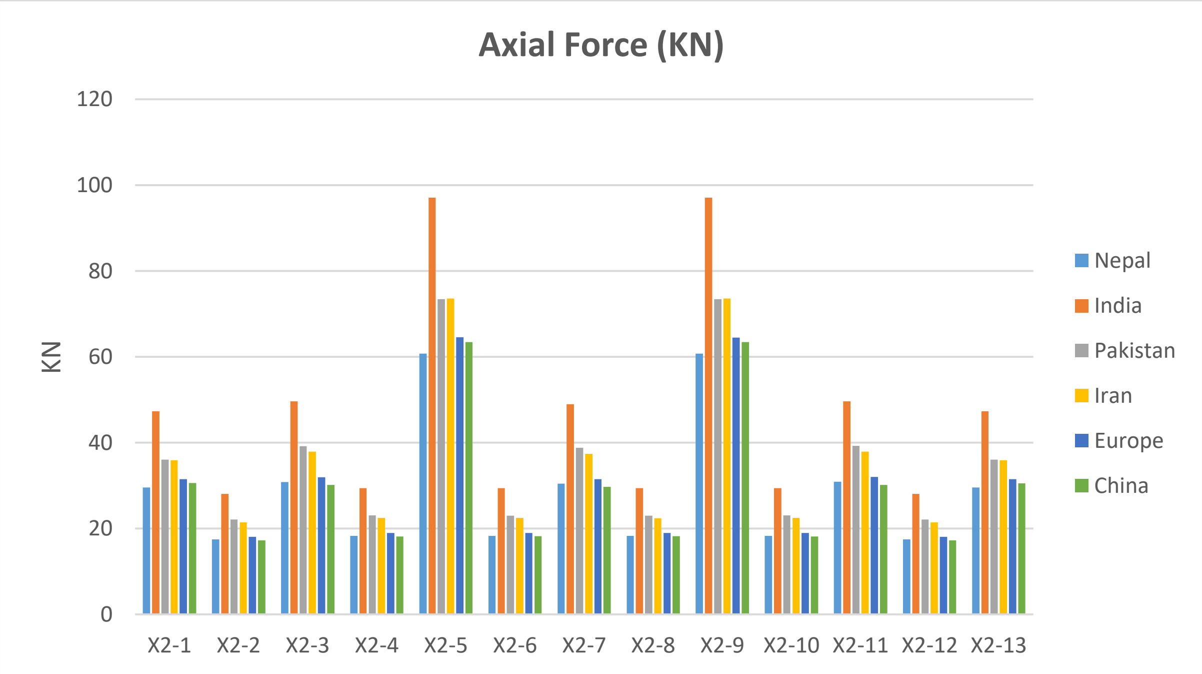

Figure 79 Comparison of axial forces, window wall, school WPL

Again looking at the elevation view of window wall along x-axis of school WPL building, we can clearly see that the axial forces have large values for the piers with large width and no windows (X2-5, X2-9) while identical distribution can be seen for piers with windows portion and piers with narrow width. Again results for critical load combination of India were the most conservative and critical load combination of Nepal, Europe and China were the most tolerant.

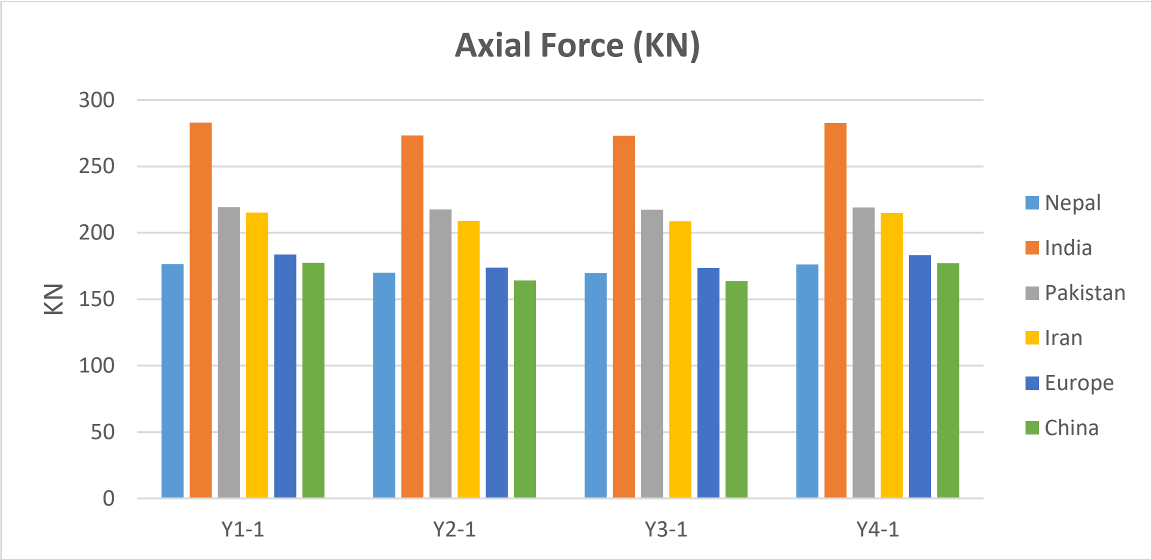

Figure 80 Comparison of axial forces, all walls along y-axis, school WPL

Considering the elevation view of walls along y-axis of school WPL building, we can notice that due to symmetry of the building, all the walls have approximately same results. Results for critical load combination of India were the most conservative and critical load combination of Nepal, Europe and China were the most tolerant.

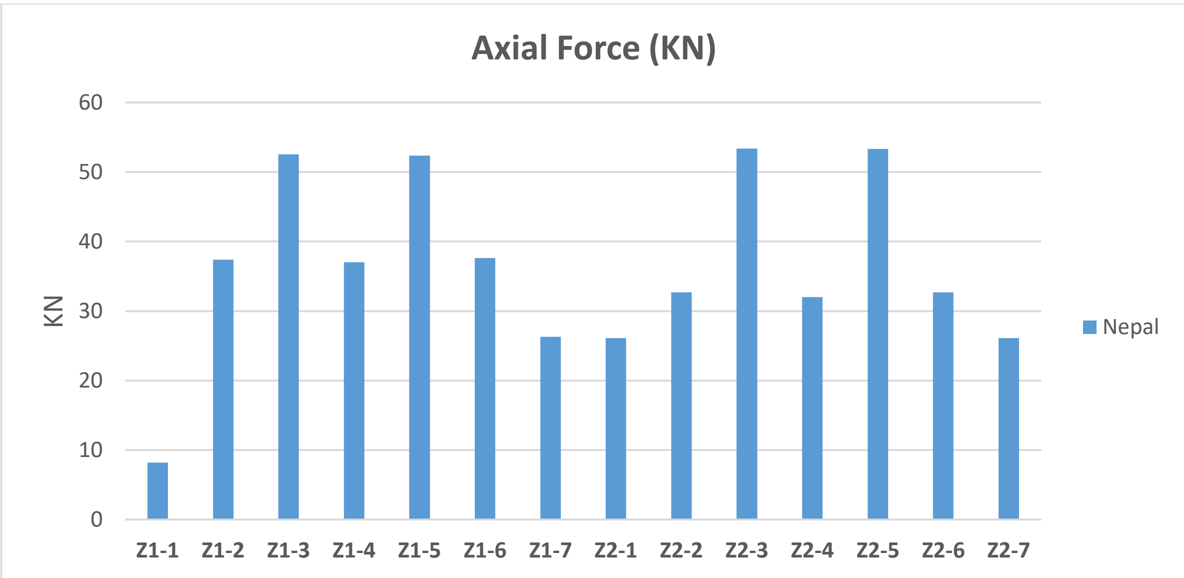

Figure 81 Comparison of axial forces, all walls along x-axis, z section, school WPL

Axial forces distribution at z levels shows us that the more is the width of the pier (Z1-3, Z1-5, Z2-3, Z2-5), the higher its axial force level is. Also we can state that the axial forces at z levels are lesser as compared to axial forces at base levels.

7.2.2.3.2 Bending moment

The bending moment at all piers were determined at base cross sections and then plotted in order to compare these results for all regions with different critical load combination. Figure 82 shows the bending moments for door wall along x- axis with piers X1-1, X1-2, X1-3, X1-4, X1-5, X1-6, X1-7, X1-8, X1-9 and X1-10. Figure 83 shows the bending moments for window wall along x-axis with piers X2-1, X2-2, X2-3, X2-4, X2-5, X2-6, X2-7, X2-8, X2-9, X2-10, X2-11, X2-12 and X2-13. Table 41 shows the data for all the piers in door wall along x-axis and Table 42 shows the data for all the piers in window wall along x-axis. Figure 84 shows the bending moments for all the walls along y- axis with piers Y1-1, Y2-1, Y3-1, Y4-1 and Table 43 shows the data for all the piers in all the walls along y-axis. Figure 85 shows the bending moments only for Nepal region for the piers at z section level for both door and window wall: Z1-1, Z1-2, Z1-3, Z1-4, Z1-5, Z1-6 Z1-7, Z2-1, Z2-2, Z2-3, Z2-4, Z2-5, Z2-6 and Z2-7. Table 44 shows the data for all the piers at z level for both door and window wall along x-axis.

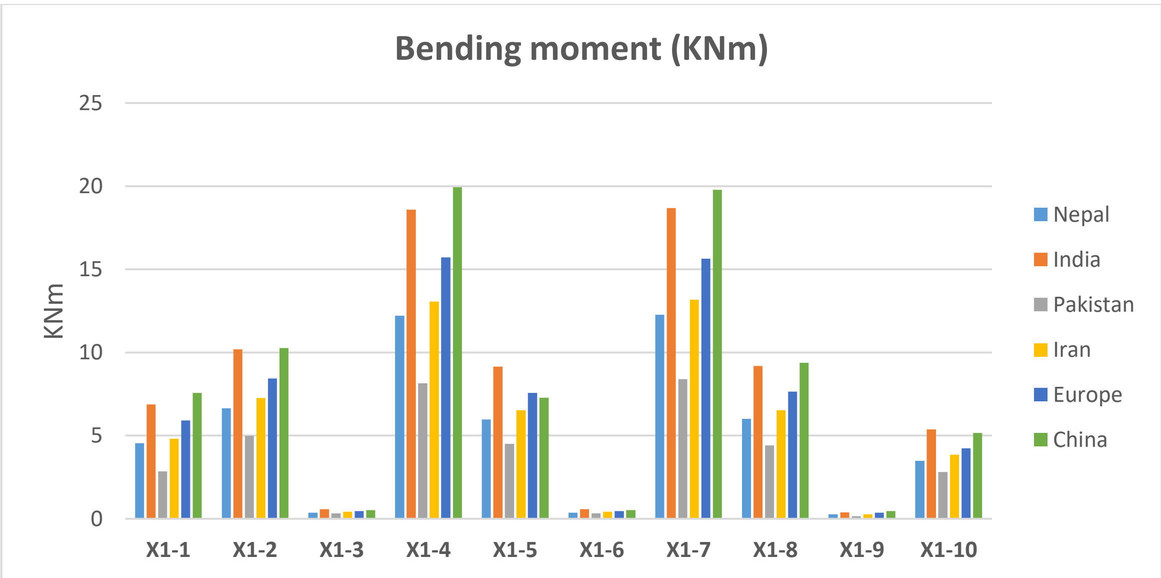

Figure 82 Comparison of bending moments, door wall, school WPL

Looking at the elevation view of door wall along x-axis of school WPL building, we can generally state that the bending moment is lower for the piers having windows portion and is maximum for piers with sizeable width. Results for China and India were the most conservative among all the countries and the critical load combination of Nepal and Iran codes were showing almost the same results. Moreover, results of Pakistan critical load combination were most tolerant.

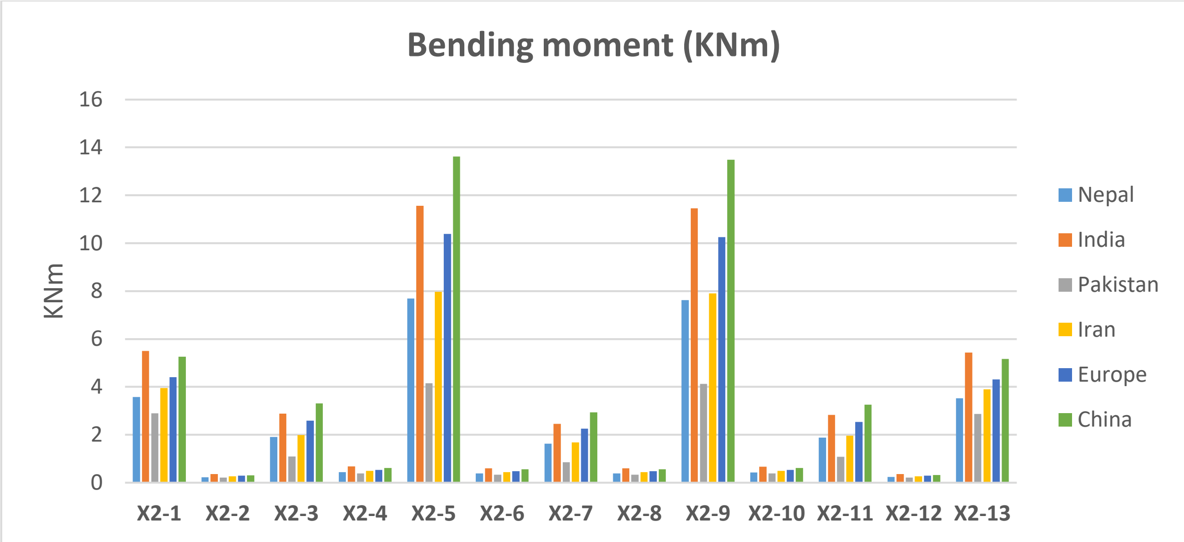

Figure 83 Comparison of bending moments, window wall, school WPL

Again looking at the elevation view of window wall along x-axis of school WPL building, we can clearly see that the bending moments have large values for the piers with large width and no windows (X2-5, X2-9) while identical distribution can be seen for piers with windows portion (X2-2, X2-4, X2-6, X2-8, X2-10 and X2-12). Piers with narrow width at either ends (X2-1, X2-13) have higher bending moment values. Again results for critical load combination of India and China were the most conservative while Pakistan was most tolerant. Moreover, critical load combination of Nepal and Iran were almost the same.

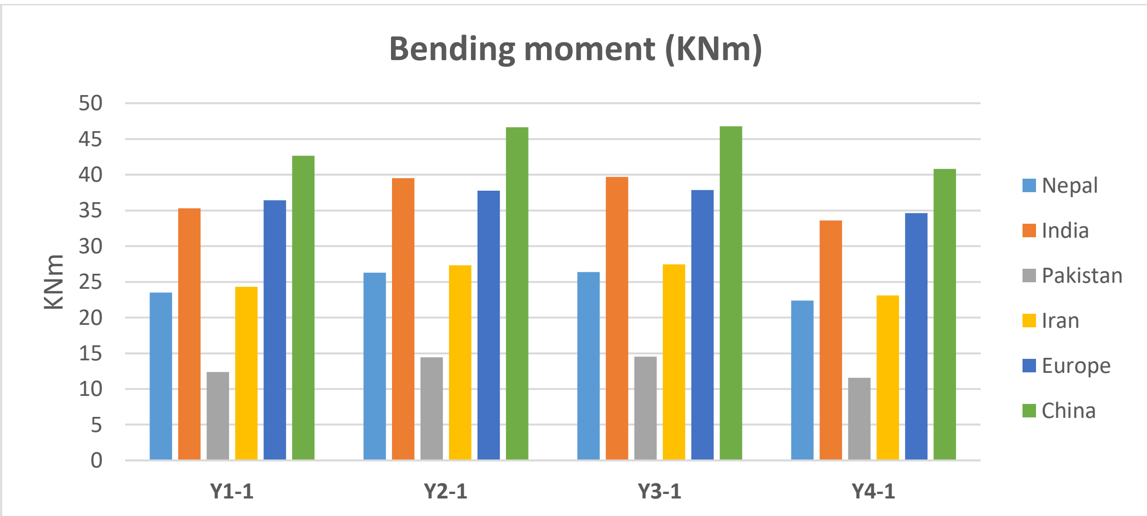

Figure 84 Comparison of bending moments, all walls along y-axis, school WPL

Considering the elevation view of walls along y-axis of school WPL building, we can notice that due to symmetry of the building, all the walls have approximately same results. Results for critical load combination of China were the most conservative and critical load combination of Pakistan were the most tolerant.

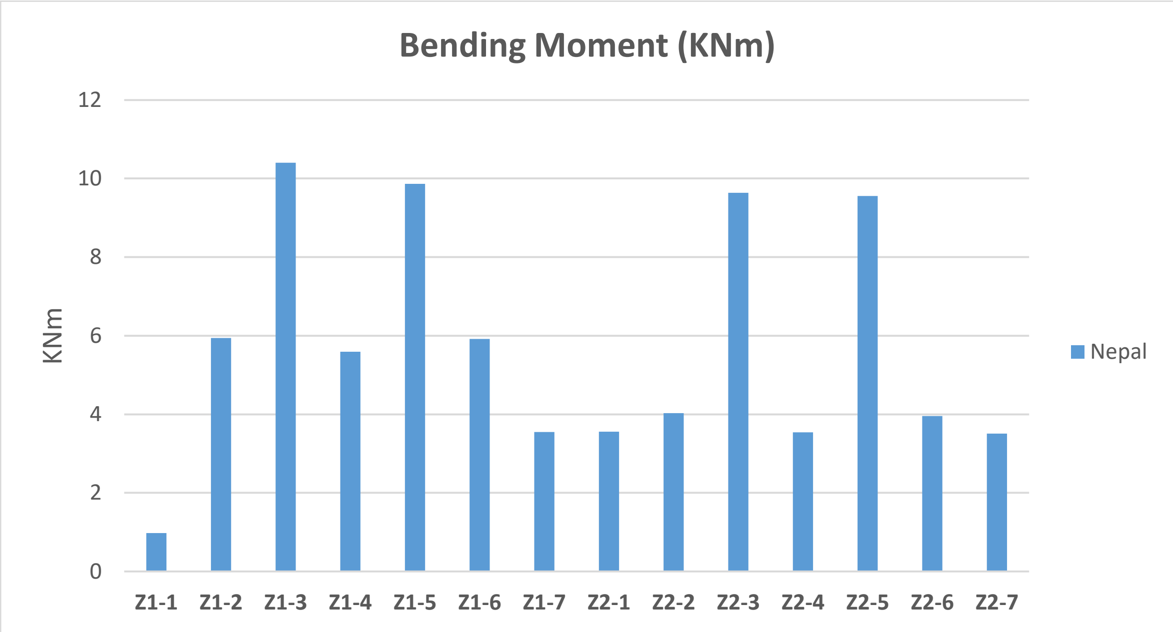

Figure 85 Comparison of bending moments, all walls along x-axis, z section, school WPL

Bending moment distribution at z levels shows us that the more is the width of the pier (Z1-3, Z1-5, Z2-3, Z2-5), the higher its bending moment level is.

7.2.2.3.3 Shear force

Shear Forces at all piers were determined at base cross sections and then plotted in order to compare these results for all regions with different critical load combination. Figure 86 shows the shear forces for door wall along x- axis with piers X1-1, X1-2, X1-3, X1-4, X1-5, X1-6, X1-7, X1-8, X1-9 and X1-10. Figure 87 shows the shear forces for window wall along x-axis with piers X2-1, X2-2, X2-3, X2-4, X2-5, X2-6, X2-7, X2-8, X2-9, X2-10, X2-11, X2-12 and X2-13. Table 45 shows the data for all the piers in door wall along x-axis and Table 46 shows the data for all the piers in window wall along x-axis. Figure 88 shows the shear forces for all the walls along y- axis with piers Y1-1, Y2-1, Y3-1, Y4-1 and Table 47 shows the data for all the piers in all the walls along y-axis. Figure 89 shows the shear forces only for Nepal region for the piers at z section level for both door and window wall: Z1-1, Z1-2, Z1-3, Z1-4, Z1-5, Z1-6 Z1-7, Z2-1, Z2-2, Z2-3, Z2-4, Z2-5, Z2-6 and Z2-7. Table 48 shows the data for all the piers at z level for both door and window wall along x-axis.

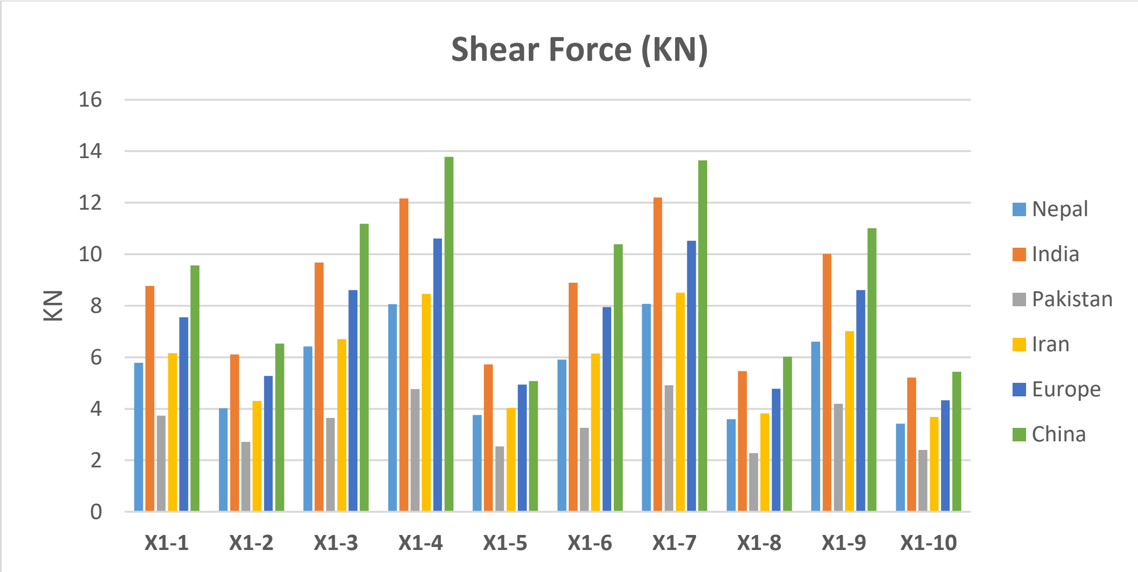

Figure 86 Comparison of shear forces, door wall, school WPL

Looking at the elevation view of door wall along x-axis of school WPL building, we can state that the shear force is high for the piers with sizeable width and having no windows portion (X1-4, X1-7) and is less for piers with no windows or doors. Results for China and India were the most conservative among all the countries and the critical load combination of Nepal and Iran codes were showing almost the same results. Moreover, results of Pakistan critical load combination were most tolerant.

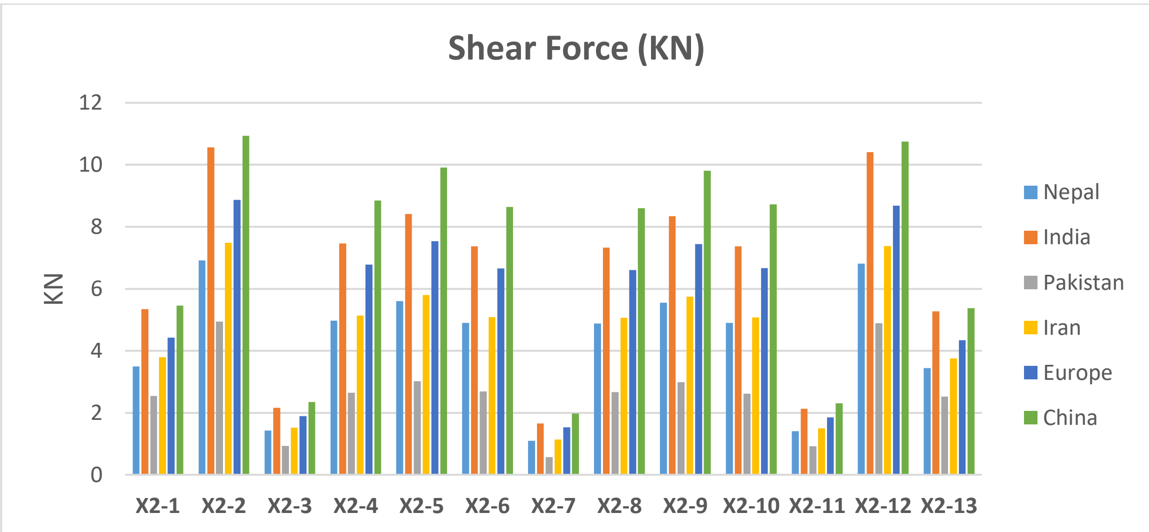

Figure 87 Comparison of shear forces, window wall, school WPL

Again looking at the elevation view of window wall along x-axis of school WPL building, we can clearly see that the shear force is high for the piers having windows portion (X2-2, X2-4, X2-6, X2-8, X-10 and X2-12) and also for piers with sizeable width (X2-5, X2-9) and is less for piers with no windows or doors. Again results for critical load combination of India and China were the most conservative while Pakistan was most tolerant. Moreover, critical load combination of Nepal and Iran were almost the same.

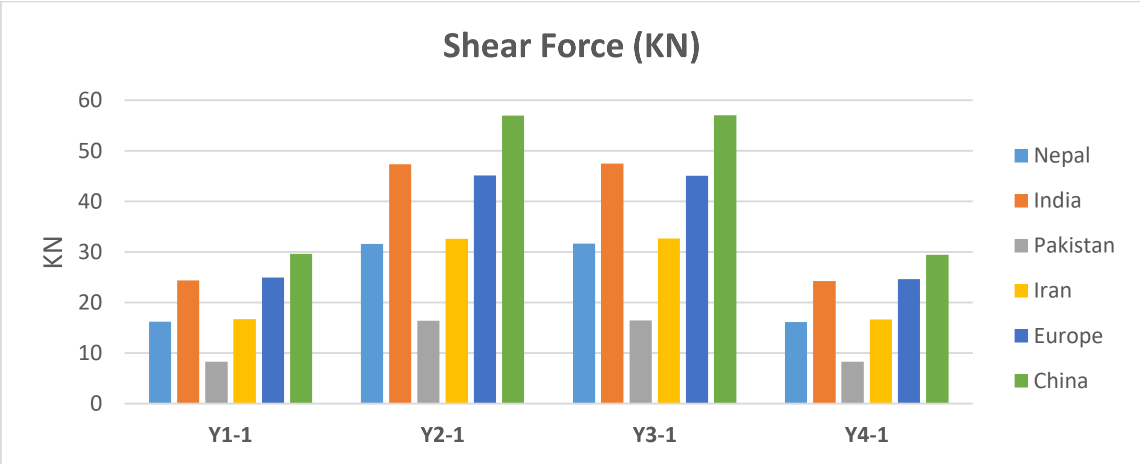

Figure 88 Comparison of shear forces, all walls along y-axis, school WPL

Considering the elevation view of walls along y-axis of school WPL building, we can notice that due to symmetry of the building, walls on outer side of building have less shear forces and vice versa. Results for critical load combination of China were the most conservative and critical load combination of Pakistan were the most tolerant. Moreover, critical load combination of Nepal and Iran were almost the same.

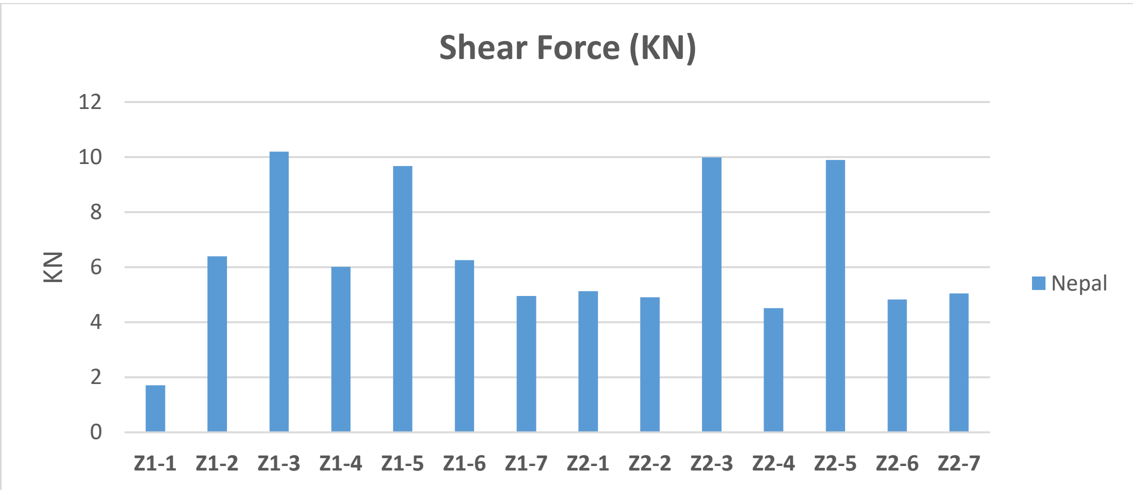

Figure 89 Comparison of shear forces, all walls along x-axis, z section, school WPL

Shear force distribution at z levels shows us that the more is the width of the pier (Z1-3, Z1-5, Z2-3, Z2-5), the higher its shear force level is.

7.2.2.4 House PL

For the internal forces estimation of house PL building, the structure is represented as a frame of piers, as is demonstrated in Figure 90. The lower end of each pier is fixed to form a cantilever pier which will represent the worst case scenario. At the plinth or base level there is a vast distribution of forces. To consider the connection of beams with the masonry pier and to be more close to the realistic behaviour of the building, we would also consider cross sections at z levels shown in elevation view in Figure 91 and Figure 92. This schematization will decrease the length of the piers and would also change the restrains of the piers considered.

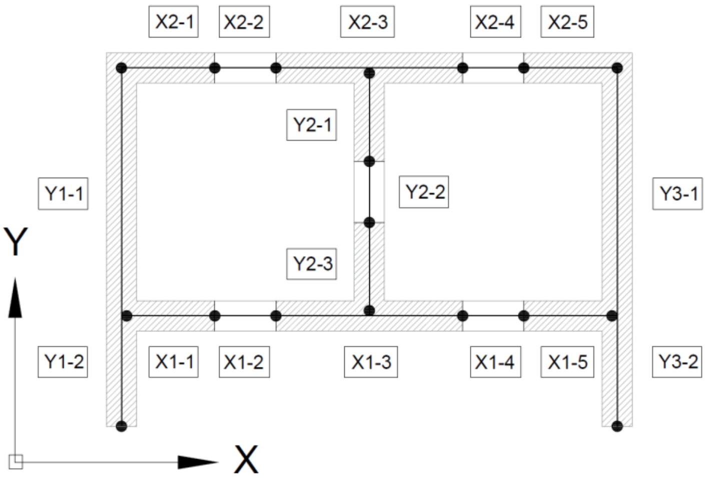

Figure 90 Piers layout for house PL

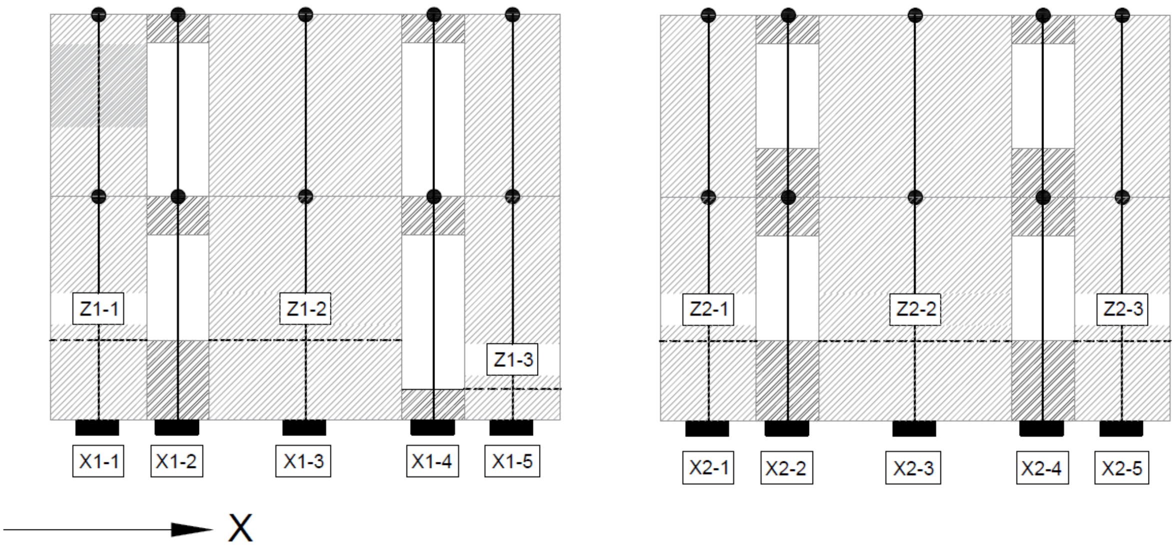

Figure 91 Piers arrangement for house PL along X axis: door wall (left); window wall (right)

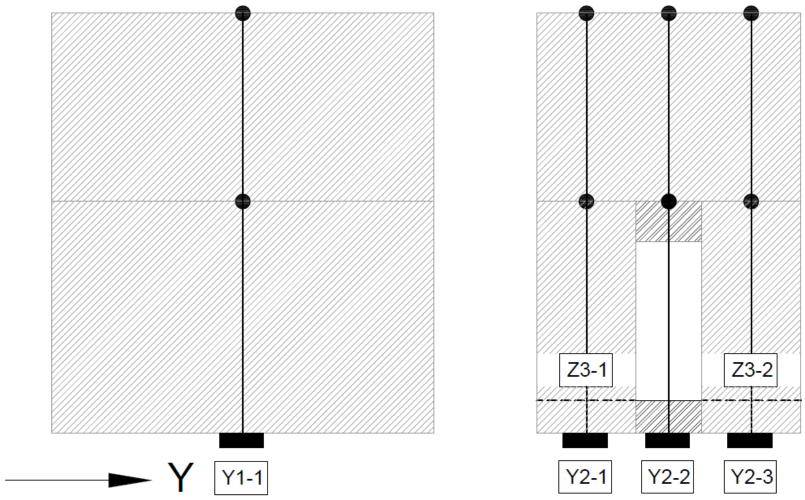

Figure 92 Piers arrangement for house PL along Y axis: exterior wall (left); interior wall (right)

7.2.2.4.1 Axial Force

Using section cut procedure in SAP2000 at base level of house PL building while looking at internal forces in z-direction of local axis, the axial forces at all piers were determined and then plotted in order to compare these results for all regions with different critical load combination. Figure 93 shows the axial forces for door wall along x- axis with piers X1-1, X1-2, X1-3, X1-4 and X1-5. Figure 94 shows the axial forces for window wall along x-axis with piers X2-1, X2-2, X2-3, X2-4 and X2-5. Table 49 shows the data for all the piers in door wall along x-axis and Table 50 shows the data for all the piers in window wall along x-axis. Figure 95 shows the axial forces for all the walls along y- axis with piers Y1-1, Y2-1, Y2-2, Y2-3, Y3-1, Y3-2 and Table 51 shows the data for all the piers in all the walls along y-axis. Figure 96 shows the axial forces only for Nepal region for the piers at z section level for both door and window wall along x axis and interior wall along y axis: Z1-1, Z1-2, Z1-3, Z2-1, Z2-2, Z2-3, Z3-1 and Z3-2. Table 52 shows the data for all the piers at z level for both door and window wall along x-axis and interior wall along y axis.

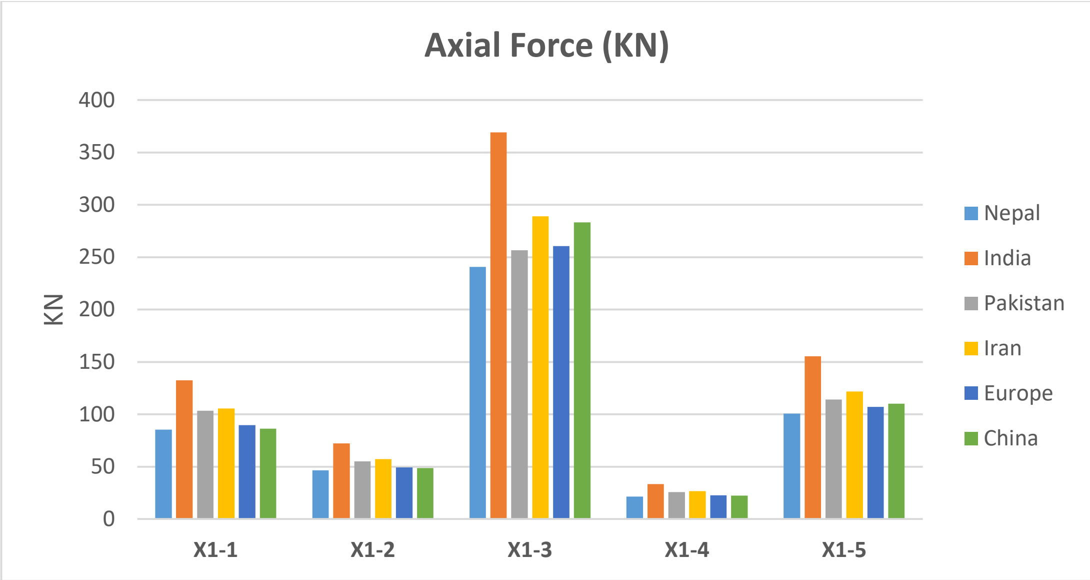

Figure 93 Comparison of axial forces, door wall, house PL

Looking at the elevation view of door wall along x-axis of house PL building, we can generally state that the axial force is lower for the piers having doors or windows portion (X1-2, X1-4) and is maximum for piers with sizeable width (X1-3). Results for India were the most conservative among all the countries and the critical load combination of Pakistan and Iran codes were showing almost the same results. Moreover, results of Nepal critical load combination were more similar to the ones of Europe and China.

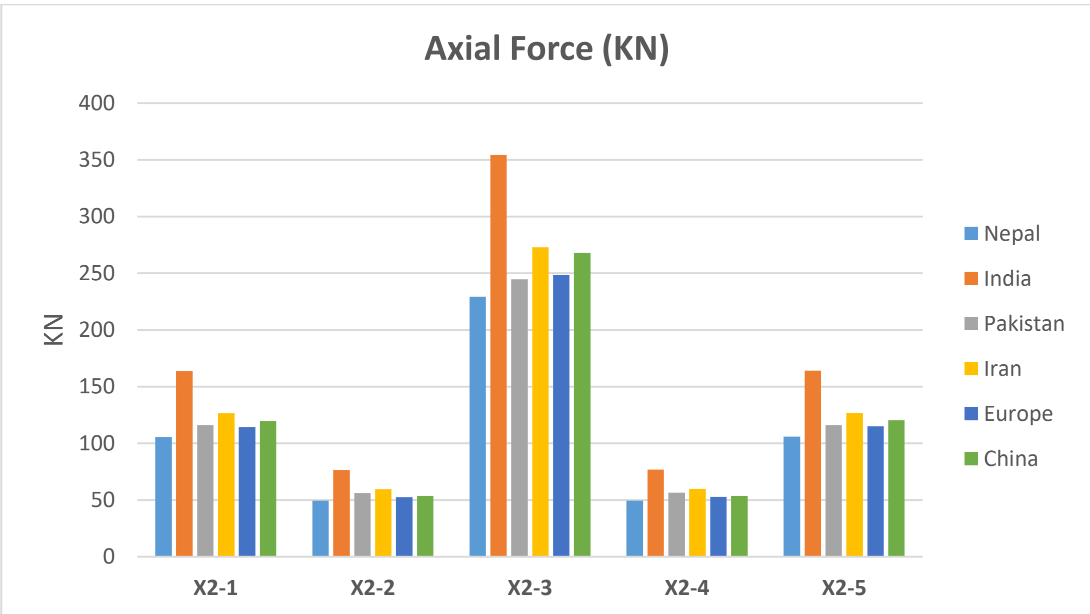

Figure 94 Comparison of axial forces, window wall, house PL

Again looking at the elevation view of window wall along x-axis of house PL building, we can clearly see that the axial forces have large values for the piers with large width and no windows (X2-3) while identical distribution can be seen for piers with windows portion and piers with narrow width. Again results for critical load combination of India were the most conservative and critical load combination of Nepal, Europe and China were the most tolerant.

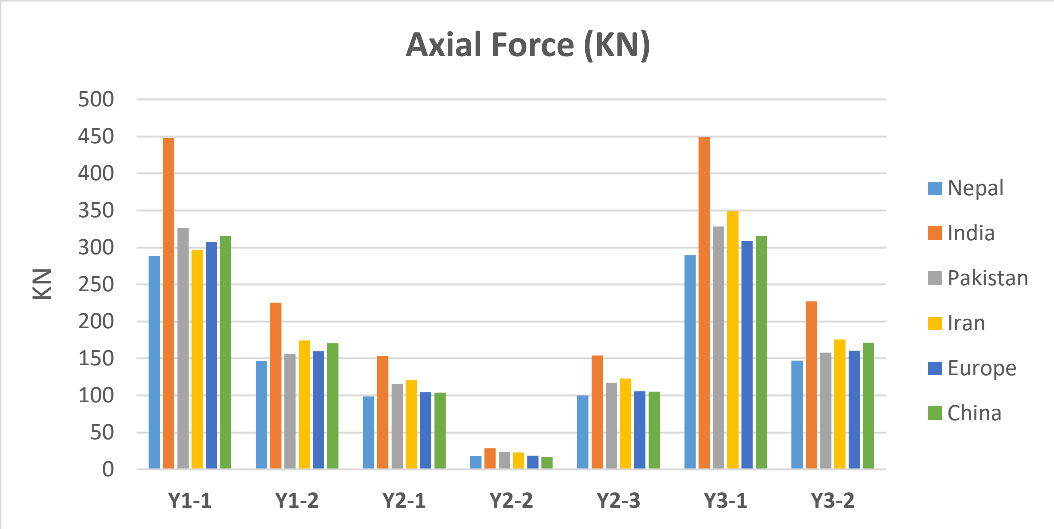

Figure 95 Comparison of axial forces, all walls along y-axis, house PL

Considering the elevation view of walls along y-axis of house PL building, we can notice that due to symmetry of the building, exterior walls have identical behaviour (Y1-1, Y1-2 and Y3-1, Y3-2). Pier with a door portion in interior wall have lowest axial forces values (Y2-2). Results for critical load combination of India were the most conservative and critical load combination of Nepal, Europe and China were the most tolerant.

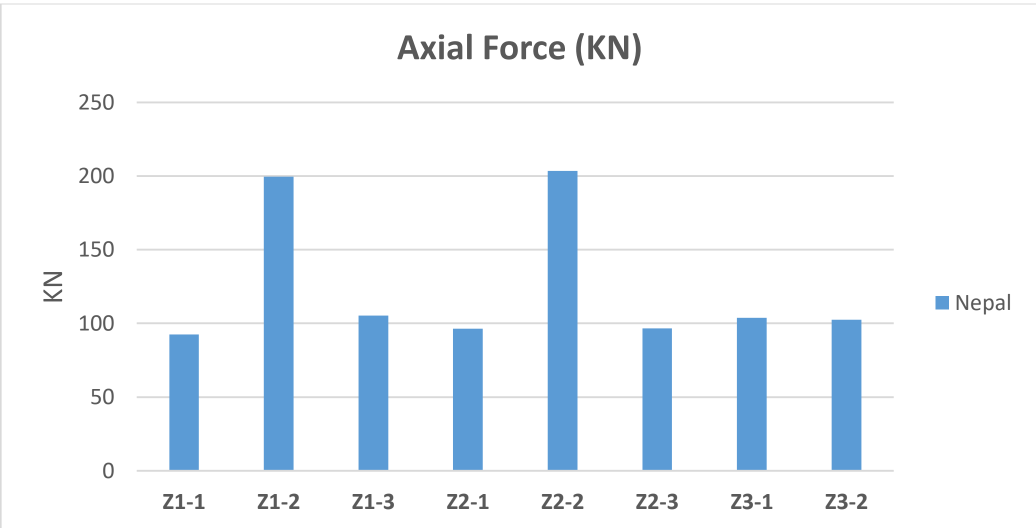

Figure 96 Comparison of axial forces, all walls along x and y axis, z section, house PL

Axial forces distribution at z levels shows us that the more is the width of the pier (Z1-2, Z2-2), the higher its axial force level is. Also we can state that the axial forces at z levels are lesser as compared to axial forces at base levels.

7.2.2.4.2 Bending moment

The bending moment at all piers were determined at base cross sections and then plotted in order to compare these results for all regions with different critical load combination. Figure 97 shows the bending moments for door wall along x- axis with piers X1-1, X1-2, X1-3, X1-4 and X1-5. Figure 98 shows the bending moments for window wall along x-axis with piers X2-1, X2-2, X2-3, X2-4 and X2-5. Table 53 shows the data for all the piers in door wall along x-axis and Table 54 shows the data for all the piers in window wall along x-axis. Figure 99 shows the bending moments for all the walls along y- axis with piers Y1-1, Y1-2, Y2-1, Y2-2, Y2-3, Y3-1, Y3-2 and Table 55 shows the data for all the piers in all the walls along y-axis. Figure 100 shows the bending moment only for Nepal region for the piers at z section level for both door and window wall along x axis and interior wall along y axis: Z1-1, Z1-2, Z1-3, Z2-1, Z2-2, Z2-3, Z3-1 and Z3-2. Table 56 shows the data for all the piers at z level for both door and window wall along x-axis and interior wall along y axis.

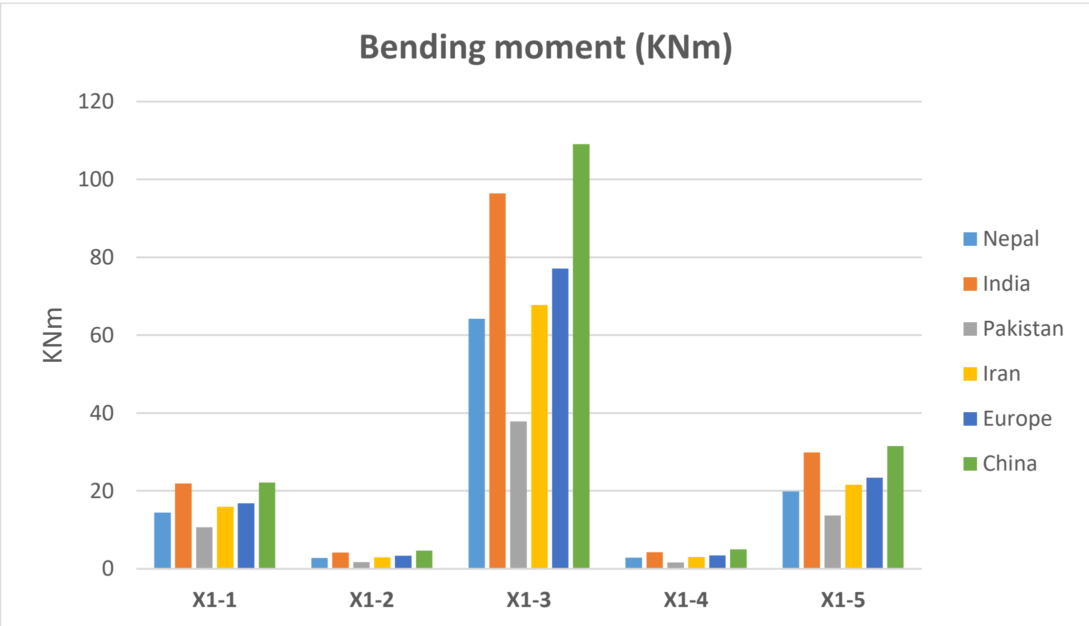

Figure 97 Comparison of bending moments, door wall, house PL

Looking at the elevation view of door wall along x-axis of house PL building, we can generally state that the bending moment is lower for the piers having doors and windows portion (X1-2, X1-4) and is maximum for piers with sizeable width (X1-3). Results for China and India were the most conservative among all the countries and the critical load combination of Nepal and Iran codes were showing almost the same results. Moreover, results of Pakistan critical load combination were most tolerant.

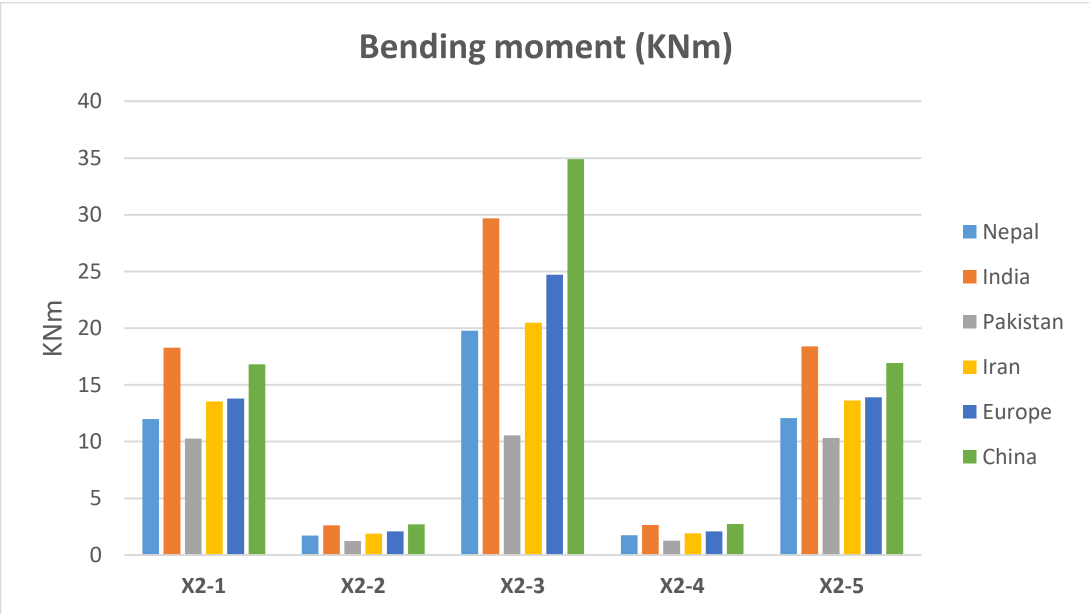

Figure 98 Comparison of bending moments, window wall, house PL

Again looking at the elevation view of window wall along x-axis of house PL building, we can clearly see that the bending moments have large values for the pier with large width and no windows (X2-3) while identical distribution can be seen for piers with windows portion (X2-2, X2-4). Again results for critical load combination of India and China were the most conservative while Pakistan was most tolerant. Moreover, critical load combination of Nepal and Iran were almost the same.

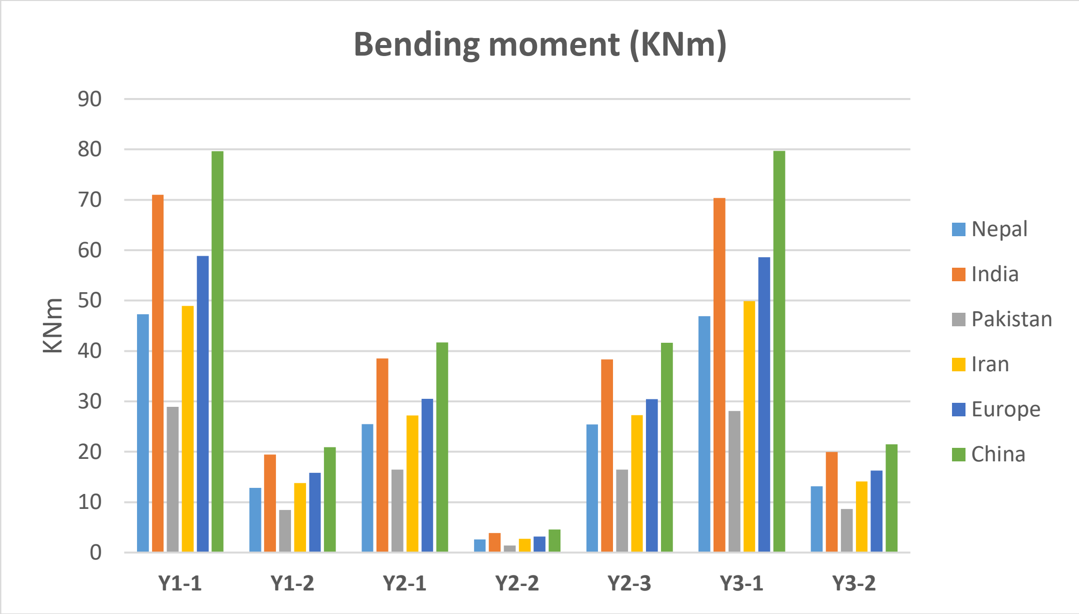

Figure 99 Comparison of bending moments, all walls along y-axis, house PL

Considering the elevation view of walls along y-axis of house PL building, we can notice that due to symmetry of the building, exterior walls have identical behaviour (Y1-1, Y1-2 and Y3-1, Y3-2). Pier with a door portion in interior wall have lowest axial forces values (Y2-2). Results for critical load combination of India and China were the most conservative and critical load combination of Pakistan were the most tolerant.

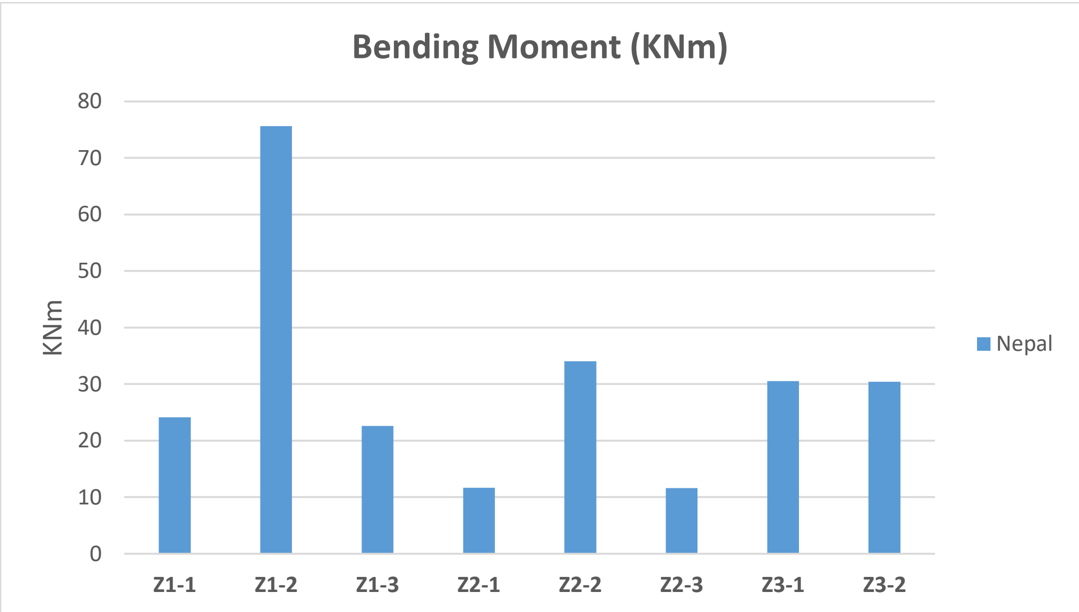

Figure 100 Comparison of bending moments, all walls along x and y axis, z section, house PL

Bending moment distribution at z levels shows us that the more is the width of the pier (Z1-2), the higher its bending moment level is. Also the bending moments at z levels of door wall are approximately double as compared to shear forces at z levels of window wall.

7.2.2.4.3 Shear force

Shear Forces at all piers were determined at base cross sections and then plotted in order to compare these results for all regions with different critical load combination. Figure 101 shows the shear forces for door wall along x- axis with piers X1-1, X1-2, X1-3, X1-4 and X1-5. Figure 102 shows the shear forces for window wall along x-axis with piers X2-1, X2-2, X2-3, X2-4 and X2-5. Table 57 shows the data for all the piers in door wall along x-axis and Table 58 shows the data for all the piers in window wall along x-axis. Figure 103 shows the shear forces for all the walls along y- axis with piers Y1-1, Y1-2, Y2-1, Y2-2, Y2-3, Y3-1, Y3-2 and Table 59 shows the data for all the piers in all the walls along y-axis. Figure 104 shows the shear forces only for Nepal region for the piers at z section level for both door and window wall along x axis and interior wall along y axis: Z1-1, Z1-2, Z1-3, Z2-1, Z2-2, Z2-3, Z3-1 and Z3-2. Table 60 shows the data for all the piers at z level for both door and window wall along x-axis and interior wall along y axis.

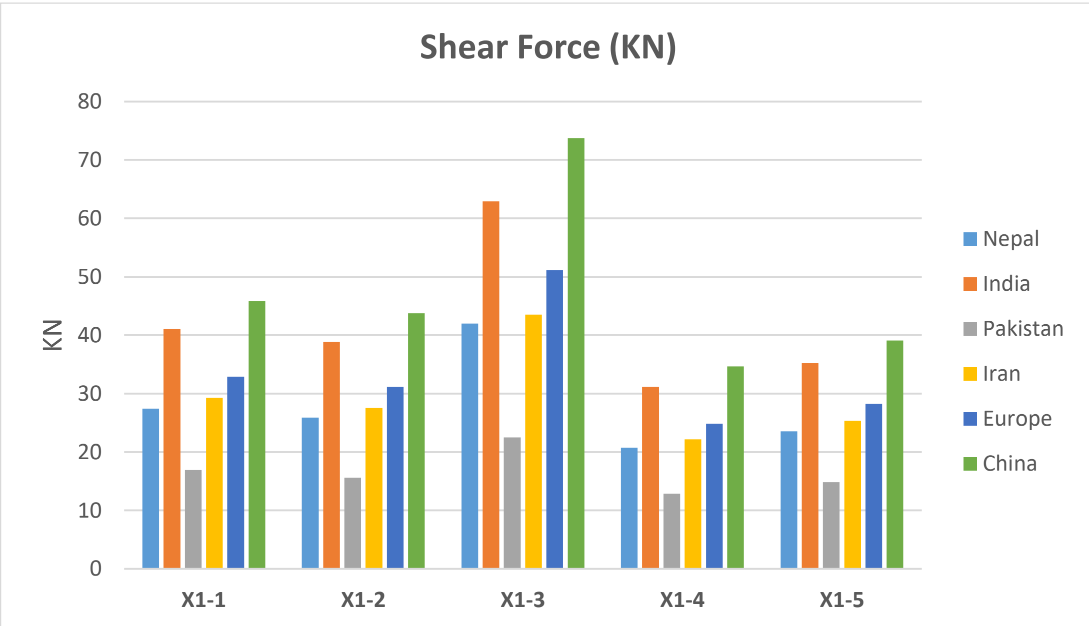

Figure 101 Comparison of shear forces, door wall, house PL

Looking at the elevation view of door wall along x-axis of house PL building, we can state that the shear force is high for the piers having sizeable width with no window or door portion (X1-3) and is less for piers with windows or doors. Results for China and India were the most conservative among all the countries and the critical load combination of Nepal and Iran codes were showing almost the same results. Moreover, results of Pakistan critical load combination were most tolerant.

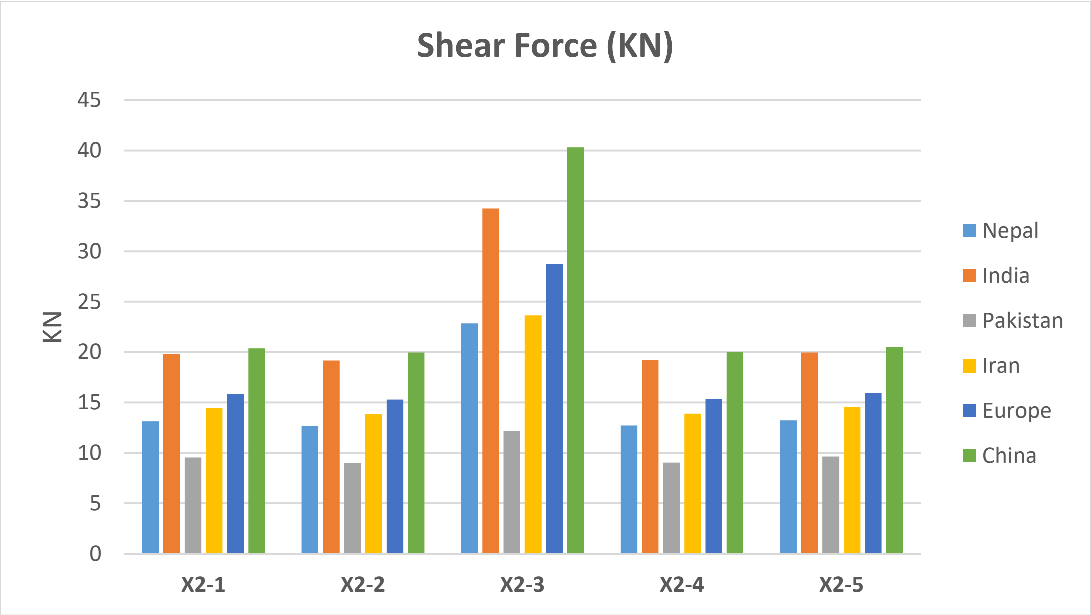

Figure 102 Comparison of shear forces, window wall, house PL

Again looking at the elevation view of window wall along x-axis of house PL building, we can clearly see that the shear force is high for the piers having sizeable width with no window or door portion (X1-3) and is less for piers with windows or doors. Again results for critical load combination of India and China were the most conservative while Pakistan was most tolerant. Moreover, critical load combination of Nepal and Iran were almost the same.

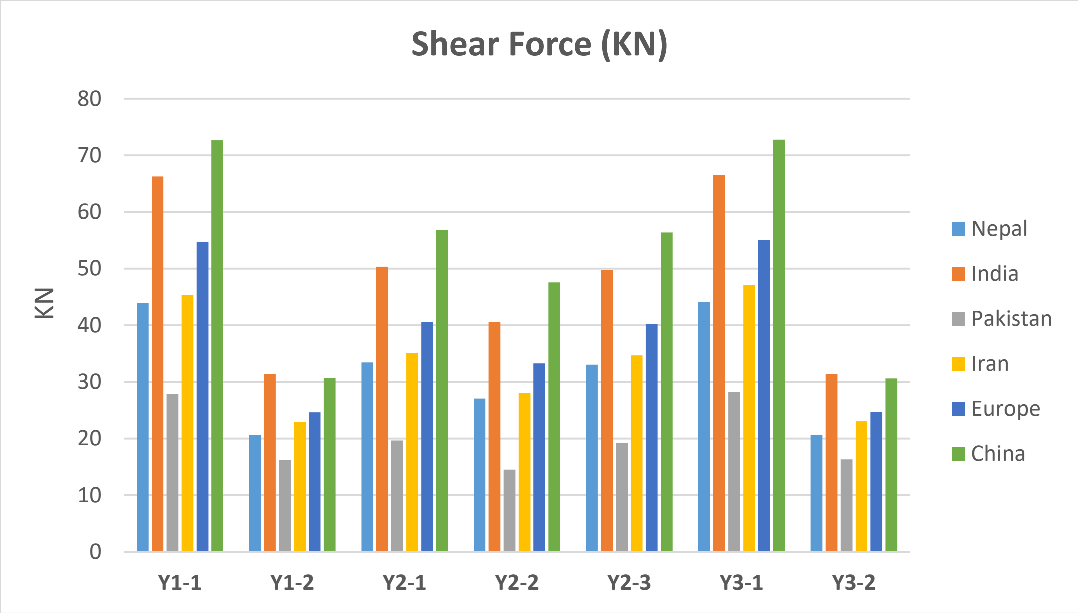

Figure 103 Comparison of shear forces, all walls along y-axis, house PL

Considering the elevation view of walls along y-axis of house PL building, we can notice that due to symmetry of the building, exterior walls have identical behaviour (Y1-1, Y1-2 and Y3-1, Y3-2). Results for critical load combination of India were the most conservative and critical load combination of Nepal, Europe and China were the most tolerant.

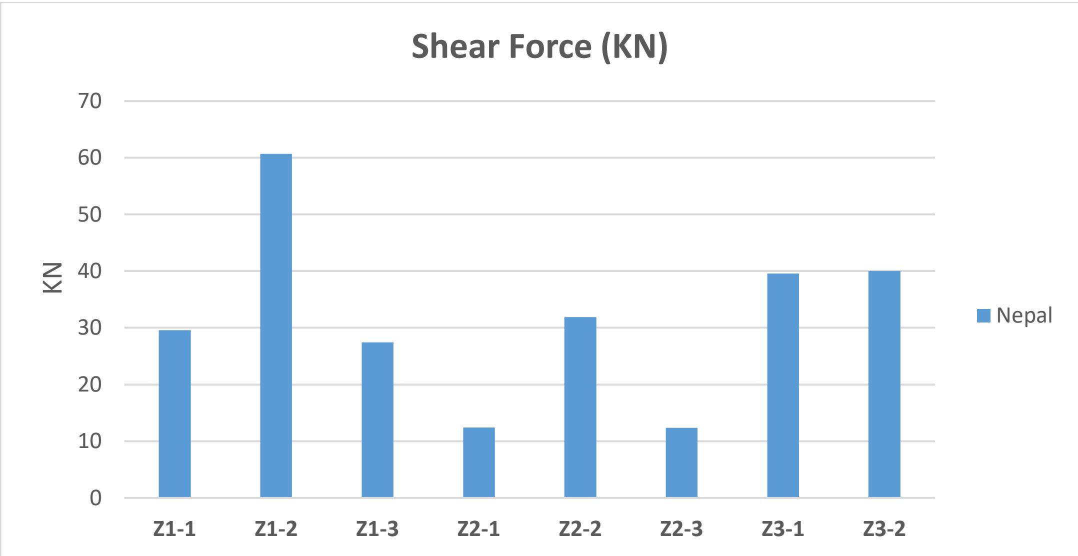

Figure 104 Comparison of shear forces, all walls along x and y axis, z section, house PL

Shear force distribution at z levels shows us that the more is the width of the pier (Z1-2), the higher its shear force level is. Also the shear forces at z levels of door wall are approximately double as compared to shear forces at z levels of window wall.

7.2.2.5 House WPL

Similar to house PL building, the internal forces estimation of house without plinth level building were less as compared to house with plinth level. The structure is represented as a frame of piers, as is demonstrated in Figure 105-Figure 107.

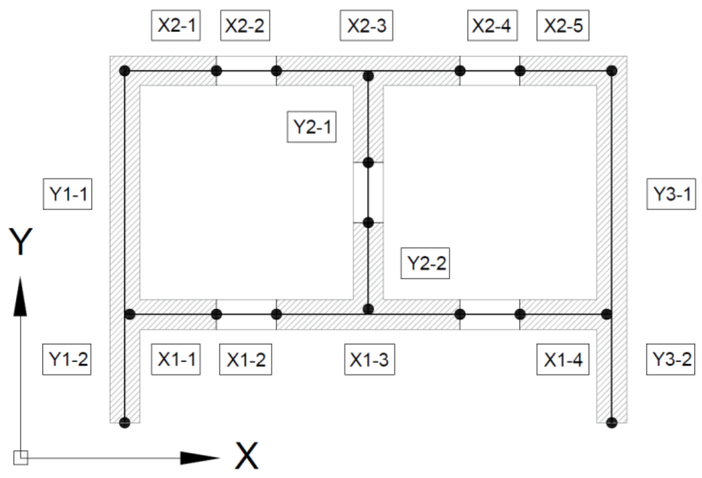

Figure 105 Piers layout for house WPL

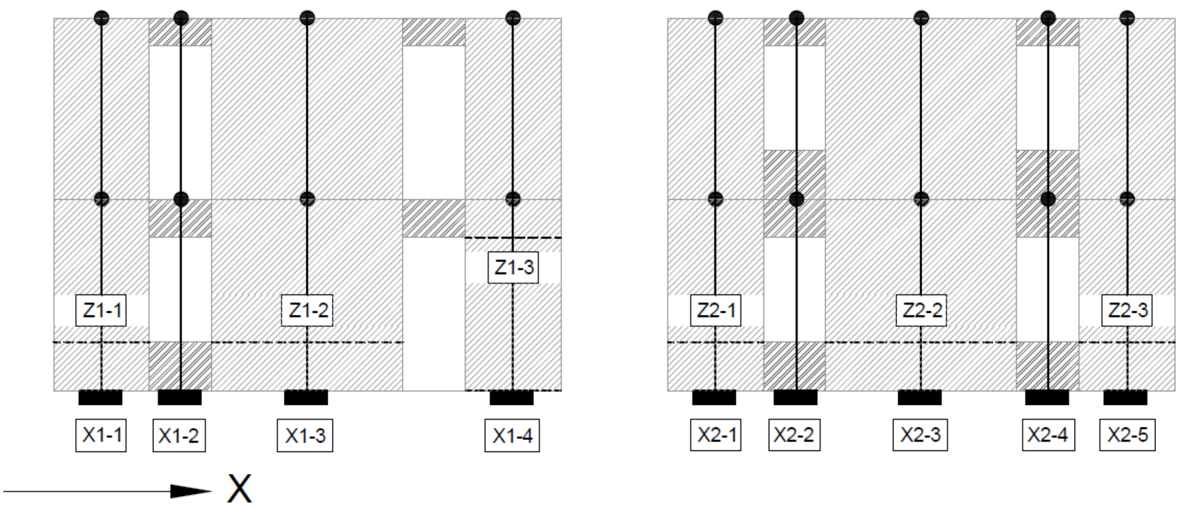

Figure 106 Piers arrangement for house WPL along X axis: door wall (left); window wall (right)

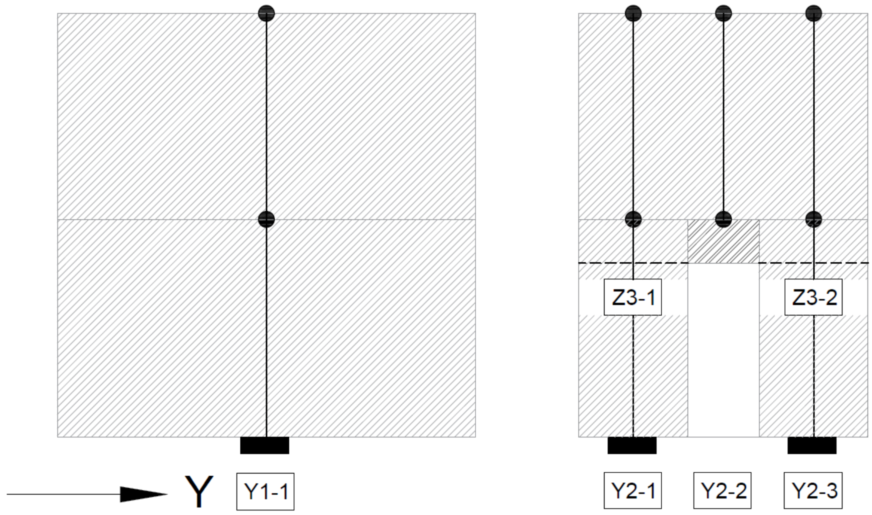

Figure 107 Piers arrangement for house WPL along Y axis: exterior wall (left); interior wall (right)

7.2.2.5.1 Axial Force

Using section cut procedure in SAP2000 at base level of house WPL building while looking at internal forces in z-direction of local axis, the axial forces at all piers were determined and then plotted in order to compare these results for all regions with different critical load combination. Figure 108 shows the axial forces for door wall along x- axis with piers X1-1, X1-2, X1-3 and X1-4. Figure 109 shows the axial forces for window wall along x-axis with piers X2-1, X2-2, X2-3, X2-4 and X2-5. Table 61 shows the data for all the piers in door wall along x-axis and Table 62 shows the data for all the piers in window wall along x-axis. Figure 110 shows the axial forces for all the walls along y- axis with piers Y1-1, Y2-1, Y2-2, Y3-1, Y3-2 and Table 63 shows the data for all the piers in all the walls along y-axis. Figure 111 shows the axial forces only for Nepal region for the piers at z section level for both door and window wall along x axis and interior wall along y axis: Z1-1, Z1-2, Z1-3, Z2-1, Z2-2, Z2-3, Z3-1 and Z3-2. Table 64 shows the data for all the piers at z level for both door and window wall along x-axis and interior wall along y axis.

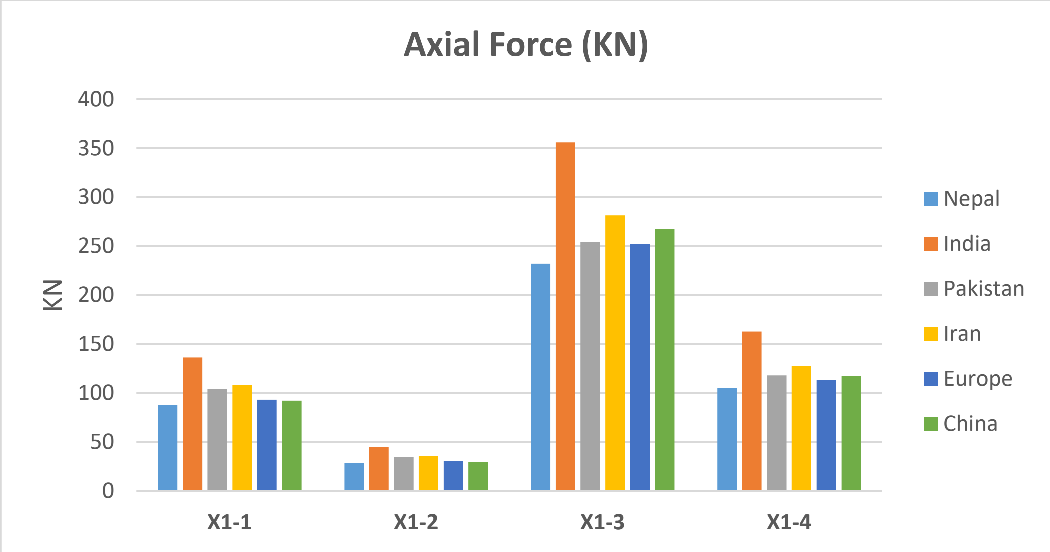

Figure 108 Comparison of axial forces, door wall, house WPL

Looking at the elevation view of door wall along x-axis of house WPL building, we can generally state that the axial force is lower for the piers having window portion (X1-2) and is maximum for piers with sizeable width (X1-3). Results for India were the most conservative among all the countries and the critical load combination of Pakistan and Iran codes were showing almost the same results. Moreover, results of Nepal critical load combination were more similar to the ones of Europe and China.

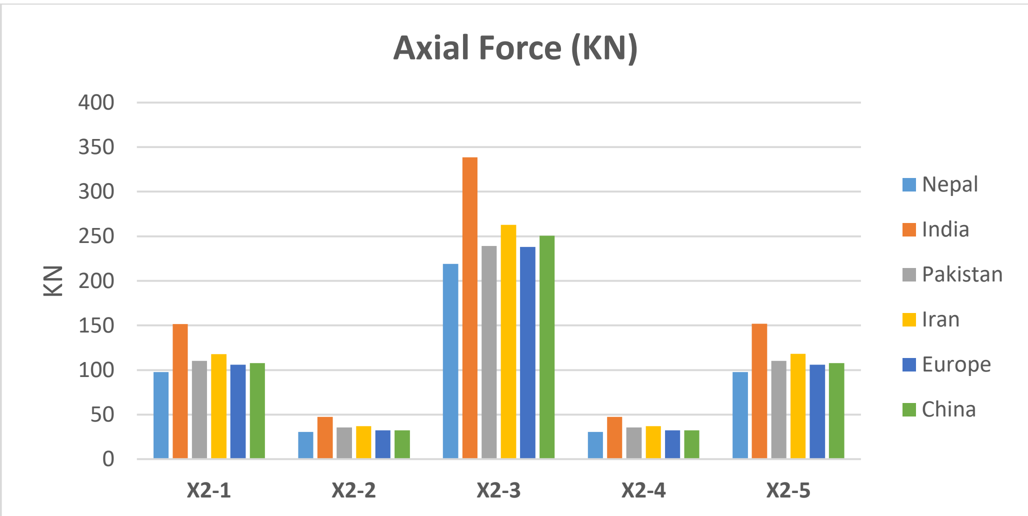

Figure 109 Comparison of axial forces, window wall, house WPL

Again looking at the elevation view of window wall along x-axis of house WPL building, we can clearly see that the axial forces have large values for the piers with large width and no windows (X2-3) while identical distribution can be seen for piers with windows portion and piers with narrow width. Again results for critical load combination of India were the most conservative and critical load combination of Nepal, Europe and China were the most tolerant.

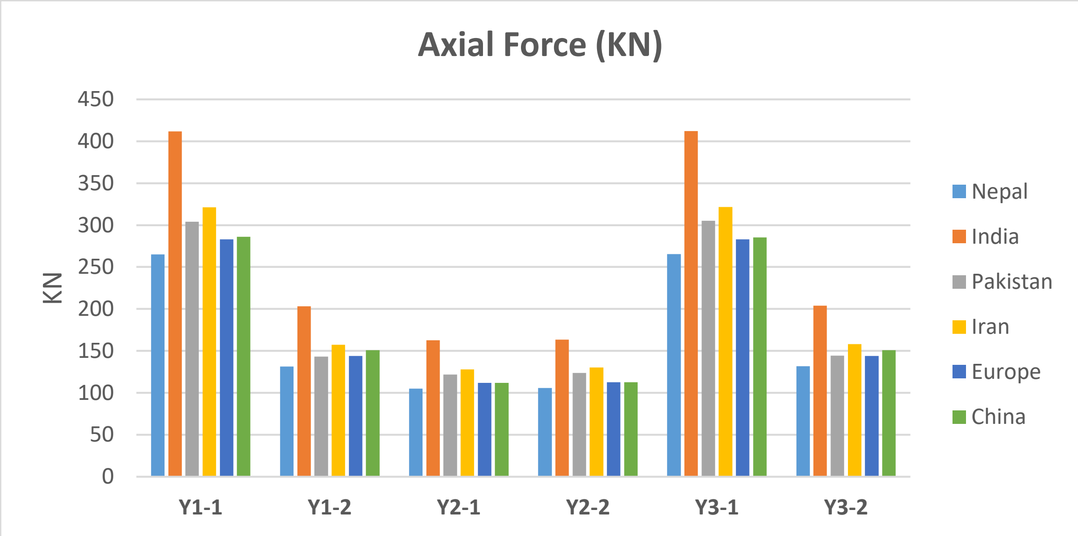

Figure 110 Comparison of axial forces, all walls along y-axis, house WPL

Considering the elevation view of walls along y-axis of house WPL building, we can notice that due to symmetry of the building, exterior walls have identical behaviour (Y1-1, Y1-2 and Y3-1, Y3-2). Pier in interior wall have lowest axial forces values (Y2-1, Y2-2). Results for critical load combination of India were the most conservative and critical load combination of Nepal, Europe and China were the most tolerant.

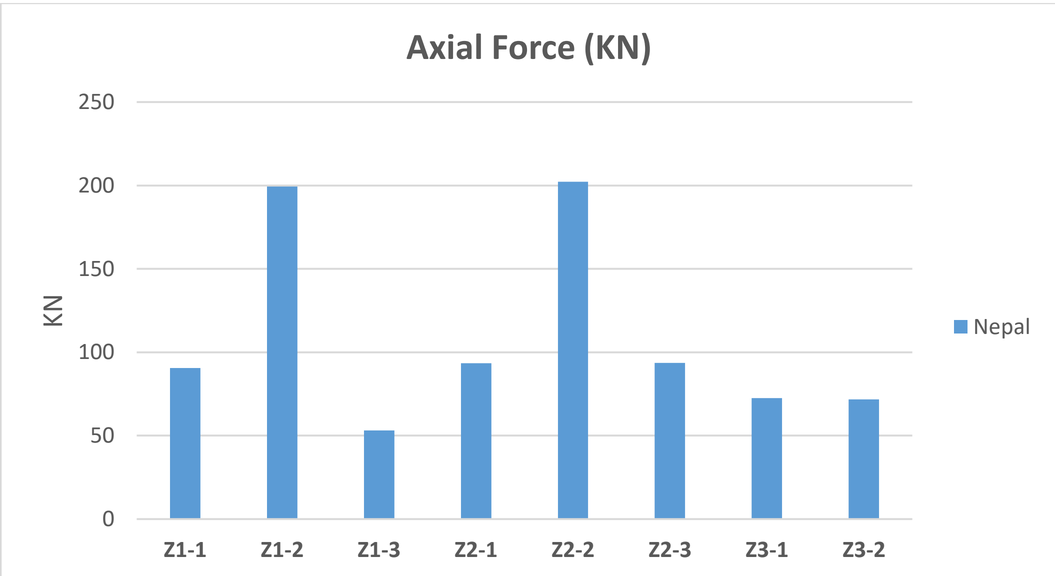

Figure 111 Comparison of axial forces, all walls along x and y axis, z section, house WPL

Axial forces distribution at z levels shows us that the more is the width of the pier (Z1-2, Z2-2), the higher its axial force level is. Also we can state that the axial forces at z levels are lesser as compared to axial forces at base levels.

7.2.2.5.2 Bending moment

The bending moment at all piers were determined at base cross sections and then plotted in order to compare these results for all regions with different critical load combination. Figure 112 shows the bending moments for door wall along x- axis with piers X1-1, X1-2, X1-3 and X1-4. Figure 113 shows the bending moments for window wall along x-axis with piers X2-1, X2-2, X2-3, X2-4 and X2-5. Table 65 shows the data for all the piers in door wall along x-axis and Table 66 shows the data for all the piers in window wall along x-axis. Figure 114 shows the bending moments for all the walls along y- axis with piers Y1-1, Y1-2, Y2-1, Y2-2, Y3-1, Y3-2 and Table 67 shows the data for all the piers in all the walls along y-axis. Figure 115 shows the bending moment only for Nepal region for the piers at z section level for both door and window wall along x axis and interior wall along y axis: Z1-1, Z1-2, Z1-3, Z2-1, Z2-2, Z2-3, Z3-1 and Z3-2. Table 68 shows the data for all the piers at z level for both door and window wall along x-axis and interior wall along y axis.

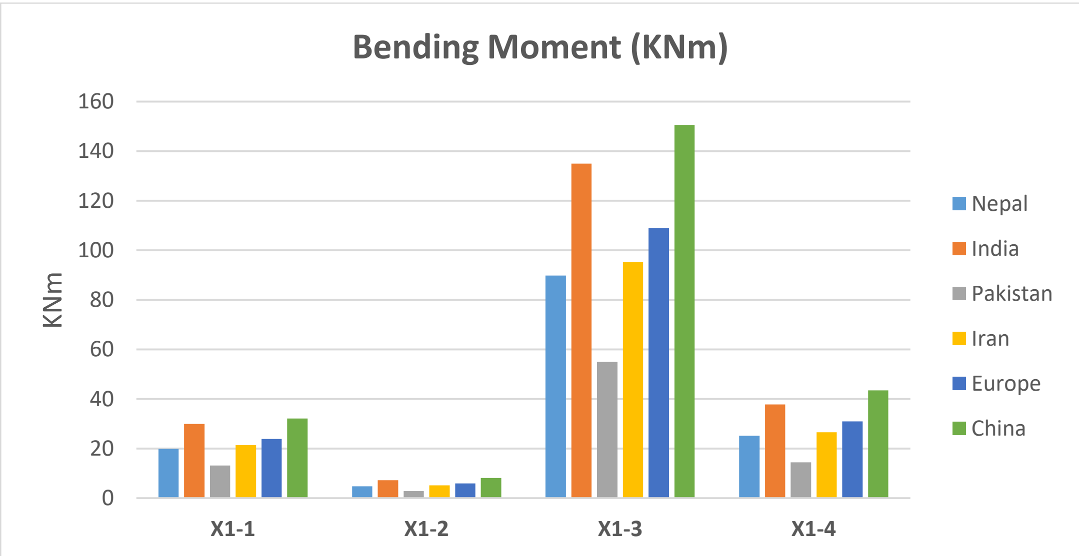

Figure 112 Comparison of bending moments, door wall, house WPL

Looking at the elevation view of door wall along x-axis of house WPL building, we can generally state that the bending moment is lower for the piers having window portion (X1-2) and is maximum for piers with sizeable width (X1-3). Results for China and India were the most conservative among all the countries and the critical load combination of Nepal and Iran codes were showing almost the same results. Moreover, results of Pakistan critical load combination were most tolerant.

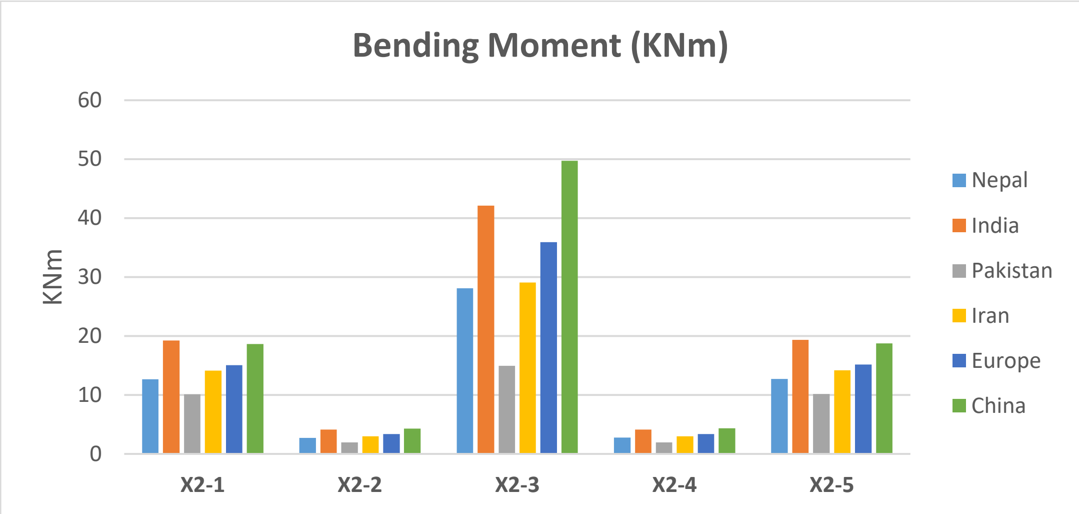

Figure 113 Comparison of bending moments, window wall, house WPL

Again looking at the elevation view of window wall along x-axis of house WPL building, we can clearly see that the bending moments have large values for the pier with large width and no windows (X2-3) while identical distribution can be seen for piers with windows portion (X2-2, X2-4). Again results for critical load combination of India and China were the most conservative while Pakistan was most tolerant. Moreover, critical load combination of Nepal and Iran were almost the same.

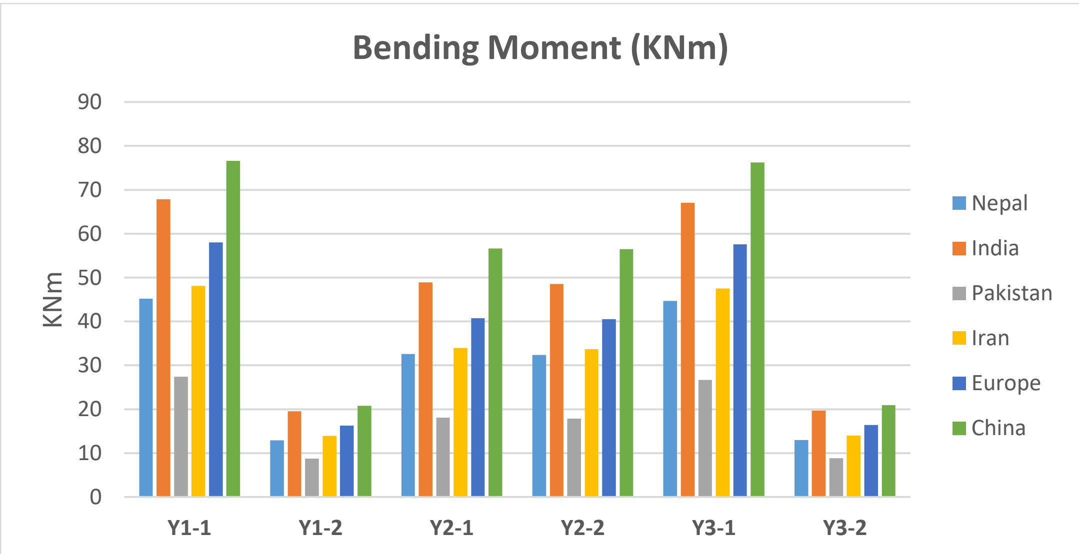

Figure 114 Comparison of bending moments, all walls along y-axis, house WPL

Considering the elevation view of walls along y-axis of house WPL building, we can notice that due to symmetry of the building, exterior walls have identical behaviour (Y1-1, Y1-2 and Y3-1, Y3-2). Pier with a door portion in interior wall have lowest axial forces values (Y2-1, Y2-2). Results for critical load combination of India and China were the most conservative and Pakistan were most tolerant.

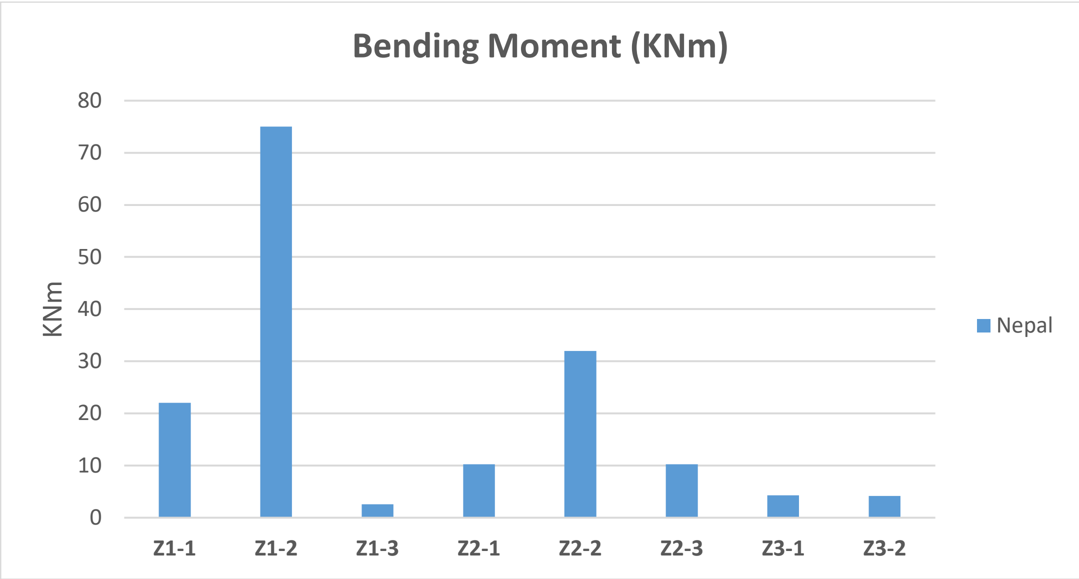

Figure 115 Comparison of bending moments, all walls along x and y axis, z section, house WPL

Bending moment distribution at z levels shows us that the more is the width of the pier (Z1-2), the higher its bending moment level is. Bending moments at z levels of door wall are approximately double as compared to shear forces at z levels of window wall. Also the higher the z section level is (Z1-3), the lower the bending moment values become.

7.2.2.5.3 Shear force

Shear Forces at all piers were determined at base cross sections and then plotted in order to compare these results for all regions with different critical load combination. Figure 116 shows the shear forces for door wall along x- axis with piers X1-1, X1-2, X1-3 and X1-4. Figure 117 shows the shear forces for window wall along x-axis with piers X2-1, X2-2, X2-3, X2-4 and X2-5. Table 69 shows the data for all the piers in door wall along x-axis and Table 70 shows the data for all the piers in window wall along x-axis. Figure 118 shows the shear forces for all the walls along y- axis with piers Y1-1, Y1-2, Y2-1, Y2-2, Y3-1, Y3-2 and Table 71 shows the data for all the piers in all the walls along y-axis. Figure 119 shows the shear forces only for

Nepal region for the piers at z section level for both door and window wall along x axis and interior wall along y axis: Z1-1, Z1-2, Z1-3, Z2-1, Z2-2, Z2-3, Z3-1 and Z3-2. Table 72 shows the data for all the piers at z level for both door and window wall along x-axis and interior wall along y axis.

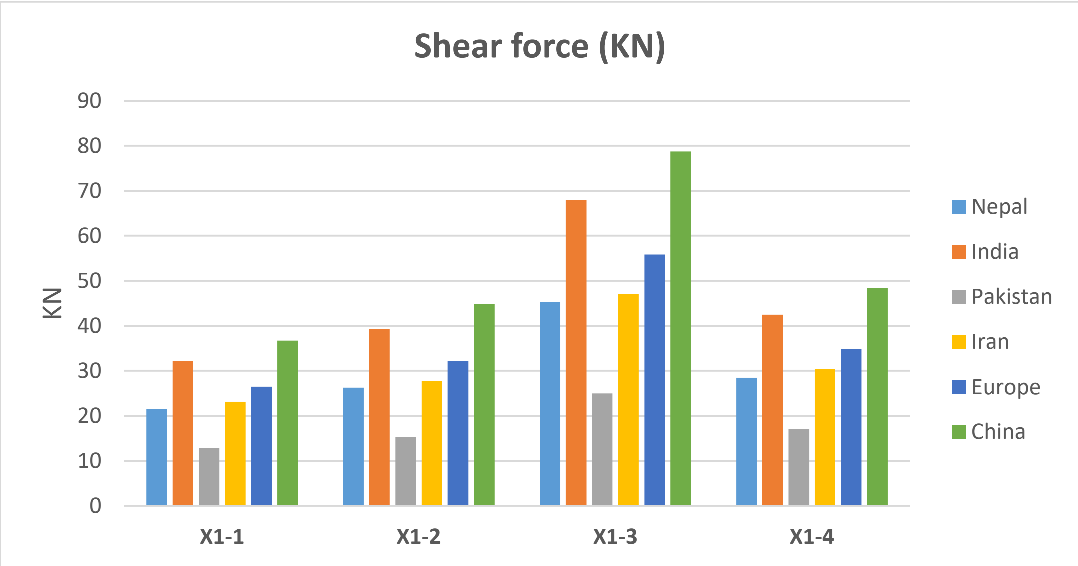

Figure 116 Comparison of shear forces, door wall, house WPL

Looking at the elevation view of door wall along x-axis of house WPL building, we can state that the shear force is high for the piers having sizeable width with no window or door portion (X1-3). Results for China and India were the most conservative among all the countries and the critical load combination of Nepal and Iran codes were showing almost the same results. Moreover, results of Pakistan critical load combination were most tolerant.

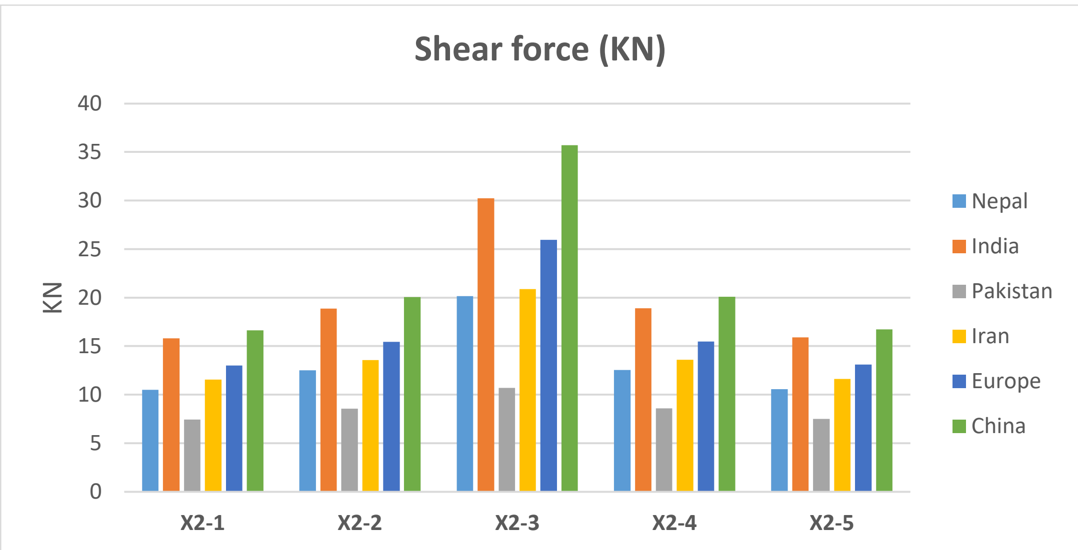

Figure 117 Comparison of shear forces, window wall, house WPL

Again looking at the elevation view of window wall along x-axis of house WPL building, we can clearly see that the shear force is high for the piers having sizeable width with no window or door portion (X1-3) and is less for piers with windows or doors. Again results for critical load combination of India and China were the most conservative while Pakistan was most tolerant. Moreover, critical load combination of Nepal and Iran were almost the same.

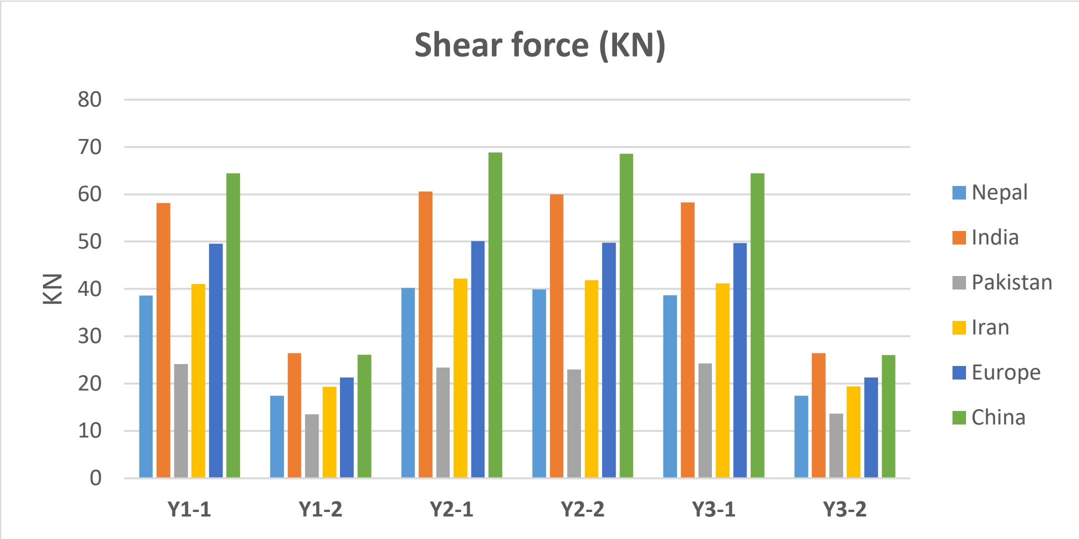

Figure 118 Comparison of shear forces, all walls along y-axis, house WPL

Considering the elevation view of walls along y-axis of house WPL building, we can notice that due to symmetry of the building, exterior walls have identical behaviour (Y1-1, Y1-2 and Y3-1, Y3-2). Results for critical load combination of India were the most conservative and critical load combination of Nepal, Europe and China were the most tolerant.

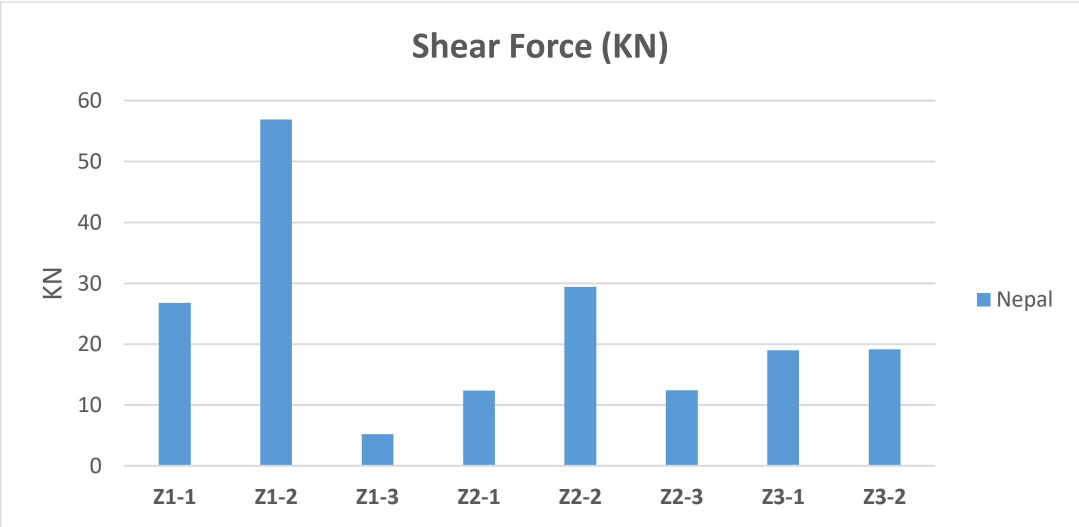

Figure 119 Comparison of shear forces, all walls along x and y axis, z section, house WPL

Shear force distribution at z levels shows us that the more is the width of the pier (Z1-2), the higher its shear force level is. Also the shear forces at z levels of door wall are approximately double as compared to shear forces at z levels of window wall.

8. Discussion and comparison between theoretical and numerical results

This paper is an attempt to contribute to a global research carried out by Smart Shelter Foundation aiming to improve current level of knowledge of masonry structure seismic behaviour and create a systematic approach to construction of non-engineered masonry buildings. As a part of the research, analytical calculations of structural response were made for the buildings presented in this case study according to national building codes of several countries, including Nepal, India, Pakistan, Iran, Europe and China.

The results of static analysis and dynamic analysis presented in the previous sections are compared to the theoretical values in terms of dead loads, fundamental periods, base shear, ratio of base shear to spectral accelerations and internal actions for both school and house buildings. This comparison is demonstrated in subsequent chapters.

8.1 Dead loads

The theoretical results were only available for buildings with plinth level (PL) therefore, the comparison will also be done only for buildings with plinth level. Figure 120 and Figure 121 shows the comparison between numerical results and theoretical results of the dead loads, including the self-weight and also the applied dead loads on the structures.

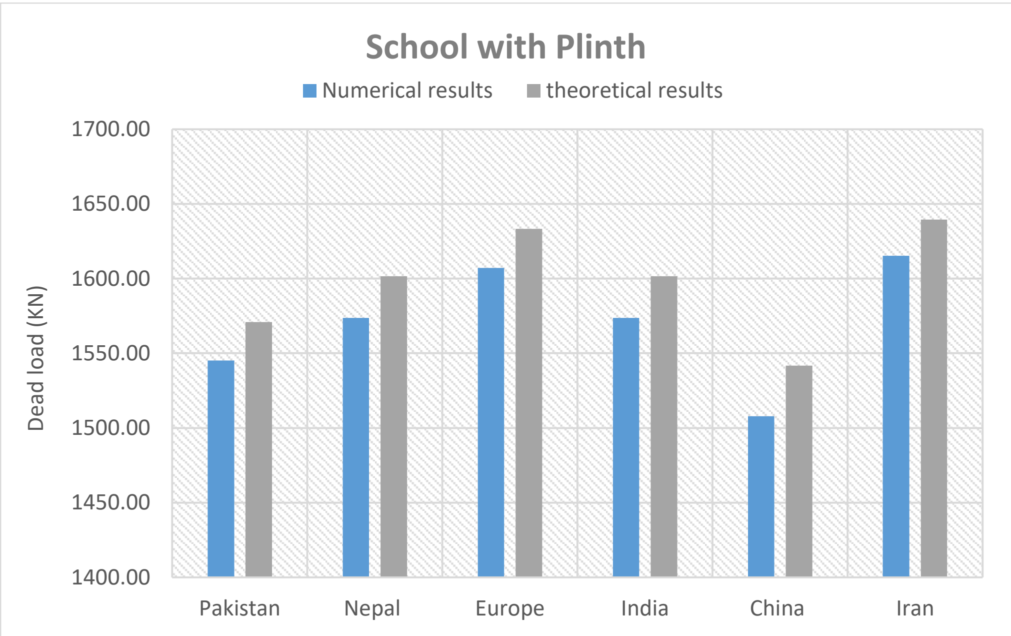

Figure 120 Comparison of dead loads, school PL

Theoretical results were more conservative as compared to the numerical results Around 2% difference was noted between numerical and theoretical results which can account for the fact that theoretical results were more detailed based oriented meaning, the dead loads of the building included the weights of doors, windows and roof structure along with the weights of masonry walls.

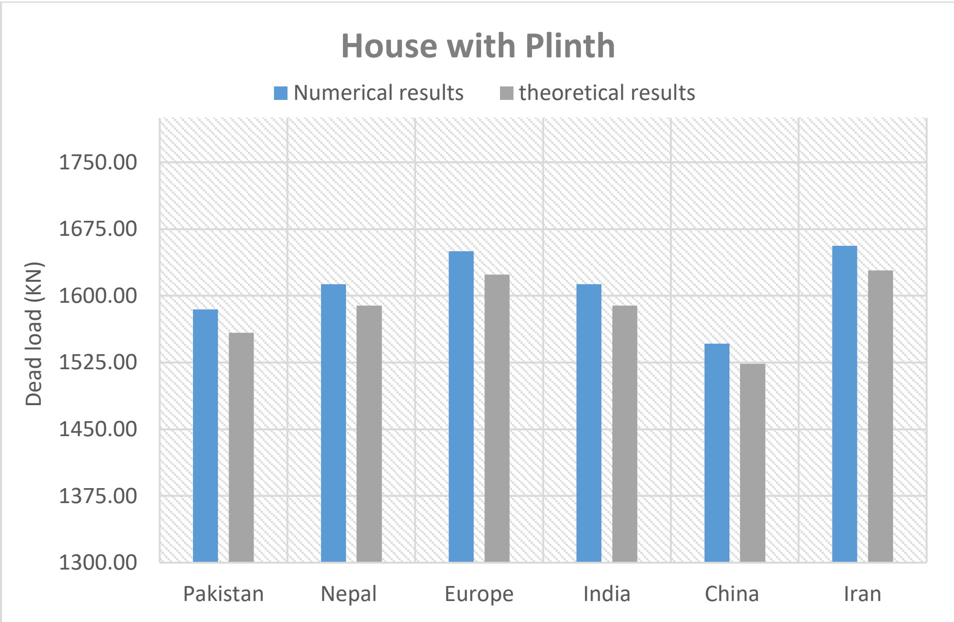

Figure 121 Comparison of dead loads, house PL

Again a difference of about 2% was determined between numerical and theoretical results. Considering house building, the numerical results were more on conservative side. This can be explained by the modelling mechanism of SAP2000 software. Since house building was more compact and had more connection points of walls as compared to school building therefore, SAP2000 can consider the materials in these connections twice, hence increasing the number of dead load of the model.

8.2 Fundamental period

The theoretical results were only available for buildings with plinth level (PL) therefore, the comparison will also be done only for buildings with plinth level. Figure 122 and Figure 123 shows the comparison between numerical results and theoretical results of the fundamental periods in both x and y axes.

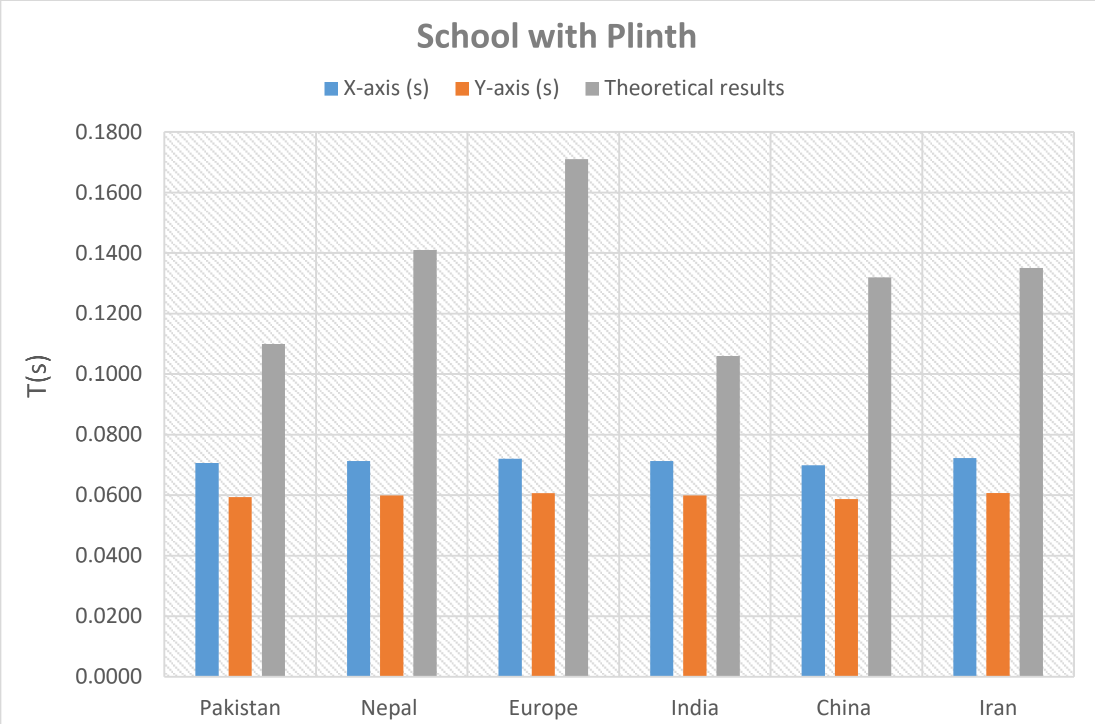

Figure 122 Comparison of fundamental periods, x and y axes, school PL

To compute the theoretical natural periods, all the building codes provide the formulas for frame structure, which is the reason we can see a huge difference between numerical and theoretical results. To model the buildings in SAP2000 software, wall system was used which is stiffer as compared to frame system and as a result of which we have lower values of periods of vibration. Also keeping in mind the percentages of mass ratio activated by these fundamental periods which is only around 30% in the case of numerical results while about 90% of mass ratio activation was considered in the case of theoretical results.

There is also a small difference between the fundamental period in x and y direction. This can be explained by the stiffness of the walls in both directions. Walls along y axis are four in number and they don't have any openings for windows and doors which makes them stiffer in that direction while on the other hand walls along x axis have openings for windows and doors which make them behave as piers connected by spandrels therefore, making them less stiff.

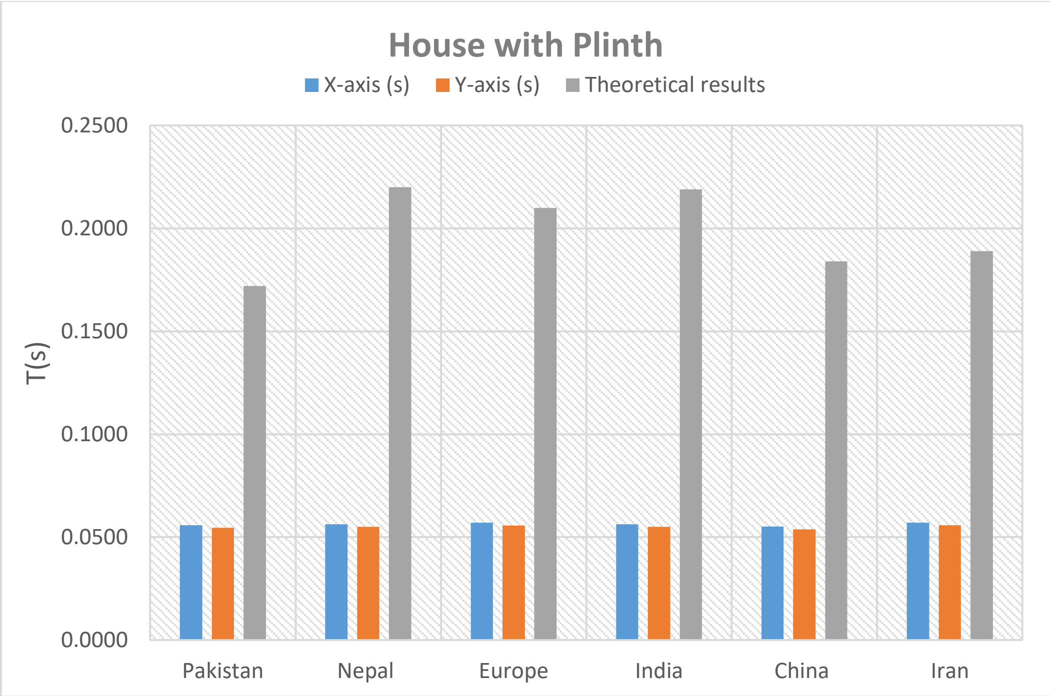

Figure 123 Comparison of fundamental periods, x and y axes, house PL

Similar to school PL building, house PL building also had large difference in numerical and theoretical results. To compute the theoretical natural periods, all the building codes provide the formulas for frame structure, which is the reason we can see a huge difference between numerical and theoretical results. To model the buildings in SAP2000 software, wall system was used which is stiffer as compared to frame system and as a result of which we have lower values of periods of vibration. Also keeping in mind the percentages of mass ratio activated by these fundamental periods which is only around 60% in the case of numerical results while about 90% of mass ratio activation was considered in the case of theoretical results.

8.3 Base shear

Basically the base shear is formulated by the multiplication of the static load to spectral acceleration. Spectral acceleration is then directly related to fundamental periods of the structure. Therefore, if we have high values of natural periods, we will get high values of spectral accelerations which will increase the values of base shear we can get after analysing a building.

The theoretical results were only available for buildings without plinth level (WPL) therefore, the comparison will also be done only for buildings without plinth level. Figure 124 and Figure

125 shows the comparison between numerical results and theoretical results of the base shear in both x and y axes.

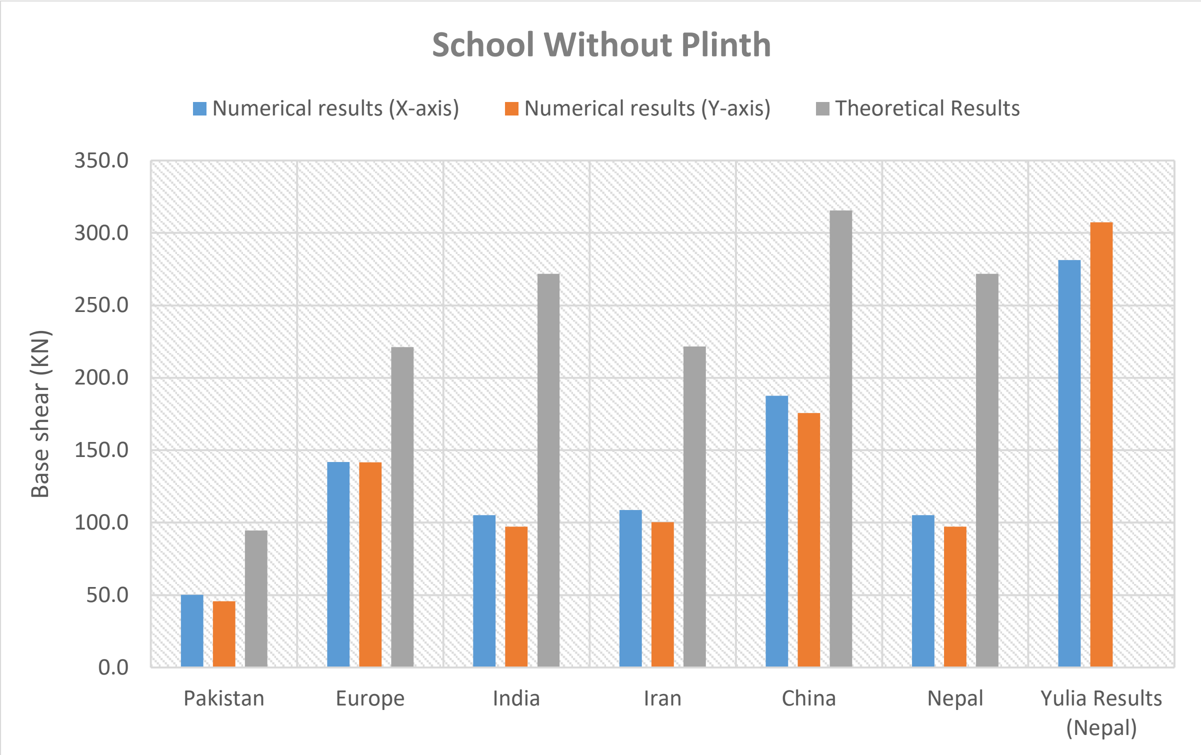

Figure 124 Comparison of base shear, x and y axes, school WPL

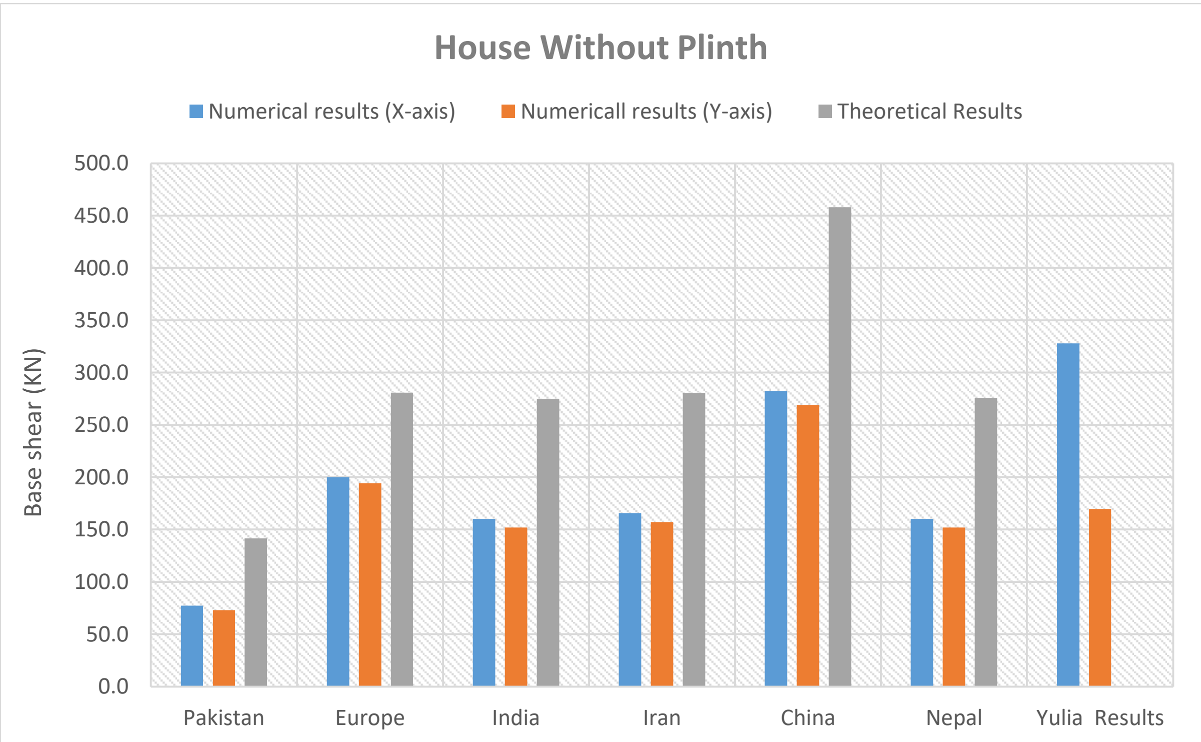

Figure 125 Comparison of base shear, x and y axes, house WPL

As explained above, base shear depends upon static load and the spectral acceleration values for a building. Theoretically 90% of mass ratio activation was considered which resulted in higher natural periods of a building which further resulted in higher spectral accelerations for a building and that is the reason for conservative base shear values of theoretical results as compared to numerical results. Yulia results for Nepal region were based on equivalent frame method and were close to theoretical results for Nepal region.

8.4 Ratio of base shear to spectral acceleration

To achieve these ratios, base shear results acquired through numerical method by the use of SAP2000 software were divided by the spectral acceleration values corresponding to the fundamental periods of numerical models. On the other hand, theoretical base shear results were divided by the maximum spectral acceleration values taken from design response spectra. The theoretical results were only available for buildings without plinth level (WPL) therefore, the comparison will also be done only for buildings without plinth level. Figure 126 shows the comparison between numerical results and theoretical results of the ratios of base shear to spectral acceleration.

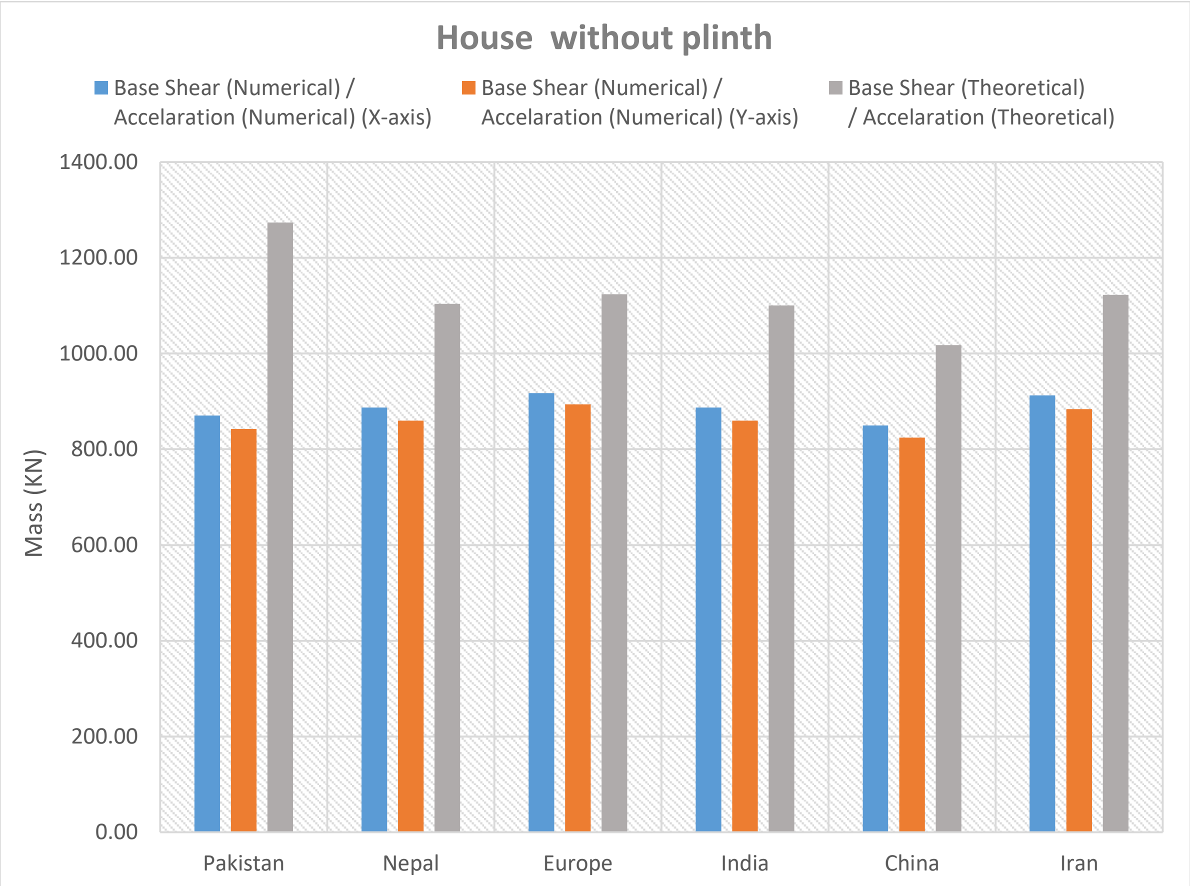

Figure 126 Comparison of ratio base shear to spectral acceleration, x and y axes, house WPL

The difference of around 20% to 30% is due to the effective mass and the spectral accelerations of every region. The theoretical results had considered 90% of mass ratio activated and the numerical results for house had about 60% of mass ratio activated. The mass ratios activated will then effect the spectral accelerations which will then effect the base shear values and eventually providing us with different ratios. The base shear values were higher in theoretical results, therefore; the ratios here were also high.

8.5 Internal actions

The theoretical results were only available for buildings without plinth level (WPL) therefore, the comparison will also be done only for buildings without plinth level. For school WPL, pier Y1-1 was taken as a sample for comparison while in case of house WPL pier X1-1 was taken as a sample for comparison.

8.5.1 Axial forces

Figure 127 and Figure 128 the comparison between numerical results and theoretical results of axial forces in pier Y1-1 for school WPL and X1-1 for house WPL respectively.

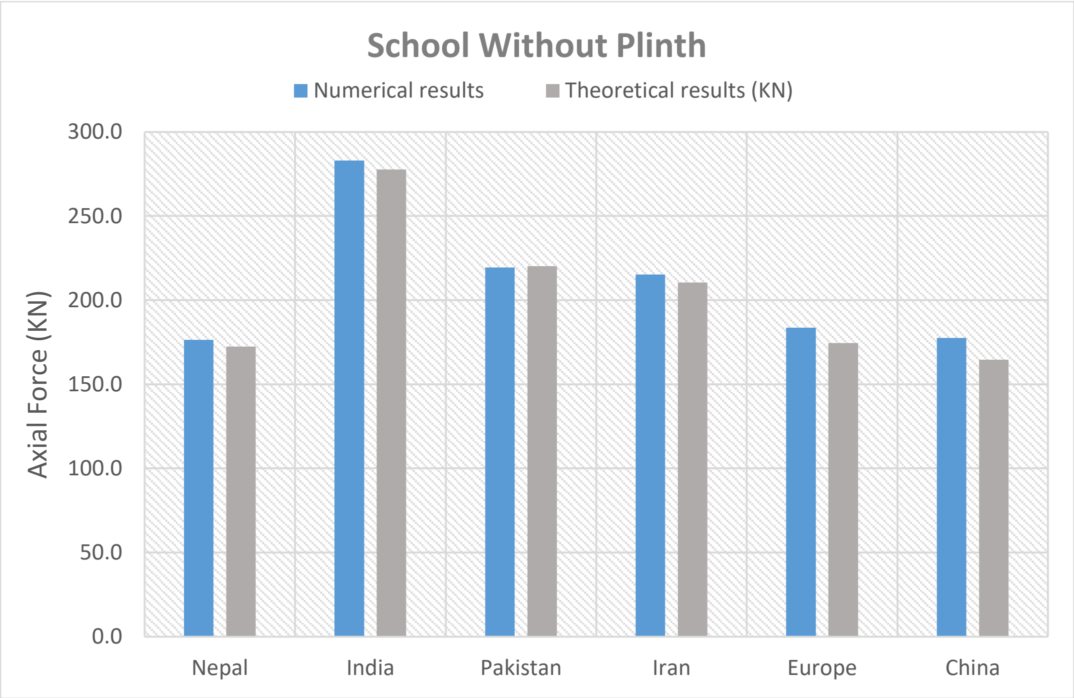

Figure 127 Comparison of axial forces, pier Y1-1, school WPL

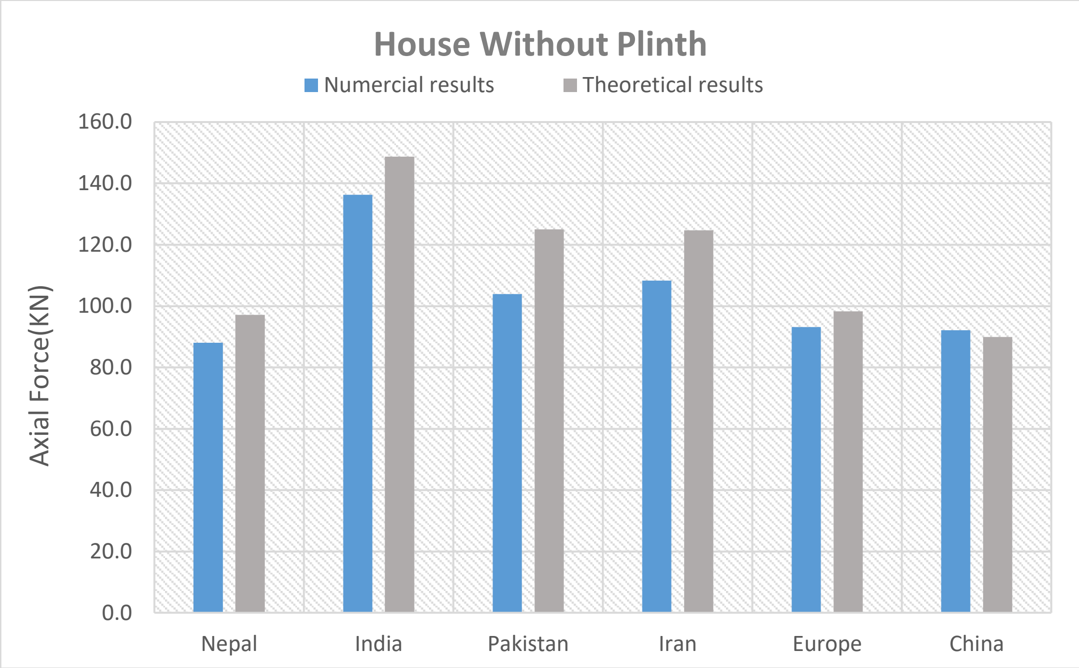

Figure 128 Comparison of axial forces, pier X1-1, house WPL

For axial force, the numerical and theoretical results were almost the same because of the similarity in terms of static loads of the buildings.

8.5.2 Bending moments

Figure 129 and Figure 130 the comparison between numerical results and theoretical results of bending moments in pier Y1-1 for school WPL and X1-1 for house WPL respectively.

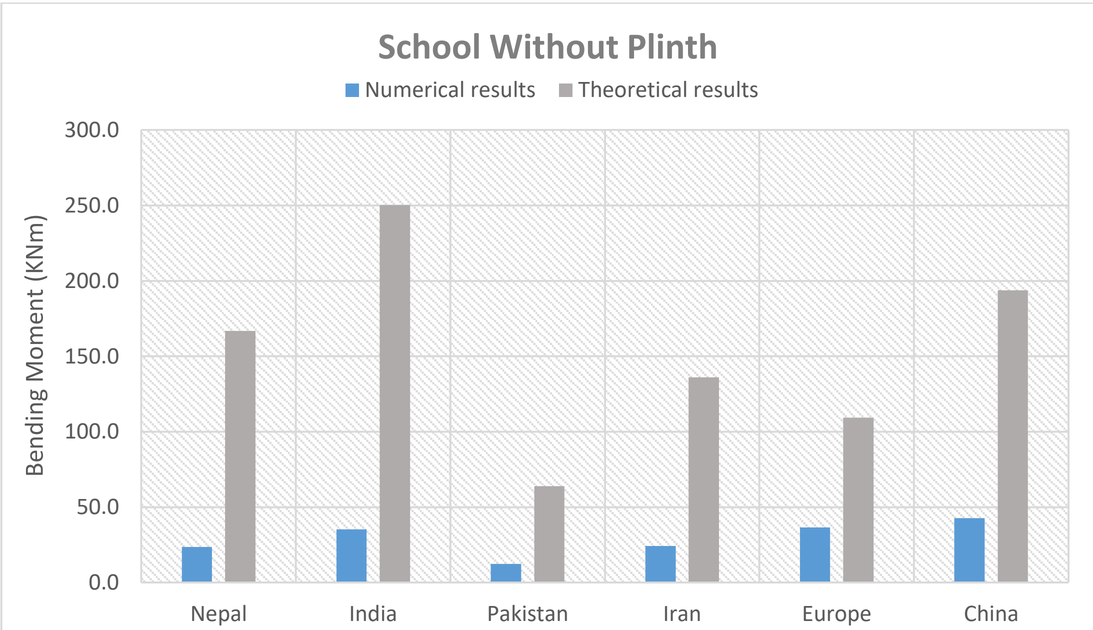

Figure 129 Comparison of bending moments, pier Y1-1, school WPL

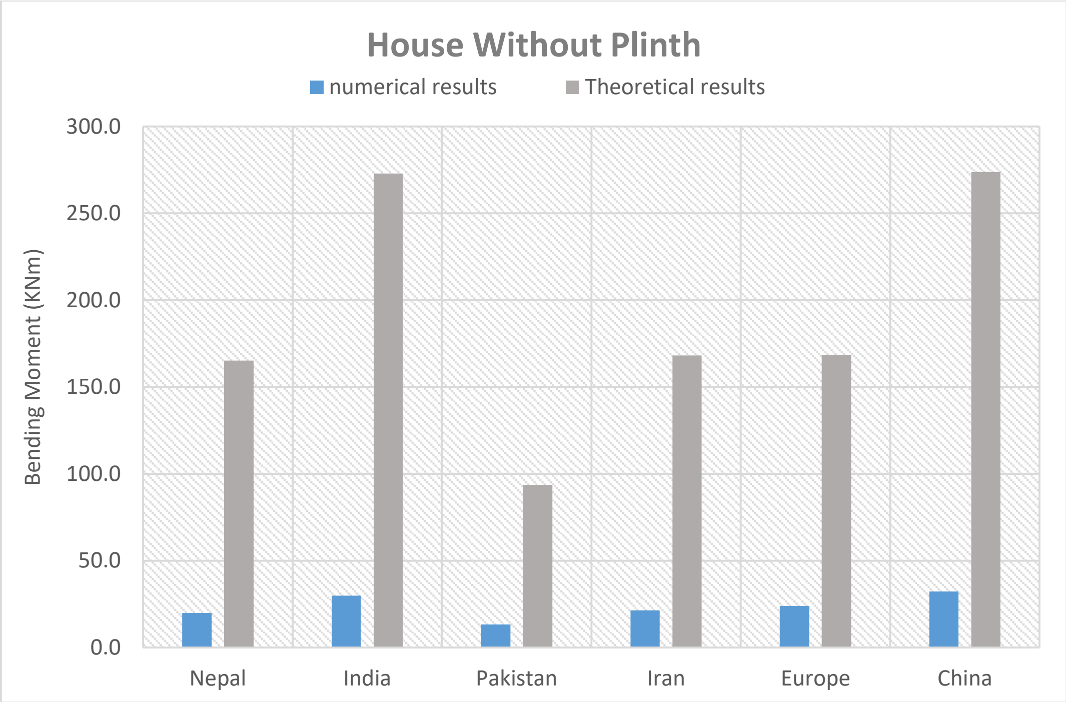

Figure 130 Comparison of bending moments, pier X1-1, house WPL

For axial force, the numerical and theoretical results had a huge difference because of the combination of two reasons. The first reason was the lateral forces (base shear), which were low for numerical results as compared to theoretical results. Therefore, if the base shear is low, the resultant bending moments will also be low. Another reason was the consideration of cantilever piers for theoretical results which is the worst case scenario and will give us conservative results. While on the other hand, wall system which had piers connected by spandrels and these spandrels helped resist the bending moment of these piers.

8.5.3 Shear Forces

Figure 131 and Figure 132 the comparison between numerical results and theoretical results of shear forces in pier Y1-1 for school WPL and X1-1 for house WPL respectively.

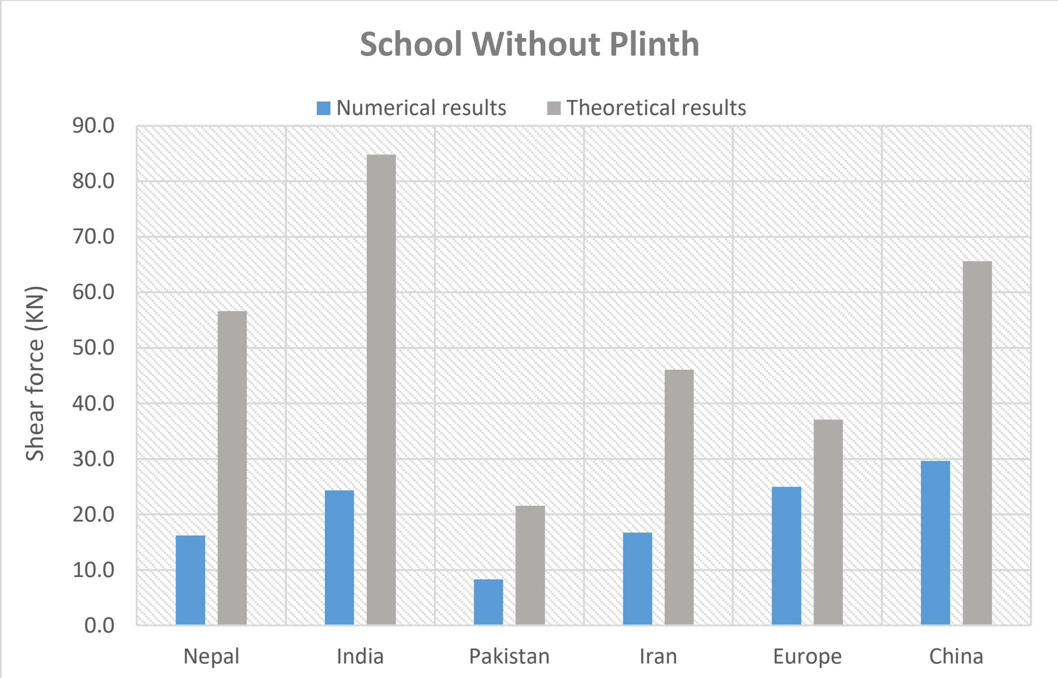

Figure 131 Comparison of shear forces, pier Y1-1, school WPL

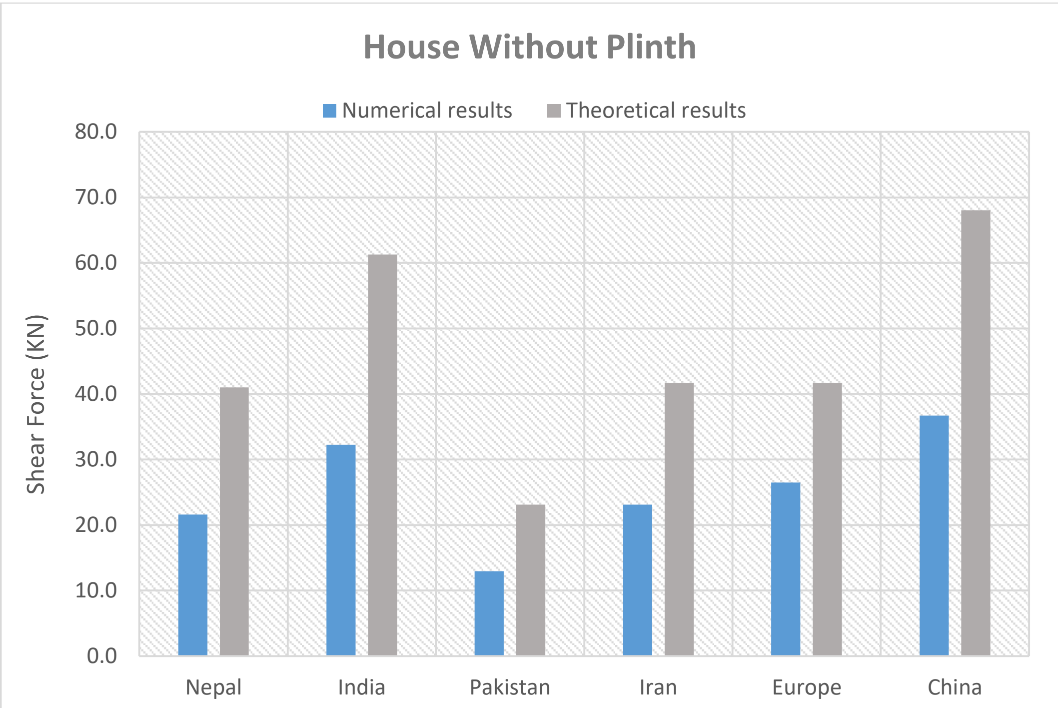

Figure 132 Comparison of shear forces, pier X1-1, house WPL

The shear forces are actually the resisting forces for applied bending moments on the structure. Therefore, if bending moments values were low for numerical results, so will be the shear forces values for numerical results and again a big difference can be seen between numerical and theoretical results.

9. Conclusion

Non-engineering rubble-stone masonry buildings comprise a significant portion of existent construction in Himalayan region. The area is famous for its seismic activity which, given exceptional vulnerability of masonry structures to earthquake loads, makes it important to research and implement new techniques for design of durable and at the same time accessible stone buildings. This report addresses, as a part of global research, the capabilities of finite element modelling and response spectrum analysis for accurate assessment of structural seismic performance.

Models with different configurations were developed using SAP2000 software. All of them were analysed for seismic behaviour based on design acceleration response spectra obtained according to different building codes. Various analysis was done which provided some solid results. These results were then compared with theoretical results and it was observed that dead loads obtained from static analysis were in alignment with the theoretical results with a small difference of around 5 percent. It can also be seen that theoretical results for natural periods were rather conservative due to the fact that these results were based on formulas provided in building codes for frame structures and not for wall systems. Furthermore, base shear results obtained from response spectrum analysis were more tolerant as compared to the theoretical results due to the fact that about 90 percent mass ratio activation was considered for theoretical calculation of natural periods which in turn gave us higher values of spectral accelerations, resulting in conservative results for seismic demand.

When analyzing the internal forces at the base of the masonry piers after application of the load combinations, axial forces were in accordance to the theoretical results considering static results were also on the same page with theoretical results. However, bending moment and shear forces results were largely tolerant because of the consideration of wall system in which piers are connected by spandrels.

The comparison established full compliance of numerical and analytical models, which serves for a more comprehensive operation of the software and informed interpretation of the results.

ACKNOWLEDGEMENTS

I would like to express my gratitude to my professor and supervisor of this project, Prof. Stefano Silvestri, and to the co-supervisor, architect Martijn Schildkamp. It would not be possible to complete the project without their constant support and valuable insight.

I would also like to extend my appreciation to Engr.Aziz-ul-Haq who works as structure engineer in Pakistan for providing me with SAP2000 software used for the analysis of this project.

Finally, I would like to thank my mother and my father for always supporting me and believing in me throughout my journey as a student.

References

Carabbio, R., Pieraccini, L., Silvestri, S., & Schildkamp, M. (2018). How Can Vernacular Construction Techniques Sustain Earthquakes: The Case of the Bhatar Buildings.

Fragiadakis. (2013). Response Spectrum Analysis of Structures Subjected to Seismic Actions. *Encyclopedia of Earthquake Engineering*.

Ondrej, & Napier, J. (2014). CSI Knowledge base.

Samayoa, J., Baraccani, S., Pieraccini, L., & Silvestri, S. (2018). Seismic Behavior of One-Storey Gabion-Box Walls Buildings.

Schildkamp, M., & Araki, Y. (2019). School Buildings in Rubble Stone Masonry With Cement Mortar in Seismic Areas: Literature Review of Seismic Codes, Technical Norms and Practical Manuals. *Frontiers in Built Environment*.

Uttamchandani, D. (2006). Guided Wave Optical Components and Devices.

Vorfolomeyeva, Y. (2021). *Non-linear static analysis of rubble stone masonry.*

TABLES

Dead Load (KN)		
Region	**School WPL**	**School PL**
Pakistan	1350.15	1545.15
Nepal	1374.57	1573.57
Europe	1404.90	1607.07
India	1374.57	1573.57
China	1319.19	1507.85
Iran	1411.00	1615.17

Table 10 Dead load for all region, School PL and School WPL

Dead Load (KN)		
Region	**House WPL**	**House PL**
Pakistan	1474.20	1558.3
Nepal	1499.60	1589.2
Europe	1534.51	1623.8
India	1499.60	1589.2
China	1438.69	1523.7
Iran	1539.90	1628.5

Table 11 Dead load for all region, House PL and House WPL

Static live load combination results		
Regions	**House with Plinth**	**House without Plinth**
Nepal	64.67	64.67
India	64.67	64.67
Pakistan	64.67	64.67
Iran	64.67	64.67
Europe	64.67	64.67
China	64.67	64.67

Table 12 Static live load results for all regions, House PL & House WPL

Static load combination results		
Regions	**School PL**	**School WPL**
Nepal	1573.57	1374.57
India	2486.24	2171.82
Pakistan	2024.15	1768.70
Iran	1938.21	1693.20
Europe	1607.07	1404.90
China	1432.46	1253.23

Table 13 Static load combination results for all regions, School PL & School WPL

Static dead load combination results		
Regions	**House with Plinth**	**House without Plinth**
Nepal	1632.53	1519.00
India	2548.74	2369.36
Pakistan	2108.47	1963.54
Iran	2052.34	1912.55
Europe	1669.43	1553.91
China	1499.65	1397.48

Table 14 Static load combination results for all regions, House PL & House WPL

Nepal response spectra coefficients	
Ta	0.1
Tc	0.5
Td	2
K	1.8
alpha	2.5
Z	0.2
Ch(T), T<Ta	1
Ch(T), Ta<T<Tc	2.5
Ch(T), Tc<T<6	2.35298135
q or R	2

Table 15 Values of coefficients, Nepal response spectra

India response spectra coefficients	
Ta	0.1
Tb	0.4
tc	4
Z	0.4
R	2
I	1

Table 16 Values of coefficients, India response spectra

Pakistan response spectra coefficients	
Ca	0.2
Cv	0.2
To	0.08
Ts	0.4
R	4.5

Table 17 Values of coefficients, Pakistan response spectra

Iran response spectra coefficients	
To	0.1
Ts	0.4
Td	2
S	1.5
alpha	2.5
A	0.2
B, 0<T<To	1
B, To<T<Ts	2.5
B, T>Ts	2.311
R	2

Table 18 Values of coefficients, Iran response spectra

China response spectra coefficients	
Ta	0.1
Tg	0.3
Td	1.5
$\eta 1$	0.02
$\eta 2$	1
Xhi	0.05
V	0.9
alpha max	0.45
Z	0.2

Table 19 Values of coefficients, China response spectra

Europe response spectra coefficients	
Tb	0.15
Tc	0.4
Td	2

S	1
ag	0.2
η	1
q	2

Table 20 Values of coefficients, Europe response spectra

School with Plinth		
Base Shear	X-axis (KN)	Y-axis (KN)
Pakistan	57.077	54.998
Nepal	119.104	116.346
Europe	155.791	166.141
India	119.104	116.346
Iran	122.982	120.03
China	211.405	209.669

Table 21 Seismic demand for school PL

School without Plinth			
Base Shear	Numerical results (X-axis) (KN)	Numerical results (Y-axis) (KN)	Theoretical Results (KN)
Pakistan	50.2	45.8	94.6
Europe	141.8	141.7	221.2
India	105.2	97.2	271.9
Iran	108.6	100.2	221.6
China	187.6	175.6	315.6
Nepal	105.2	97.2	271.9
Yulia Results (Nepal)	281.28	307.46	

Table 22 Seismic demand for school WPL

House with Plinth		
Base Shear	X-axis (KN)	Y-axis (KN)
Pakistan	84.818	82.125
Nepal	175.288	170.017
Europe	215.196	211.666
India	175.288	170.017
Iran	181.412	175.957
China	308.626	300.127

Table 23 Seismic demand for house PL

House without Plinth			
Base Shear	Numerical results (X-axis) (KN)	Analytical results (Y-axis) (KN)	Theoretical Results (KN)
Pakistan	77.3	73.1	141.5
Europe	200.1	194.3	280.9
India	160.2	151.9	275.1
Iran	165.7	157.2	280.6
China	282.7	269.3	457.9
Nepal	160.2	151.9	276.0
Yulia Results	328.05	169.87	

Table 24 Seismic demand for house WPL

Axial Force (KN)						
Section	Nepal	India	Pakistan	Iran	Europe	China
X1-1	33.637	53.7	40.066	40.602	36.308	35.776
X1-2	11.533	18.482	14.246	14.058	12.03	11.727
X1-3	43.235	69.26	53.194	52.646	45.338	44.062
X1-4	28.515	45.759	35.638	34.863	29.533	28.453

X1-5	67.606	107.857	80.099	81.478	72.278	72.3
X1-6	12.2	19.563	15.159	14.893	12.686	12.318
X1-7	41.935	67.255	52.125	51.201	43.683	42.155
X1-8	28.324	45.46	35.456	34.643	29.299	28.202
X1-9	68.02	108.492	80.416	81.93	72.747	72.924
X1-10	12.188	19.545	15.15	14.881	12.671	12.299
X1-11	41.94	67.258	52.104	51.202	43.692	42.182
X1-12	27.008	43.384	34.048	33.099	27.988	26.642
X1-13	32.526	51.939	38.844	39.287	34.983	34.483

Table 25 Comparison of axial forces, door wall, school PL

Axial Force (KN)						
Section	Nepal	India	Pakistan	Iran	Europe	China
X2-1	32.607	52.059	38.868	39.367	35.245	34.667
X2-2	27.574	44.269	34.6	33.75	28.566	27.366
X2-3	29.192	46.937	37.105	35.861	30.199	28.489
X2-4	29.152	46.764	36.32	35.611	30.269	29.222
X2-5	65.134	103.953	77.447	78.572	69.595	69.376
X2-6	29.152	46.753	36.249	35.592	30.274	29.296
X2-7	29.009	46.655	36.965	35.658	29.909	28.202
X2-8	29.121	46.708	36.234	35.561	30.209	29.238
X2-9	65.079	103.87	77.418	78.515	69.487	69.273
X2-10	29.155	46.768	36.322	35.614	30.279	29.229
X2-11	29.21	46.963	37.115	35.879	30.233	28.523
X2-12	27.565	44.258	34.602	33.743	28.545	27.343
X2-13	32.475	51.865	38.829	39.238	34.994	34.391

Table 26 Comparison of axial forces, window wall, school PL

Axial Force (KN)						
Section	Nepal	India	Pakistan	Iran	Europe	China
Y1-1	199.265	319.376	246.319	242.799	207.381	201.591
Y2-1	188.18	302.789	240.854	231.354	192.325	181.629
Y3-1	187.951	302.449	240.745	231.123	192.18	181.228
Y4-1	198.31	317.899	245.524	241.735	206.13	200.199

Table 27 Comparison of axial forces, all walls along y-axis, school PL

Axial Force (KN)	
Section	Nepal
Z1-1	32.863
Z1-2	37.787
Z1-3	53.018
Z1-4	37.319
Z1-5	52.793
Z1-6	38.023
Z1-7	26.737
Z2-1	26.493
Z2-2	33.088
Z2-3	53.859
Z2-4	32.261
Z2-5	53.826
Z2-6	33.106
Z2-7	26.504

Table 28 Comparison of axial forces, all walls along x-axis, z section, school PL

Bending Moment (KNm)						
Section	Nepal	India	Pakistan	Iran	Europe	China
X1-1	4.2378	6.5495	3.5625	4.7254	5.0342	6.0853
X1-2	1.462	2.2193	0.95	1.5581	1.8704	2.4072
X1-3	3.2683	4.964	2.1434	3.4859	4.1818	5.3632
X1-4	0.5191	0.7917	0.3632	0.5612	0.6549	0.8278
X1-5	7.6424	11.5254	4.4618	8.0032	9.7783	13.1004
X1-6	1.2832	1.9365	0.7562	1.3472	1.6691	2.1969
X1-7	2.8366	4.2988	1.7961	3.0086	3.6586	4.7264
X1-8	0.4812	0.7333	0.3313	0.5189	0.613	0.7737
X1-9	7.741	11.7065	4.745	8.1648	9.7883	13.0233
X1-10	1.2731	1.9184	0.7306	1.3316	1.6562	2.1997
X1-11	2.7148	4.0961	1.5931	2.847	3.531	4.6551
X1-12	0.2745	0.417	0.1785	0.2916	0.3851	0.4575
X1-13	2.9935	4.6466	2.6566	3.374	3.4951	4.1491

Table 29 Comparison of bending moments, door wall, school PL

Bending Moment (KNm)						
Section	Nepal	India	Pakistan	Iran	Europe	China
X2-1	3.0295	4.7071	2.715	3.4224	3.6054	4.1816
X2-2	0.307	0.47	0.2247	0.3328	0.4144	0.4832
X2-3	1.1067	1.6753	0.6859	1.17	1.4517	1.8618
X2-4	0.6295	0.9648	0.4723	0.6888	0.7997	0.9735
X2-5	5.3468	8.036	2.9263	5.5491	7.0236	9.3929
X2-6	0.5627	0.8575	0.3882	0.6068	0.7293	0.9068
X2-7	0.9001	1.3502	0.4727	0.9292	1.2159	1.607
X2-8	0.562	0.8565	0.388	0.6061	0.7264	0.905
X2-9	5.2974	7.9622	2.9036	5.4987	6.9266	9.2971

X2-10	0.6229	0.955	0.4691	0.6821	0.7886	0.9611
X2-11	1.0878	1.647	0.6768	1.1506	1.4165	1.8259
X2-12	0.3138	0.4803	0.2297	0.3401	0.4248	0.494
X2-13	2.983	4.6376	2.6948	3.3752	3.5164	4.0908

Table 30 Comparison of bending moments, window wall, school PL

Bending Moment (KNm)						
Section	Nepal	India	Pakistan	Iran	Europe	China
Y1-1	29.7284	44.6775	15.8357	30.7974	45.2698	53.5891
Y2-1	27.961	42.0862	15.56	29.113	39.2531	49.3131
Y3-1	27.9721	42.1117	15.6337	29.1413	39.1388	49.2457
Y4-1	27.3154	40.9975	14.1947	28.2037	41.6135	49.6383

Table 31 Comparison of bending moments, all walls along y-axis, school PL

Bending Moment (KNm)	
Section	Nepal
Z1-1	3.7558
Z1-2	6.2581
Z1-3	10.8295
Z1-4	5.9895
Z1-5	10.1136
Z1-6	6.2749
Z1-7	4.0379
Z2-1	4.0168
Z2-2	4.3794
Z2-3	10.1025
Z2-4	3.8706
Z2-5	10.0041

Z2-6	4.2954
Z2-7	3.9712

Table 32 Comparison of bending moments, all walls along x-axis, z section, school PL

Shear Force (KN)						
Section	Nepal	India	Pakistan	Iran	Europe	China
X1-1	4.08	6.217	2.82	4.391	5.056	6.51
X1-2	5.394	8.242	3.884	5.845	6.684	8.454
X1-3	3.366	5.082	1.999	3.535	4.373	5.742
X1-4	7.213	10.871	4.154	7.539	9.358	12.441
X1-5	6.348	9.529	3.406	6.568	8.219	11.192
X1-6	3.3	4.953	1.757	3.411	4.325	5.844
X1-7	2.88	4.323	1.539	2.979	3.803	5.098
X1-8	6.555	9.853	3.598	6.804	8.556	11.495
X1-9	6.238	9.377	3.437	6.478	8.015	10.9
X1-10	3.553	5.361	2.09	3.724	4.563	6.075
X1-11	3.617	5.511	2.494	3.89	4.532	5.791
X1-12	7.793	11.875	5.388	8.385	9.692	12.452
X1-13	3.604	5.467	2.319	3.834	4.515	5.938

Table 33 Comparison of shear forces, door wall, school PL

Shear Force (KN)						
Section	Nepal	India	Pakistan	Iran	Europe	China
X2-1	3.601	5.491	2.507	3.881	4.481	5.734
X2-2	7.686	11.765	5.673	8.366	9.574	11.918
X2-3	3.616	5.514	2.521	3.896	4.582	5.77
X2-4	6.111	9.238	3.708	6.436	7.968	10.352
X2-5	6.055	9.11	3.377	6.301	7.905	10.558

X2-6	5.384	8.087	2.907	5.576	7.155	9.51
X2-7	2.602	3.903	1.369	2.686	3.472	4.633
X2-8	5.355	8.044	2.891	5.546	7.1	9.456
X2-9	6.004	9.033	3.354	6.248	7.804	10.458
X2-10	6.032	9.12	3.67	6.356	7.821	10.202
X2-11	3.566	5.439	2.497	3.845	4.489	5.675
X2-12	7.579	11.605	5.619	8.257	9.378	11.719
X2-13	3.56	5.428	2.484	3.838	4.41	5.661

Table 34 Comparison of shear forces, window wall, school PL

Shear Force (KN)						
Section	Nepal	India	Pakistan	Iran	Europe	China
Y1-1	20.322	30.484	10.466	20.952	30.59	36.921
Y2-1	38.185	57.278	19.963	39.41	52.967	68.51
Y3-1	38.137	57.206	19.949	39.361	52.698	68.386
Y4-1	20.006	30.009	10.322	20.629	29.805	36.293

Table 35 Comparison of shear forces, all walls along y-axis, school PL

Shear Force (KN)	
Section	Nepal
Z1-1	5.588
Z1-2	6.939
Z1-3	11.234
Z1-4	6.667
Z1-5	10.503
Z1-6	6.837
Z1-7	4.865
Z2-1	4.997

Z2-2	5.397
Z2-3	10.949
Z2-4	5.007
Z2-5	10.843
Z2-6	5.292
Z2-7	4.907

Table 36 Comparison of shear forces, all walls along x-axis, z section, school PL

Axial Force (KN)						
Section	Nepal	India	Pakistan	Iran	Europe	China
X1-1	32.814	52.426	39.381	39.685	35.169	34.597
X1-2	44.625	71.541	55.277	54.439	46.78	45.145
X1-3	17.744	28.501	22.383	21.75	18.332	17.553
X1-4	64.471	103.039	77.661	78.037	68.542	67.654
X1-5	43.423	69.684	54.281	53.1	45.225	33.541
X1-6	17.721	28.462	22.338	21.718	18.324	17.551
X1-7	64.814	103.56	77.9	78.405	68.952	68.196
X1-8	43.732	70.172	54.606	53.464	45.578	43.759
X1-9	17.003	27.327	21.549	20.869	17.57	16.718
X1-10	29.673	47.49	36.185	36.038	31.612	30.687

Table 37 Comparison of axial forces, door wall, school WPL

Axial Force (KN)						
Section	Nepal	India	Pakistan	Iran	Europe	China
X2-1	29.574	47.33	36.053	35.914	31.543	30.602
X2-2	17.482	28.087	22.088	21.439	18.068	17.26
X2-3	30.862	49.622	39.231	37.914	31.977	30.168
X2-4	18.311	29.408	23.064	22.437	18.948	18.157
X2-5	60.754	97.138	73.454	73.61	64.57	63.491

X2-6	18.331	29.43	23.021	22.443	18.997	18.252
X2-7	30.458	48.982	38.794	37.436	31.479	29.684
X2-8	18.314	29.405	23.012	22.425	18.963	18.219
X2-9	60.733	97.106	73.443	73.588	64.527	63.451
X2-10	18.318	29.418	23.068	22.444	18.961	18.169
X2-11	30.877	49.644	39.238	37.929	32.006	30.196
X2-12	17.48	28.083	22.089	21.437	18.061	17.253
X2-13	29.557	47.306	36.06	35.901	31.494	30.551

Table 38 Comparison of axial forces, window wall, school WPL

Axial Force (KN)						
Section	Nepal	India	Pakistan	Iran	Europe	China
Y1-1	176.429	282.948	219.344	215.286	183.565	177.457
Y2-1	169.888	273.362	217.542	208.879	173.751	164.121
Y3-1	169.645	273	217.423	208.632	173.459	163.682
Y4-1	176.198	282.577	219.053	215.003	183.211	177.217

Table 39 Comparison of axial forces, all walls along y-axis, school WPL

Axial Force (KN)	
Section	Nepal
Z1-1	8.171
Z1-2	37.386
Z1-3	52.538
Z1-4	37.035
Z1-5	52.355
Z1-6	37.619
Z1-7	26.287
Z2-1	26.09

Z2-2	32.681
Z2-3	53.364
Z2-4	32.023
Z2-5	53.348
Z2-6	32.699
Z2-7	26.107

Table 40 Comparison of axial forces, all walls along x-axis, z level, school WPL

Bending Moment (KNm)						
Section	Nepal	India	Pakistan	Iran	Europe	China
X1-1	4.5365	6.8741	2.8598	4.81	5.9179	7.5729
X1-2	6.6458	10.1854	4.9814	7.2532	8.4323	10.2597
X1-3	0.37	0.5751	0.3319	0.4193	0.4544	0.5119
X1-4	12.2235	18.5848	8.146	13.0703	15.7229	19.9347
X1-5	5.9751	9.1604	4.4991	6.5271	7.5772	7.2896
X1-6	0.3733	0.579	0.3267	0.4208	0.4577	0.5247
X1-7	12.2761	18.6959	8.4001	13.1824	15.6503	19.7781
X1-8	6.0114	9.1984	4.4058	6.5358	7.6386	9.3844
X1-9	0.2612	0.3939	0.1511	0.2727	0.3605	0.4522
X1-10	3.4865	5.3702	2.8043	3.8546	4.2471	5.1576

Table 41 Comparison of bending moments, door wall, school WPL

Bending Moment (KNm)						
Section	Nepal	India	Pakistan	Iran	Europe	China
X2-1	3.5718	5.5064	2.9014	3.9571	4.404	5.2622
X2-2	0.2322	0.3623	0.2175	0.2643	0.2914	0.3132
X2-3	1.9086	2.8769	1.0952	1.995	2.5947	3.3159
X2-4	0.4363	0.6766	0.382	0.4918	0.534	0.6164

X2-5	7.6944	11.5589	4.1564	7.9734	10.3904	13.6185
X2-6	0.3875	0.6	0.3329	0.4351	0.4778	0.5546
X2-7	1.635	2.4525	0.8554	1.6875	2.2601	2.9311
X2-8	0.3889	0.6021	0.3336	0.4366	0.4801	0.5572
X2-9	7.6248	11.4547	4.1235	7.9022	10.2586	13.485
X2-10	0.4326	0.6711	0.3802	0.488	0.5279	0.6096
X2-11	1.8769	2.8294	1.0797	1.9624	2.5367	3.2558
X2-12	0.2338	0.3647	0.2189	0.2661	0.2938	0.3156
X2-13	3.5193	5.4277	2.8763	3.9033	4.3073	5.1622

Table 42 Comparison of bending moments, window wall, school WPL

Bending Moment (KNm)						
Section	Nepal	India	Pakistan	Iran	Europe	China
Y1-1	23.5126	35.3198	12.3776	24.3239	36.4364	42.634
Y2-1	26.2775	39.5339	14.443	27.3195	37.7818	46.6339
Y3-1	26.3935	39.7129	14.5424	27.4488	37.8659	46.7926
Y4-1	22.389	33.5998	11.5784	23.1066	34.6402	40.824

Table 43 Comparison of bending moments, all walls along y-axis, school WPL

Bending moment (KNm)	
Section	Nepal
Z1-1	0.9784
Z1-2	5.9401
Z1-3	10.3989
Z1-4	5.5933
Z1-5	9.8622
Z1-6	5.9203
Z1-7	3.548

Z2-1	3.5604
Z2-2	4.0258
Z2-3	9.6374
Z2-4	3.545
Z2-5	9.5511
Z2-6	3.9573
Z2-7	3.5116

Table 44 Comparison of bending moments, all walls along x-axis, z level, school WPL

Shear Force (KN)						
Section	Nepal	India	Pakistan	Iran	Europe	China
X1-1	5.783	8.776	3.729	6.156	7.548	9.566
X1-2	4.015	6.11	2.709	4.303	5.27	6.533
X1-3	6.426	9.68	3.649	6.705	8.611	11.182
X1-4	8.06	12.168	4.772	8.461	10.609	13.787
X1-5	3.764	5.729	2.543	4.036	4.94	5.08
X1-6	5.911	8.891	3.267	6.145	7.952	10.382
X1-7	8.068	12.199	4.915	8.505	10.524	13.646
X1-8	3.601	5.458	2.278	3.821	4.774	6.021
X1-9	6.608	10.015	4.188	7.011	8.607	11.013
X1-10	3.418	5.214	2.401	3.689	4.332	5.435

Table 45 Comparison of shear forces, door wall, school WPL

Shear Force (KN)						
Section	Nepal	India	Pakistan	Iran	Europe	China
X2-1	3.495	5.345	2.548	3.797	4.426	5.461
X2-2	6.914	10.561	4.938	7.483	8.867	10.936
X2-3	1.426	2.166	0.933	1.521	1.891	2.351

X2-4	4.97	7.461	2.646	5.138	6.784	8.846
X2-5	5.6	8.412	3.018	5.801	7.536	9.906
X2-6	4.901	7.368	2.685	5.09	6.652	8.641
X2-7	1.103	1.654	0.577	1.138	1.528	1.976
X2-8	4.877	7.332	2.674	5.066	6.606	8.595
X2-9	5.551	8.337	2.994	5.75	7.441	9.81
X2-10	4.905	7.364	2.615	5.072	6.666	8.723
X2-11	1.405	2.135	0.923	1.499	1.854	2.312
X2-12	6.813	10.41	4.888	7.38	8.684	10.747
X2-13	3.449	5.277	2.523	3.75	4.346	5.379

Table 46 Comparison of shear forces, window wall, school WPL

Shear Force (KN)						
Section	Nepal	India	Pakistan	Iran	Europe	China
Y1-1	16.247	24.372	8.341	16.749	24.994	29.626
Y2-1	31.602	47.404	16.439	32.605	45.144	56.961
Y3-1	31.658	47.487	16.476	32.663	45.084	57.036
Y4-1	16.18	24.27	8.317	16.68	24.632	29.462

Table 47 Comparison of shear forces, all walls along y-axis, school WPL

Shear Force (KN)	
Section	Nepal
Z1-1	1.7
Z1-2	6.398
Z1-3	10.198
Z1-4	6.016
Z1-5	9.679
Z1-6	6.255

Z1-7	4.956
Z2-1	5.129
Z2-2	4.91
Z2-3	9.989
Z2-4	4.508
Z2-5	9.897
Z2-6	4.825
Z2-7	5.044

Table 48 Comparison of shear forces, all walls along y-axis, z level, school WPL

Axial Force (KN)						
Section	Nepal	India	Pakistan	Iran	Europe	China
X1-1	85.306	132.479	103.277	105.396	89.536	86.225
X1-2	46.613	72.136	55.025	57.34	49.142	48.792
X1-3	240.646	369.19	256.465	289.083	260.707	283.094
X1-4	21.556	33.424	25.602	26.508	22.751	22.417
X1-5	100.529	155.525	113.955	121.891	107.214	110.094

Table 49 Comparison of axial forces, door wall, house PL

Axial Force (KN)						
Section	Nepal	India	Pakistan	Iran	Europe	China
X2-1	105.68	163.732	115.931	126.412	114.429	119.808
X2-2	49.298	76.548	56.226	59.599	52.559	53.494
X2-3	229.343	354.212	244.621	272.904	248.479	267.891
X2-4	49.355	76.635	56.28	59.667	52.649	53.579
X2-5	105.933	164.112	116.134	126.703	114.797	120.215

Table 50 Comparison of axial forces, window wall, house PL

Axial Force (KN)						
Section	Nepal	India	Pakistan	Iran	Europe	China
Y1-1	288.506	447.723	326.678	296.77	307.402	315.394
Y1-2	146.167	225.618	156.26	174.203	159.532	170.639
Y2-1	98.689	153.148	115.596	120.571	104.389	103.763
Y2-2	18.276	28.473	23.313	22.941	18.91	17.217
Y2-3	99.858	154.208	117.374	123.01	105.502	105.113
Y3-1	289.473	449.214	328.384	349.527	308.378	315.852
Y3-2	147.206	227.224	157.913	175.647	160.478	171.279

Table 51 Comparison of axial forces, all walls along y-axis, house PL

Axial Force (KN)	
Section	Nepal
Z1-1	92.461
Z1-2	199.596
Z1-3	105.228
Z2-1	96.441
Z2-2	203.449
Z2-3	96.67
Z3-1	103.781
Z3-2	102.562

Table 52 Comparison of axial forces, all walls along x and y axis, z section, house PL

Bending Moment (KNm)						
Section	Nepal	India	Pakistan	Iran	Europe	China
X1-1	14.4549	21.8755	10.6715	15.8837	16.8481	22.1695
X1-2	2.7907	4.197	1.7143	2.9634	3.3485	4.6605
X1-3	64.1727	96.3718	37.8542	67.7092	77.1147	109.0473
X1-4	2.8526	4.2633	1.5864	2.9967	3.4545	4.9652
X1-5	19.8345	29.9121	13.6839	21.5462	23.3583	31.5

Table 53 Comparison of bending moments, door wall, house PL

Bending Moment (KNm)						
Section	Nepal	India	Pakistan	Iran	Europe	China
X2-1	11.9801	18.28	10.2598	13.5418	13.7924	16.8092
X2-2	1.7261	2.6126	1.2366	1.8825	2.0699	2.6933
X2-3	19.7865	29.6814	10.5561	20.4949	24.7112	34.9071
X2-4	1.7413	2.6353	1.2497	1.9003	2.0875	2.715
X2-5	12.0567	18.3947	10.327	13.632	13.8923	16.9209

Table 54 Comparison of bending moments, window wall, house PL

Bending Moment (KNm)						
Section	Nepal	India	Pakistan	Iran	Europe	China
Y1-1	47.2846	71.0126	28.8904	48.9369	58.869	79.6469
Y1-2	12.8661	19.4522	8.4624	13.7682	15.8407	20.9349
Y2-1	25.5075	38.5326	16.4816	27.2084	30.5313	41.6799
Y2-2	2.6113	3.9074	1.4112	2.7215	3.2015	4.5822
Y2-3	25.4495	38.3443	16.444	27.2604	30.4615	41.6583
Y3-1	46.9085	70.3346	28.1253	49.9185	58.5781	79.6934
Y3-2	13.1883	19.9478	8.6469	14.0927	16.255	21.4825

Table 55 Comparison of bending moments, all walls along y-axis, house PL

Bending Moment (KNm)	
Section	Nepal
Z1-1	24.1518
Z1-2	75.6405
Z1-3	22.5852
Z2-1	11.6613
Z2-2	34.0301
Z2-3	11.6073
Z3-1	30.5078
Z3-2	30.4218

Table 56 Comparison of bending moments, all walls along x and y axis, z section, house PL

Shear Force (KN)						
Section	Nepal	India	Pakistan	Iran	Europe	China
X1-1	27.399	41.049	16.916	29.31	32.879	45.797
X1-2	25.915	38.865	15.605	27.525	31.122	43.712
X1-3	41.971	62.9	22.47	43.547	51.154	73.739
X1-4	20.761	31.135	12.85	22.185	24.84	34.645
X1-5	23.53	35.182	14.817	25.365	28.217	39.068

Table 57 Comparison of shear forces, door wall, house PL

Shear Force (KN)						
Section	Nepal	India	Pakistan	Iran	Europe	China
X2-1	13.128	19.825	9.56	14.433	15.844	20.374
X2-2	12.688	19.165	8.979	13.841	15.281	19.949
X2-3	22.841	34.261	12.156	23.651	28.766	40.322

X2-4	12.736	19.237	9.041	13.905	15.343	19.996
X2-5	13.217	19.958	9.642	14.538	15.949	20.496

Table 58 Comparison of shear forces, window wall, house PL

Shear Force (KN)						
Section	Nepal	India	Pakistan	Iran	Europe	China
Y1-1	43.925	66.27	27.899	45.395	54.754	72.634
Y1-2	20.639	31.351	16.235	22.943	24.651	30.654
Y2-1	33.422	50.322	19.675	35.102	40.598	56.758
Y2-2	27.089	40.623	14.533	28.094	33.263	47.601
Y2-3	33.073	49.753	19.266	34.71	40.227	56.405
Y3-1	44.112	66.552	28.19	47.063	55.028	72.782
Y3-2	20.687	31.424	16.349	23.027	24.696	30.65

Table 59 Comparison of shear forces, all walls along y-axis, house PL

Shear Force (KN)	
Section	Nepal
Z1-1	29.564
Z1-2	60.672
Z1-3	27.442
Z2-1	12.414
Z2-2	31.87
Z2-3	12.359
Z3-1	39.594
Z3-2	40.008

Table 60 Comparison of shear forces, all walls along x and y axis, z section, house PL

Axial Force (KN)						
Section	Nepal	India	Pakistan	Iran	Europe	China
X1-1	88.031	136.271	103.961	108.261	93.197	92.118
X1-2	28.945	44.829	34.866	35.833	30.49	29.664
X1-3	232.197	356.04	253.916	281.527	251.992	267.35
X1-4	105.435	162.737	117.94	127.677	113.318	117.53

Table 61 Comparison of axial forces, door wall, house WPL

Axial Force (KN)						
Section	Nepal	India	Pakistan	Iran	Europe	China
X2-1	97.777	151.641	110.37	118.003	105.842	107.644
X2-2	30.513	47.442	35.574	37.125	32.527	32.352
X2-3	219.137	338.603	239.215	262.743	237.894	250.51
X2-4	30.542	47.488	35.603	37.159	32.572	32.395
X2-5	97.913	151.845	110.48	118.159	106.049	107.875

Table 62 Comparison of axial forces, window wall, house WPL

Axial Force (KN)						
Section	Nepal	India	Pakistan	Iran	Europe	China
Y1-1	265.176	411.795	304.123	321.164	282.901	286.03
Y1-2	131.414	203.018	143.125	157.456	143.77	150.779
Y2-1	104.917	162.614	121.771	127.977	111.8	111.797
Y2-2	105.87	163.333	123.638	130.218	112.623	112.752
Y3-1	265.406	412.179	305.144	321.704	283.004	285.493
Y3-2	131.859	203.732	144.206	158.187	144.092	150.648

Table 63 Comparison of axial forces, all walls along y-axis, house WPL

Axial Force (KN)	
Section	Nepal
Z1-1	90.554
Z1-2	199.401
Z1-3	53.143
Z2-1	93.442
Z2-2	202.148
Z2-3	93.593
Z3-1	72.453
Z3-2	71.793

Table 64 Comparison of axial forces, all walls along x and y axis, z section, house WPL

Bending moment (KNm)						
Section	Nepal	India	Pakistan	Iran	Europe	China
X1-1	19.8597	29.9089	13.1802	21.4259	23.8777	32.176
X1-2	4.8131	7.2226	2.8603	5.094	5.886	8.1652
X1-3	89.7348	134.9492	54.9063	95.2441	109.0653	150.5583
X1-4	25.1961	37.7375	14.4065	26.5306	30.9569	43.4163

Table 65 Comparison of bending moments, door wall, house WPL

Bending moment (KNm)						
Section	Nepal	India	Pakistan	Iran	Europe	China
X2-1	12.6546	19.2265	10.0845	14.1147	15.0574	18.6467
X2-2	2.7249	4.1184	1.9308	2.9718	3.3345	4.2871
X2-3	28.0768	42.1173	14.9052	29.0686	35.9249	49.7264
X2-4	2.7398	4.1405	1.9444	2.9895	3.3523	4.3076

X2-5	12.7127	19.3131	10.1371	14.1841	15.1306	18.731

Table 66 Comparison of bending moments, window wall, house WPL

Bending moment (KNm)						
Section	Nepal	India	Pakistan	Iran	Europe	China
Y1-1	45.1885	67.8666	27.3825	48.0936	57.9965	76.5799
Y1-2	12.8963	19.5073	8.7172	13.8869	16.2518	20.7938
Y2-1	32.5533	48.8761	18.0911	33.9614	40.7676	56.6455
Y2-2	32.3475	48.5527	17.8228	33.6945	40.5541	56.4669
Y3-1	44.6861	67.0383	26.6592	47.492	57.5458	76.2618
Y3-2	12.9922	19.6574	8.7926	13.9891	16.3825	20.9359

Table 67 Comparison of bending moments, all walls along y-axis, house WPL

Bending Moment (KNm)	
Section	Nepal
Z1-1	22.0407
Z1-2	75.0133
Z1-3	2.5847
Z2-1	10.2431
Z2-2	31.9675
Z2-3	10.2143
Z3-1	4.2513
Z3-2	4.1289

Table 68 Comparison of bending moments, all walls along x and y axis, z section, house WPL

Shear Force (KN)						
Section	Nepal	India	Pakistan	Iran	Europe	China
X1-1	21.608	32.245	12.921	23.106	26.474	36.705
X1-2	26.232	39.32	15.318	27.704	32.131	44.862
X1-3	45.236	67.933	24.991	47.086	55.811	78.713
X1-4	28.474	42.458	17.019	30.48	34.879	48.399

Table 69 Comparison of shear forces, door wall, house WPL

Shear Force (KN)						
Section	Nepal	India	Pakistan	Iran	Europe	China
X2-1	10.508	15.804	7.425	11.542	13.005	16.622
X2-2	12.509	18.869	8.545	13.561	15.425	20.048
X2-3	20.163	30.243	10.681	20.868	25.938	35.718
X2-4	12.538	18.913	8.589	13.603	15.461	20.071
X2-5	10.578	15.91	7.483	11.623	13.089	16.73

Table 70 Comparison of shear forces, window wall, house WPL

Axial Force (KN)						
Section	Nepal	India	Pakistan	Iran	Europe	China
Y1-1	38.577	58.155	24.097	41.019	49.58	64.434
Y1-2	17.407	26.407	13.534	19.335	21.3	26.109
Y2-1	40.238	60.552	23.377	42.198	50.111	68.847
Y2-2	39.898	59.953	22.939	41.864	49.767	68.569
Y3-1	38.652	58.271	24.288	41.153	49.7	64.424
Y3-2	17.412	26.417	13.608	19.367	21.296	26.049

Table 71 Comparison of shear forces, all walls along y-axis, house WPL

Shear Force (KN)	
Section	Nepal
Z1-1	26.785
Z1-2	56.922
Z1-3	5.208
Z2-1	12.364
Z2-2	29.398
Z2-3	12.428
Z3-1	19.019
Z3-2	19.152

Table 72 Comparison of shear forces, all walls along x and y axis, z section, house WPL

School with Plinth		
Region	Numerical results	theoretical results
Pakistan	1545.15	1570.8
Nepal	1573.57	1601.6
Europe	1607.07	1633.3
India	1573.57	1601.6
China	1507.85	1541.8
Iran	1615.17	1639.4

Table 73 Comparison of dead loads, school PL

House with Plinth		
Region	Numerical results	theoretical results
Pakistan	1584.84	1558.3
Nepal	1613.13	1589.2

Europe	1650.03	1623.8
India	1613.13	1589.2
China	1546.25	1523.7
Iran	1656.39	1628.5

Table 74 Comparison of dead loads, house PL

School with Plinth					
Region	**First Fundamental period**		**Percentage of mass ratio activated**		**Fundamental period**
	X-axis (s)	Y-axis (s)	X-axis (%)	Y-axis (%)	Theoretical results
Pakistan	0.0707	0.0593	30.29	28.56	0.11
Nepal	0.0713	0.0599	30.30	28.56	0.141
Europe	0.0721	0.0606	30.26	28.57	0.171
India	0.0713	0.0599	30.30	28.56	0.106
China	0.0698	0.0587	30.23	28.58	0.132
Iran	0.0723	0.0607	30.29	28.56	0.135

Table 75 Comparison of fundamental periods, x and y axes, school PL

House with Plinth					
Region	**First Fundamental period**		**% of mass ratio activated**		**Fundamental period**
	X-axis (s)	Y-axis (s)	X-axis (%)	Y-axis (%)	Theoretical results
Pakistan	0.0559	0.0545	58.20	56.95	0.172
Nepal	0.0563	0.0550	58.20	56.94	0.22
Europe	0.0570	0.0557	58.20	56.96	0.21
India	0.0563	0.0550	58.20	56.94	0.219
China	0.0552	0.0538	58.19	56.97	0.184
Iran	0.0571	0.0558	58.20	56.94	0.189

Table 76 Comparison of fundamental periods, x and y axes, house PL

School without Plinth			
Base Shear	Numerical results (X-axis)	Numerical results (Y-axis)	Theoretical Results
Pakistan	50.2	45.8	94.6
Europe	141.8	141.7	221.2
India	105.2	97.2	271.9
Iran	108.6	100.2	221.6
China	187.6	175.6	315.6
Nepal	105.2	97.2	271.9
Yulia Results (Nepal)	281.28	307.46	

Table 77 Comparison of base shear, x and y axes, theoretical results, school WPL

House without Plinth			
Base Shear	Numerical results (X-axis)	Analytical results (Y-axis)	Theoretical Results
Pakistan	77.3	73.1	141.5
Europe	200.1	194.3	280.9
India	160.2	151.9	275.1
Iran	165.7	157.2	280.6
China	282.7	269.3	457.9
Nepal	160.2	151.9	276.0
Yulia Results	328.05	169.87	

Table 78 Comparison of base shear, x and y axes, house WPL

Base Shear (Numerical) / Acceleration (Numerical)	**Base Shear (Numerical) / Acceleration (Numerical)**	**Base Shear (Theoretical) / Acceleration (Theoretical)**
X-axis	Y-axis	X-axis
870.38	842.56	1273.50
887.47	859.63	1104.00
917.45	894.10	1123.60
887.47	859.63	1100.40
850.03	824.65	1017.56
912.43	883.89	1122.40

Table 79 Comparison of ratio base shear to spectral acceleration, x and y axes, house WPL

School without Plinth		
Region	Numerical results	Theoretical results (KN)
Nepal	176.4	172.4
India	282.9	277.6
Pakistan	219.3	220.1
Iran	215.3	210.5
Europe	183.6	174.4
China	177.5	164.5

Table 80 Comparison of axial forces, pier Y1-1, school WPL

House without Plinth		
Region	Numercial results	Theoretical results
Nepal	88.0	97.1
India	136.3	148.7
Pakistan	104.0	125
Iran	108.3	124.7
Europe	93.2	98.3

China	92.1	89.9

Table 81 Comparison of axial forces, pier X1-1, house WPL

School without Plinth		
Region	Numerical results	Theoretical results
Nepal	23.5	166.8
India	35.3	250.3
Pakistan	12.4	63.9
Iran	24.3	136
Europe	36.4	109.3
China	42.6	193.7

Table 82 Comparison of bending moments, pier Y1-1, school WPL

House without Plinth		
Region	numerical results	Theoretical results
Nepal	19.9	165.2
India	29.9	272.9
Pakistan	13.2	93.6
Iran	21.4	168.1
Europe	23.9	168.3
China	32.2	273.8

Table 83 Comparison of bending moments, pier X1-1, house WPL

School without Plinth		
Region	Numerical results	Theoretical results
Nepal	16.2	56.6

India	24.4	84.8
Pakistan	8.3	21.6
Iran	16.7	46.1
Europe	25.0	37.1
China	29.6	65.6

Table 84 Comparison of shear forces, pier Y1-1, school WPL

House without Plinth		
Region	Numerical results	Theoretical results
Nepal	21.6	41
India	32.2	61.3
Pakistan	12.9	23.1
Iran	23.1	41.7
Europe	26.5	41.7
China	36.7	68

Table 85 Comparison of shear forces, pier X1-1, house WPL